MASTERARBEIT / MASTER'S THESIS

Titel der Masterarbeit / Title of the Master's Thesis

„A protective role of silicon in mosses under abiotic stress?"

verfasst von / submitted by

Stephan Manhalter, BSc

angestrebter akademischer Grad / in partial fulfilment of the requirements for the degree of

Master of Science (MSc)

Wien, 2017 / Vienna 2017

Acknowledgements

Wien, 06.06.2017   Stephan Manhalter

Table of Contents

1 Abstract

Within the last decade, multiple papers addressed the topic of silicon as beneficial or even essential element in plant nutrition for selected crops like *Zea mays* or *Oryza sativa*. These and other studies linked plant available silicon to drought tolerance, heavy metal stress tolerance and pathogen defense. Yet there is not much published on the role of silicon in bryophytes, even though some species contain up to 10% of silicon dioxide in biomass.

The conducted experiments sought to explain the influence of plant available silicon, provided as sodium orthosilicate, on stress response in bryophytes, in this case the model organism *Physcomitrella patens* (Hedw., syn. *Aphanorhegma patens*) and the heavy metal tolerant *Pohlia drummondii* (C. Müll.) Andrews. In three experiments the mosses were cultivated on solid, initially copper free media, half of the petri dishes with 0.5 mM sodium orthosilicate and the other half without additional silicon. The first experiment focused on Cu treatments with added concentrations of 0.1, 1 and 10 mM $CuCl_2$. In the second experiment half of the plants were treated with UV-B radiation for 10 h a day after the fourth week of cultivation. In the last experiment, the mosses were treated with 0.2, 0.4 and 0.6 Osm NaCl to look at stress caused by salinity. Images of the cultures were taken every week and the plants were harvested after a period of seven weeks. Image analysis, spectrophotometry, staining of reactive oxygen species (ROS) and cell measurement were employed to find decisive evidence linking silicon to the viability and general fitness of the plant.

In the Cu experiment, Si treatment led to a decrease of Cu accumulation in the protonemata of *P. drummondii* in 1 mM Cu treated samples. In the UV experiment, Si led to a strong increase in biomass in combination with UV treatment of *P. drummondii*. In case of *P. patens,* the biomass of the same treatment was equal to the control, while the UV treatment yielded lower biomass. The 0.4 Osm NaCl treated *P. patens* performed on par with the control, but was outperformed by the Si treated and both 0.2 Osm NaCl/0.2 Osm NaCl & Si treated samples in the salinity experiment. It also gained more biomass than the *P. drummondii* samples of the same treatment, supporting the hypothesis that *P. patens* is more salt tolerant than some other mosses.

2 Zusammenfassung

Im letzten Jahrzehnt haben viele Publikationen Silizium als förderliches oder gar essentielles Element im Pflanzenbau besprochen. Dies gilt vor allem für einige Nutzpflanzen, wie zum Beispiel *Zea mays* oder *Oryza sativa*. Diese und weitere Studien verbanden pflanzenverfügbares Silizium mit Resistenz gegen Dürre, Schwermetallstress und Pathogene. Bisher wurde allerdings nicht viel über die Rolle von Silizium in Moosen publiziert, obwohl einige Spezies bis zu 10% Siliziumdioxid in der Trockenmasse beinhalten.

Die durchgeführten Experimente versuchten den Einfluss von pflanzenverfügbarem Silizium, in der Form von Natrium-Orthosilikat, auf die Stressreaktion von Moosen, zu erklären. Der Modelorganismus *Physcomitrella patens* (Hedw. Syn. *Aphanorhegma patens*) und die schwermetalltolerante Spezies *Pohlia drummondii* (C. Müll.) Andrews, wurden untersucht. In drei Experimenten wurden die Moose auf festen, ursprünglich kupferfreien, Medien kultiviert. Die Hälfte der Petrischalen wurde mit 0,5 mM Natrium-Orthosilikat behandelt und die andere Hälfte wurde siliziumfrei belassen. Im ersten Experiment lag der Fokus auf der Kupferbehandlung mit $CuCl_2$, welches den Medien in Konzentrationen von 0,1, 1 und 10 mM zugefügt wurde. Im zweiten Experiment wurde die Hälfte der Pflanzen mit UV-B Strahlung behandelt, jeweils 10 Stunden am Tag, beginnend nach der vierten Woche Kultivierung. Im letzten Experiment wurden die Moose mit 0,2, 0,4 und 0,6 Osm NaCl behandelt, um Salzstress zu untersuchen. Die Kulturen wurden jede Woche fotografiert und die Pflanzen wurden nach sieben Wochen geerntet. Um ausschlaggebende Beweise für die Verbindung von Silizium und Überleben, beziehungsweise Gesundheit der Pflanze zu finden, wurden Bildanalysen, Spektrofotometrie, Sauerstoffradikalfärbung (ROS) und Zellvermessungen durchgeführt.

Im Kupferexperiment führte die Si-Behandlung zu einer Abnahme des Kupfergehalts im Protonema der mit 1 mM Cu behandelten *P. drummondii* Proben. Im UV Experiment führte Si in Kombination mit UV-B Strahlung zu einer starken Biomassezunahme bei *P. drummondii*. Im Fall von *P. patens* war die Biomasse der gleichen Behandlung gleich hoch wie in der Kontrolle, während die UV Behandlung eine geringere Biomasse aufwies. Im Salinitätsexperiment lagen die mit 0,4 Osm NaCl behandelten *P. patens* Kulturen in ihrer Biomasse mit den Kontrollkulturen gleichauf, wurden aber von den Si-behandelten und den 0,2 Osm NaCl/0,2 Osm NaCl & Si behandelten Proben übertroffen. In diesem Falle, nahm die Biomasse auch mehr zu, als vergleichsweise bei *P. drummondii*. Dies unterstützt die Hypothese, nach der *P. patens* eine höhere Salztoleranz hat, als so manche andere Moose.

3 Introduction

Recent research is increasingly focusing on breeding species of stress tolerant crops for human consumption or industrial use, to reduce the impact of climate change, soil salinization and environmental pollution on annual yields and product quality (Feller, 2016; Liu et al., 2016). In some species of higher plants (maize, rice) Si has been found to increase tolerance to several abiotic and biotic stressors (Kim et al., 2016; Malčovská et al., 2014a; Malčovská et al., 2014b; Shakoor, 2014; Vaculík, 2009; Vaculíková et al., 2016) and in *Glycine max* it is thought to mobilize Zn in Zn limiting conditions (Pascual et al., 2016). In wheat, barley and cucumber beneficial effects on growth have been observed (Dragisic Maksimovic et al., 2012; Ma et al., 2001). Many abiotic stress response pathways are highly conserved in the plant kingdom and developed before bryophytes and higher land plants diverged (Kroemer et al., 2004). This is one of the reasons why we focused on mosses in our experiments.

For this study, different species of bryophytes were chosen as a model, because of the conservative character of some abiotic stress tolerance pathways and their basal position in the evolutionary lineage of land plants. The aim was to investigate the physiological changes caused by treatment with plant available silicon under abiotic stress (heavy metal, UV-B, salinity).

3.1 Bryophytes

Bryophytes *sensu stricto*, commonly referred to as mosses, are the sister group to hornworts and all tracheophytes, which diverged from the liverworts about 480-430 million years ago, during the mid-Ordovician to lower Silurian period (Qiu et al., 2006). Similar to higher plants, they are diplo-haplonts but the haploid phase is more prominent. This means, they only have one set of chromosomes for the longer timespan of their lifecycle, which is the opposite in higher plants. It vastly improves capabilities for genetic manipulation (Knight et al., 1988). The haploid phase is known as gametophyte, since it will produce the gametes to later form the sporophyte, the diploid phase. Furthermore, the gametophyte can be divided in the gametophore, a branching or unbranching system of stems with spirally or bilateral symmetrically distributed phylloids (Frahm and Frey, 2004) with one or more cell-layers (middle rib) and highly branched, filamentous protonema, which in many species forms rhizoids and attaches the moss to the substrate. The protonema additionally can be differentiated into chloronema and caulonema. Both are photosynthetically active, but chloronemata contain more chloroplasts and assimilate the most. They also form brood cells or gemma for asexual reproduction and as point of origin for more protonemata. Caulonemata on the other hand behave more like other tip growing filaments (pollen tubes, root hairs, hyphae), and upon division, form oblique cell walls. Another function is their sense for gravity provided by amyloplasts (Pressel et al., 2008 and references therein). They also grow faster than chloronema, which makes them a prime model to study cell elongation and cytoskeleton, as well as endo-/exocytosis and vesicle transport (Vidali et al., 2009).

In general mosses are pioneer plants, which, similar to lichens, live in rather extreme habitats, as long as there is enough precipitation or available water. The possible habitats include rocks, acidic and calcareous soils, cliff seeps, waterfall areas, stream sides as well as tree bark and bogs (Glime, 2017). Their desiccations tolerance, facilitated by poikilohydry and quick recovery, supports them in seasonally dry habitats, or on exposed rock (Oliver et al., 2005), but some species also withstand other stress factors, like salinity (*Physcomitrella patens*; Frank et al. (2005)), or exposure to heavy metals (*Pohlia drummondii*, Wernitznig (2009 and references therein), Url (1956)). Like in other plants, cell wall components, especially the low-methylesterified pectins, like homogalacturonan (HGA) provide an ion-exchange capacity for bi- and trivalent cations (Krzesłowska, 2011). According to Krzesłowska et al. (2009), mosses actively increase their ca-

pacity to handle heavy metals by forming more pectinous cell wall thickenings and by sequestering heavy metal ions into the apoplast. While HGA saturated with Ca^{2+}-ions is rather stable, other ions, like Cu^{2+} or Fe^{2+} which also have a higher binding affinity, will negatively impact the cell wall stability (Fry, 1998).

3.2 Silicon

Silicon is the second most abundant element in the earth's crust after oxygen and before aluminum (Lutgens and Tarbuck, 2000). Most of it is bound as oxide in minerals like quartz, glimmer or feldspar; elementary silicon can only be produced artificially. The sheer abundance as well as bio-mineralization of silica in some organisms (radiolaria, diatoms, horsetails etc.) make it an interesting candidate for research. So far artificial culture media rarely contained additional silicon, although it is plant available in soil solutions in concentrations of 0.1 to 0.5 mM (Lindsay, 1979). It is technically very difficult to work "silicon free" though, as even highly purified water contains trace amounts of silicon ($2*10^{-5}$ mM, 0.5 ppb), because the uncharged form of mono-silicic acid (H_4SiO_4) simply passes through the ion exchangers for laboratory-grade water and any glass instruments or containers could add silicon to the prepared medium (Werner and Roth, 1983). According to Trembath-Reichert et al. (2015) *Physcomitrella patens* has transmembrane Si-transporters of an aquaporine subfamily called nodulin 26-like intrinsic protein (NIP). While *Oryza sativa* for example has type I, II and III, of which type II and III are said to transport orthosilicic acid, *P. patens* has only a variant of type II. In some species of crops (*Cucumis melo*, *C. sativa*, *Phaseolus vulgaris*) the transporters were bred out to soften the rind or improve palatability. According to He et al. (2015), most silicon that is incorporated into the cell wall of plants (*O. sativa*) is in the hemicellulose fraction (61.7%).

3.3 Stress

Stress is a significant long term deviation from the average "optimal" conditions of the habitat. This excludes short time fluctuations or regular rhythms (sunny/cloudy days, day-night cycle). Since plants cannot flee from their stressors, the only options they have are stress avoidance and stress tolerance. In plants, most stressors will induce few specific effects, but a very similar overall response, like reduced growth rate.

The concept of plant stress after Lichtenthaler (1998) constitutes of four phases, the fourth being regeneration of the plant, if the stress event was not too severe.

1: Response phase: initial alarm reaction, after initiation of stress event

- Deviation of functional norm
- Decline of vitality
- Catabolic processes exceed anabolism

2: Restitution phase: plant attempts to resist, stress event still ongoing

- Adaptation processes
- Repair processes
- Hardening (reactivation of anabolism)

3: End phase: plant exhaustion, especially under long-term stress

- Stress intensity too high
- Overcharge of the adaptation capacity
- Chronic disease or death

4: Regeneration phase: if the stressor is removed and the damage was not too high, partial or full recovery of the plant is possible.

Here we focus mostly on abiotic stress, which is defined as a condition that is significantly different from the optimum and is caused by environmental factors, excluding pathogens like fungi, bacteria and viruses, herbivores, other plants or anthropogenic influence. Abiotic stress includes a full range of factors (after Kreeb, 1974; Levitt, 1980):

- Radiation: deficiency, excess, UV
- Temperature: heat, cold, frost
- Water: dry air, dry soil, flooding/hypoxia
- Gases: oxygen deficiency, shifted CO_2-O_2 ratio, volcanic gases
- Minerals: deficiency, excess, imbalance, salinity, heavy metals, acidity, alkalinity
- Mechanical: wind, wounding

Most stress factors will induce the generation of reactive oxygen species (ROS), which will cause damage on membranes and DNA. The plant has enzymes to reduce ROS, like Cu/Zn superoxide dismutase (Yamasaki et al., 2008), which help countering the negative impact, but it will bind part of the plant's resources to counter the effect and repair damages, so that it will lead to a reduction of growth.

3.4   Copper and heavy metals

Heavy metals are omnipresent, but mostly in low concentrations. Through natural and anthropogenic influence, they might accumulate locally. Examples for such influences are erosion and mining, leading to heavy metal enriched creeks and spoil heaps or slag deposits. Those areas can be multiple millennia old, dating back to Celts or Romans. Through further erosion the remains of spoil heaps or slag deposits can contaminate the surrounding substrate (Greger, 2004). The area then becomes inhospitable or uninhabitable for un-adapted organisms and higher plants (Gregory and Bradshaw, 1965).

According to Nieboer and Richardson (1980) and Appenroth (2010), metals are divided into three groups:

1. A-metals: They have a high affinity to oxygen groups in macro molecules (carboxyl- and alcohol groups). Those are especially alkaline earths, Li, Na, Ca and Cs.
2. B-metals: They are characterized by their affinity to sulfur and nitrogen (sulfohydryl- and amino groups). Examples are Cu, Pd, Ag, Au, Pt and Hg.
3. Transition metals: This group sums up all other metals, which do not fit into the other two groups. For example, Cr, Mn, Fe, Co, Ni, Zn, Cd, Sn and Pb.

Higher concentrations of heavy metals will cause coagulation of proteins, like a heat shock (Lepeschkin, 1924). This would cause the metabolism to halt and effectively kill the cell. Some metals, like silver and mercury have a fixating influence, but others will distort the cell struc-

tures, if high concentrations are applied (Klemm, 1895). Lower concentrations of heavy metals might lead to competition for uptake with essential micronutrients and can cause chlorosis, necrosis or slowed growth caused by micronutrient deficiency. In some cases they also negatively influence plant anatomy, like the roots of maize and poplar (Stoláriková et al., 2012; Vaculík et al., 2012).

Heavy metals also can have a significant influence on cell wall stability. Very important in this context are pectins, for example homogalacturonans (HGA) and rhamnogalacturonans (RGA). They are well defined, but structurally heterogenous and comprise about 30% of the primary cell wall (Scheller et al., 2007). Cell wall stability furthermore depends on the level of methylesterification of the pectins, the pH, as well as oxygen radicals (Fry, 1998). Bi- and trivalent ions of heavy metals often have a higher affinity to the carboxyl and alcohol groups of HGA and RGA than Ca-ions (Krzesłowska, 2011 and references therein). The higher affinity of Cu and other heavy metals to HGA and RGA increases both the stability of the cell wall and influences the activity of pectin methyl esterase (PME) and its inhibitors (PMEI) through direct detection (wall associated kinase like, WAKL) or detection of "eggbox" HGA structures with metal ions (wall associated kinase, WAK) (Decreux and Messiaen, 2005; Hou et al., 2005), leading to a signal cascade for stress response.

Here we focused on copper, a micronutrient cation, that was provided as inorganic salt ($CuCl_2$). It is often used as catalyst in redox processes (Schlee, 1986) and is part of plastocyanin and oxidase enzymes. Most of the copper in a plant cultivated on non-contaminated substrate, is found in the chloroplasts (Libbert, 1987). Copper is, after cadmium and mercury, one of the most toxic heavy metals. Its toxicity also significantly depends on the associated anion (Sassmann et al., 2015a). The copper-anion will mostly bind to peptide groups of proteins/polypeptides or the amino group of polypeptides and amino acids (Küntzel and Dröscher, 1940). In higher plants, it is instead transported as amino acid complex (Ernst, 1972; Schiller, 1974). Another preferred binding site for heavy metal ions are SH groups of proteins (Ross and Old, 1973).

3.5 UV-B, pigments and photoprotection

UV radiation is the, for humans invisible, short wave electromagnetic radiation between visible light and X-rays. The weaker UV-A radiation ranges from 380-315 nm wavelength, while the UV-B spectrum ranges from 315 to 280 nm. The stronger UV-C, which, under natural conditions, is completely absorbed by the upper layers of atmospheric air, ranges from 280 to 200 nm wavelength (DIN 5031, 1984). Since part of the UV-B radiation passes both the ozone layer and the atmospheric air layers below, intense irradiation, as might happen higher up in the mountains or on a clear day in summer can cause severe damage to plant cells, especially to DNA, proteins, lipids and membranes (Hollosy, 2002). DNA damage needs to be repaired before replication for the next cell division, and membrane damage needs to be repaired to prevent cell death. Other effects of UV irradiation on plants would be a reduction of chlorophyll and an increase in carotenes, to protect the other pigments (Pavlović et al., 2014).

Plant pigments are carbohydrates with conjugated double-bonds and/or aromatic rings, which allow for excitation of individual electrons by incoming light (absorption spectrum) and emission of light quanta of lower energy (emission spectrum). Chlorophylls are chelate complexes of porphyrin-ring derivates and a Mg^{2+} central atom. If the pH drops into the acidic, part of the chlorophyll will lose its Mg-ion, turning into a pheophytin. Pheophytins are still active in photo-

synthesis, by transporting electrons within the light harvesting complex (LHC) of Photosystem II (PS-II). The investigation of the phaeophytinisation after Ronen and Galun (1984) allows for estimation of chlorophyll acidification, that leads to loss of the Mg-ion of the chelate complex. Protochlorophylls are an oxidized version of chlorophylls that are reduced to chlorophylls when exposed to light. Carotenes both transport electrons in the LHC and provide protection against singlet oxygen (O·), the production of which is partially caused by UV irradiation. Most light absorption of the LHC happens around 450-500 nm and around 650-680 nm wavelength (Fig. 1).
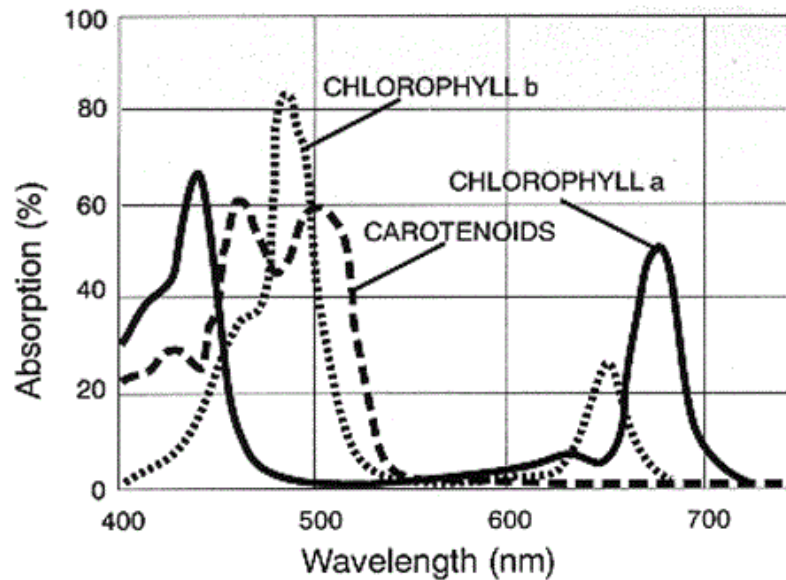
Fig. 1: Light absorption spectrum of plant pigments after Whitmarsh and Govindjee (1999, Fig. 5).

While some reported, Si induced, UV protection mechanisms, like an increase of surface wax, are not biologically possible in bryophytes, the UV radiation can still be shielded by amorphous silica in the cell walls, a process which is evident at least in other species and higher plants (Benvenuto et al., 2013; Tripathi et al., 2017 and references therein).

3.6 Salinity

Oversalination of arable land was discussed by Jacobsen and Adams (1958) as a reason for the downfall of ancient Mesopotamia. While generally irrigation is necessary in arid climates, under the wrong circumstances the improvements in yield will not last for long. In his manuscript for the book "Exploiting the Earth" (John Hopkins University Press), Cowen (manuscript, 2004) mentions four factors that are important for sustainable irrigation in arid climates:

- An abundant supply of water of good quality with low amount of salt or pollutants.
- Well-drained soil to avoid formation of salt crusts by evaporating water.
- Good regional drainage to avoid salt accumulating in the soil.
- A supply of fertilizer to reintroduce nitrogen and essential minerals, which get washed out by irrigation.

If any of those factors are not provided, the soil quality will deteriorate over time and cause loss of yield, until the soil is oversalinated and only very few, specialized breeds or species will grow at all.

One example for plants, which can deal with elevated levels of salt in the substrate, is *Oryza sativa*. It possesses a Na^+/H^+ exchanger, that pumps sodium out of the cells. When it was initially discovered in *Arabidopsis thaliana*, it was named salt overly sensitive 1 (SOS1) protein. Its homolog in rice was therefore named OsSOS1. Together with two kinases, which form a complex (SOS2/SOS3), it is part of the salt overly sensitive pathway to sense and respond to high intracellular concentrations of sodium, by pumping out sodium ions in exchange for protons. Since homologs of SOS1 were also found in *P. patens*, the pathway is considered to be highly conservative (Martínez-Atienza et al., 2007 and references therein).

If plants are unable to deal with salt stress, it will cause detrimental effects, like reduction of growth, accelerated development, senescence and death. These are caused by the osmotic stress or by sensitivity to sodium and/or chloride. Severe salinity shock may also lead to programmed cell death. Salt stress will also induce abscisic acid synthesis, which will in turn lead to stomata closure, if it is transported to the guard cells. As a result, photosynthesis declines because of reduced gas exchange and photoinhibition and oxidative stress increase, as if the plant was going through a dry period. Another effect of salt stress is the inhibition of cell expansion directly, or caused by abscisic acid. Sodium also will compete with potassium for uptake, which leads to potassium deficiency. Increased calcium on the other hand can counter this through "an intracellular signaling pathway that regulates expression and activity of potassium and sodium transporters." (Zhu, 2001). It may also be responsible for direct suppression of non-selective cation channel activity.

3.7 Hypotheses

Our main hypothesis, based on some of the reports of beneficial effects of Si in higher plants was, that plants that have access to Si would be better in coping with stress, leading to lower amount of reactive oxygen species (ROS) and more vitality and growth. For this purpose, we applied ROS dyes, measured biomass and pigment content.

Based on prior investigations by Sassmann et al. (2015a), we hypothesized, that increased abiotic stress would lead to more biomass investment into protonemata. Therefore, if Si application would significantly reduce the stress, it would also show in the protonema/gametophore ratio.

It was also important to investigate, if added Si would influence the bioavailability of other supplied elements, like Cu, in the heavy element treatment. This was investigated using a simulation approach with MINTEQ V 3.1 (Gustafsson, 2016).

Another hypothesis dealt with the supposed alleviation of UV damage by Si application, which would be attributed to physical filtering or scattering of the light, if Si is deposited in the cell wall for example.

We also hypothesized, that the effects of Si might be higher in so-called heavy metal mosses, species that are adapted to deal with heavy metals and their toxicity.

4 Material and Methods

4.1 Moss species

For our experiments, two species of bryophyte were compared:

- *Pohlia drummondii* (C. Müll.) Andrews, Bryaceae, a heavy metal adapted moss, which prefers Cu contaminated sites (Fig. 2 A,
- A).
- *Physcomitrella patens* (Hedw.) [syn.: *Aphanorhegma patens* (Hedw.) Lindb.], Funariaceae which is a fully sequenced model organism with many mutant lines available (Fig. 2 B,
- B).

P. patens has been cultured in our lab for years, but originally was gifted by Ralf Reski Lab (Freiburg, Germany).
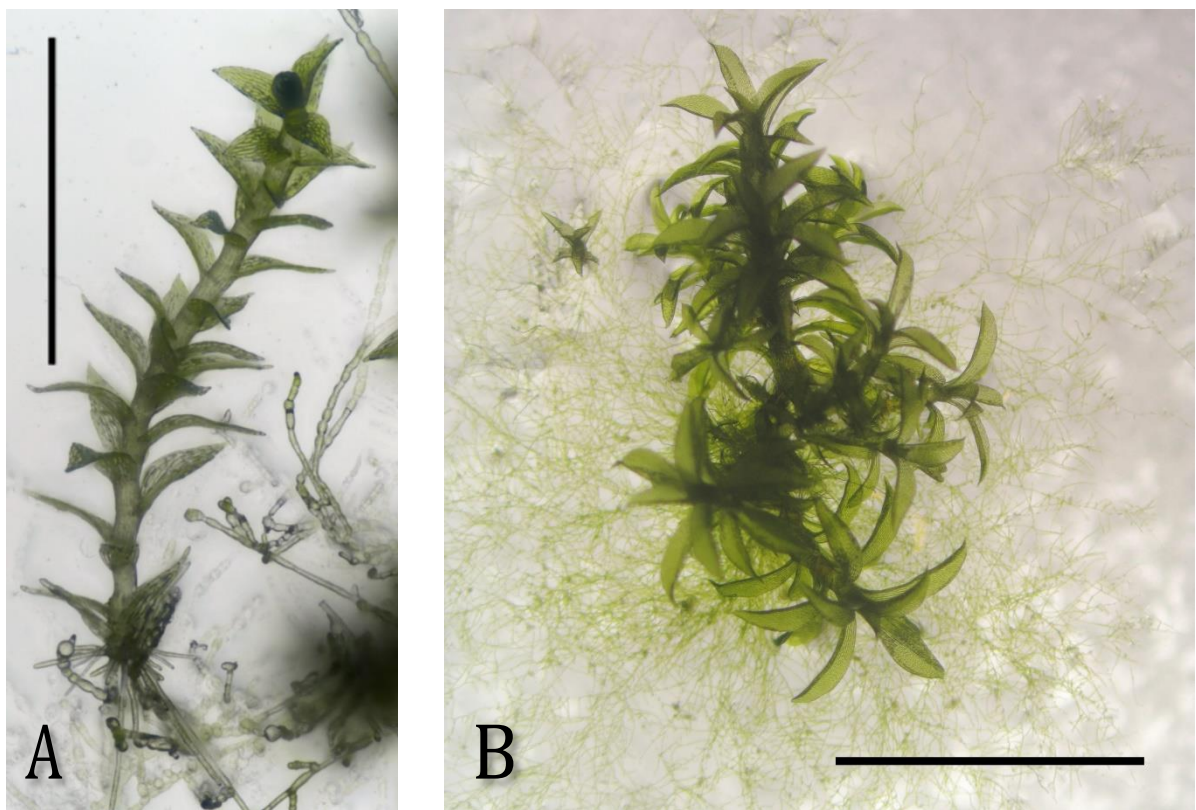

Fig. 2: Macro shots of A: *Pohlia drummondii*, bar: 1 mm; B: *Physcomitrella patens*, bar: 1 cm.
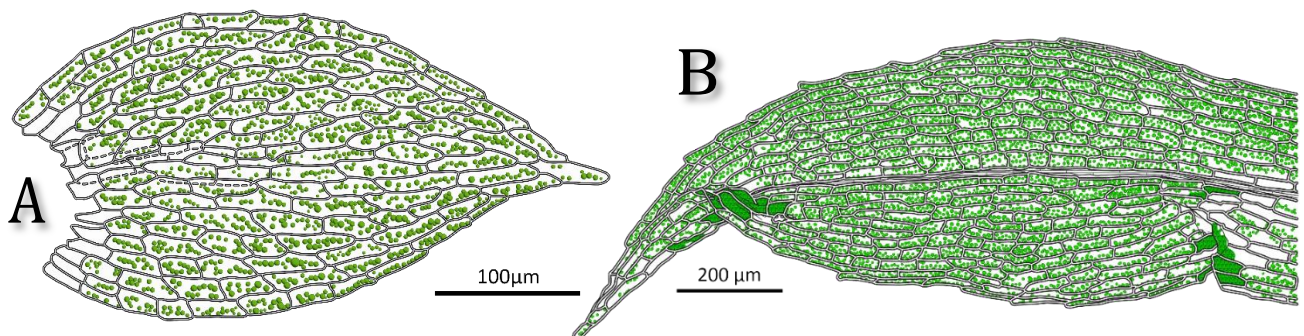

Fig. 3: Anatomic illustration of A: *Pohlia drummondii* leaf;
B: *Physcomitrella patens* leaf.

1.1 Culture

Moss cultures were set up on sterilized cellophane on solid agar media to enable harvesting of protonemata additionally to gametophores which were needed for the experiments. Pieces of gametophores or protonemata were ground and the resulting cell suspension was used to start new cultures.

The media were always based on the Hoagland ($PpNO_3$) medium by Vidali et al. (2009), which was modified to be technically free from copper. The pH was adjusted to 5.8 using HCl or KOH under constant mixing on a magnetic stirrer (Schott instruments electrode blue line pH meter). The media composition is listed in Tab. 1.

Tab. 1: Composition of the $PpNO_3$ media per liter.

Compound	Amount	Concentration (final)
$MgSO_4 \cdot 7\,H_2O$	254 mg	1030 μM
KH_2PO_4	250 mg	1860 μM
H_3BO_3	614 μg	9930 nM
$MnCl_2 \cdot 4H_2O$	389 μg	1966 nM
$CoCl_2 \cdot 6\,H_2O$	55 μg	231 nM
$ZnSO_4 \cdot 7\,H_2O$	55 μg	191 nM
KI	28 μg	169 nM
$Na_2MoO_4 \cdot 2\,H_2O$	25 μg	103 nM
$Ca(NO_3)_2 \cdot 4\,H_2O$	800 mg	3300 μM
Di-ammonium tartrate	500 mg	2700 μM
$FeSO_4 \cdot 7\,H_2O$	12.5 mg	45 μM
Agar	7g	

4.1.1 Silicon and copper

To investigate the effect of copper (Cu) in addition to silicon on *Physcomitrella patens* and *Pohlia drummondii*, eight different solid media were prepared (Tab 2; further referred to by the abbreviations in Tab. 2).

Tab. 2: List of abbreviations of the different used media for the heavy metal experiment and their modifications concerning $NaSiO_4$ and $CuCl_2$ content.

Abbreviation	$NaSiO_4$ [mM]	$CuCl_2$ [mM]
Con	0	0
Si	0.5	0
Con 0.1	0	0.1
Si 0.1	0.5	0.1
Con 1	0	1
Si 1	0.5	1
Con 10	0	10
Si 10	0.5	10

Silicon was provided in a final concentration of 0.5 mM in the form of sodium orthosilicate ("liquid glass", Tiger). To get a 1 M stock solution, 10 ml liquid glass with a molarity of about 6 M·L^{-1} were diluted by adding 51.7 ml deionized water. 0.5 ml of that stock were further diluted with 99.5 ml deionized water to get 100 ml of a 5 mM stock. 100 ml of the 5 mM stock were used to create 1 L of 0.5 mM medium.

Copper was provided as $CuCl_2$ in concentrations of 0.1, 1 and 10 mM. The higher concentrated Cu media needed additional modification, since the $CuCl_2$ interfered with gel formation of the added Agar. For both media with 1 mM $CuCl_2$ 0.6 g Agar were added to 200 ml medium, while for the 10 mM Cu & Si medium 2.6 g Agar on 200 ml and for the 10 mM Cu medium 5.6 g Agar on 200 ml had to be added. After autoclaving and reheating in the microwave, the media were poured into 9 cm Petri dishes (Greiner Bio-one) in the sterile workbench (Ehret Aura-V 130) and stored in sterilized Ziploc (Ziploc slider) bags in the fridge until use. Shortly before inoculation with the mosses, the agar in the dishes was topped with sterilized cellophane disks (A. A. Packaging Limited).

One petri dish of moss material was ground using a tissue grinder (Omni tip homogenizing kit) with autoclaved tips in 4 ml of sterilized *A. dest* for 30 sec. and 90 µl of the moss suspension was spread on the cellophane disk of each petri dish. Every treatment – species combination was prepared in three repetitions, sealed with Parafilm (Bemis) and put in the cultivation cabinet at 21°C with a 14/10 hour day/night rhythm for seven weeks. Images of protonemal development on the whole dish were taken every week using a digital camera and a 90 mm macro objective (Nikon 1J1).

4.1.2 Silicon and UV-B

As an alternative for copper stress, UV-B radiation was tested. For this experiment, only two variations of Agar media were used. The control medium used in the previous experiments and the Si spiked medium with 0.5 mM sodium orthosilicate. Half of the samples were treated with UV-B radiation for 10 hours a day in the 14/10 hour day/night cycle (10h night, 2h light, 10h light + UV-B, 2 h light; Tab. 3), starting after four weeks of cultivation. The UV-B Lamp (Multiple Ray Lamp, Analytik Jena, 365 nm) has an irradiation intensity of 28.6 mW/dm^2 at 20 cm distance, which is about the distance we used for the experiment. The rest of the procedure was identical to the previous experiment.

Tab. 3: List of abbreviations of the different treatments for the UV-B experiment and the media modifications concerning $NaSiO_4$ as well as UV-B treatment. N = not treated.

Abbreviation	NaSiO$_4$ [mM]	UV-B
Con	0	N
Si	0.5	N
Con UV	0	Week 4+
Si UV	0.5	Week 4+

4.1.3 Silicon and salinity

In a third set of experiments, salinity (NaCl) was tested as a stress factor. Eight different media were prepared for this experiment, one for control, like in the previous experiments and three spiked with 0.2, 0.4 and 0.6 M NaCl, as well as another set of four plates that were additionally spiked with Si (Tab. 4).

Tab. 4: List of abbreviations of the different used media for the salinity experiment and their modifications concerning NaSiO$_4$ and NaCl content.

Abbreviation	NaSiO$_4$ [mM]	NaCl [M]
Con	0	0
0.2	0	0.2
0.4	0	0.4
0.6	0	0.6
Si	0.5	0
Si 0.2	0.5	0.2
Si 0.4	0.5	0.4
Si 0.6	0.5	0.6

4.2 Biomass

Gain of biomass was measured as protonemal growth in the petri dish [cm^2] by taking photos once a week (Nikon 1J1 & 90mm macro objective) of both the dishes and a sheet of millimeter paper as reference. Actual measurements were conducted using a macro that was adjusted to optimize distinction between moss and background/artifacts for area measurements, using Fiji image analysis software (Fig. 4).
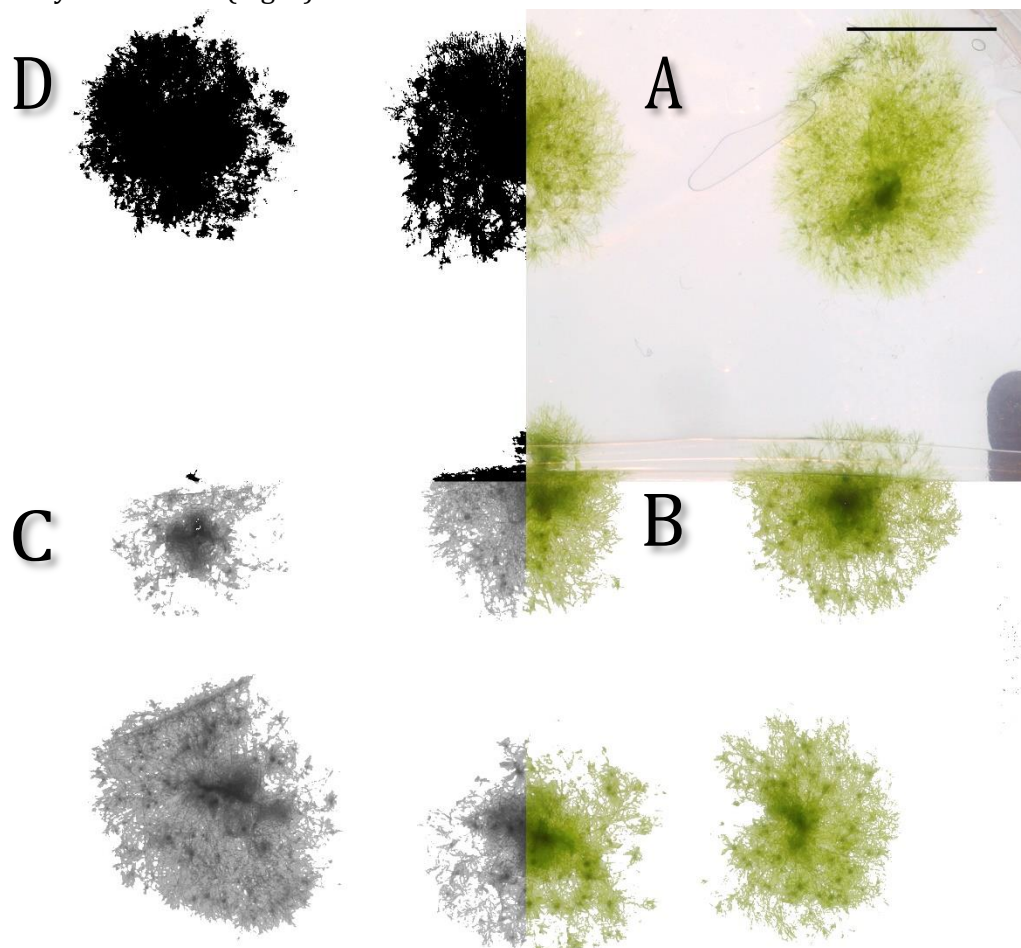

Fig. 4: *P. patens*, week 7, all steps from initial photo till measurable area A: original photo, B: exclusion of background, C: conversion to 8-bit grayscale, D: adjustment of threshold. bar: 1 cm

4.3 Gametophore-Protonema Ratio (G-P ratio)

The Gametophore-Protonema Ratio (G-P ratio) is defined after Sassmann et al. (2015a) and used as another indicator for abiotic stress. Similar to the biomass measurements, a slightly different setup for the same macro as mentioned for biomass calculation was used to calculate the area covered by gametophores, which had a darker green than the area only covered by protonema. Both the value from this measurement and the value from the initial biomass calculation were used to calculate the G-P ratio.

4.4 Reactive oxygen species

Reactive oxygen species (ROS) are a byproduct of aerobic metabolism and usually quickly reduced by enzymes and antioxidants. If the plant is under stress, the production of ROS increases and cellular components suffer heavy damage, sometimes leading to cell death. Therefore, detection and visualization of ROS can be a tool to localize and indirectly quantify stressed tissue. To be able to analyze and quantify the detrimental effect of the copper, UV-B and NaCl treatment on the plant metabolism/ROS production, and the influence of silicon in this regard, staining with nitrotetrazolium blue chloride (NBT) and 3, 3'-diaminobenzidine (DAB) was conducted. NBT forms a dark blue, insoluble formazan compound with O_2^-, while DAB turns into a reddish-brown precipitate through oxidation by H_2O_2 in the presence of peroxidase.

4.4.1 Nitrotetrazolium blue chloride (NBT)

Samples were submersed in 0.1 % solution of NBT (Sigma-Aldrich) in 50 mM potassium phosphate buffer (KH_2PO_4; pH 6.0) with 10mM sodium acid (NaN_3). Like for DAB staining, the samples were infiltrated in low vacuum for 10 min. Samples were then stored at room temperature for 36 h.

4.4.2 3, 3'-diaminobenzidine (DAB)

Gametophores were stained using a 0.1 % solution of DAB (Sigma-Aldrich) in 10 mM MES buffer (2-(N-morpholino) ethane sulfonic acid; pH 6.1). The samples were infiltrated in low vacuum for 10 min, and kept in the dark at room temperature for 36 h.

4.4.3 Further analysis

To eliminate chlorophyll pigments in the samples, the staining solution was exchanged with a solution made of 3 parts 96% ethanol, 1 part glycerol and 1 part acetic acid (v/v/v) after Daudi and O'Brien (2012), and boiled at ~80 °C for 10 minutes. The decolorized samples were then put onto glass slides and photographed (Nikon Eclipse Ni, Nikon DS-Ri2). To quantify the staining of ROS, the proportion of stained and unstained stem areas were calculated, leading to percentage values, which were then used for statistical analysis. In the salinity experiment the lack of gametophores forced us to use an intensity approach instead. In the image of the protonemata, a homogenously stained area was selected using the freehand selection tool of Fiji Image analysis software. The mean value of a resulting bell shaped color histogram (red for DAB and blue for NBT) was used to quantify staining intensity. Higher staining intensity led to lower values and lower staining to higher values, for proper representation the values were inverted by deducing them from 255 (maximum possible value).

4.5 Pigment analysis

To quantify the pigment content and derive information about plant health, we used pigment extraction and a spectrophotometric approach. Therefore a single individual per petri dish was divided into gametophores and protonemata, which was imbibed in 1 ml N,N-dimethylformamide (DMF), covered with aluminum foil and stored in the fridge for 10 days. After this period the wells of a polypropylene (PP) 96-well plate were filled with 200 µl of the extracts for measurement. Some wells were left empty or filled with unused DMF for reference. A Tecan infinite M200 spectrophotometer was used to measure the optical density at six different wavelengths to calculate the pigment content (Tab. 5). The number of flashes was always 25 at a bandwidth of 9 nm. For each wavelength, multiple reads per well (MRW) were performed in a 3x3 grid with 800 µm distance from the well border. We also allowed 100 ms settling time. The formulas used are listed in Tab. 6. The content was calculated as mg·g^{-1} dry weight, for which the tissues were dried at 65 °C for 3 days after extraction. For weighing of the samples a Sartorius Acculab ATILON scale (±0.1 mg) was used. For further reference, the abbreviations in Tab. 5 will be used to address the pigments individually. For comparison, the extraction was also conducted with di-methyl sulfoxide (DMSO) for the UV-B and the salinity treatment experiment. Additionally measurements at 415 and 435 nm wavelength were conducted in the last two experiments to estimate the phaeophytinisation after Ronen and Galun (1984). The quotient between the optical densities of both data points was compared to their table, to estimate acidification of chlorophyll pigments.

Tab. 5: List of measured wavelengths and which pigment calculations they were needed for. Light grey denotes indirect use through *Chla* and *Chlb* calculation. *Chl*: chlorophyll, *ProtChl*: protochlorophyllids, *Ph*: pheophytins, *Car*: carotenoids, *t*: total.

Wavelength	Chla	Chlb	Chl t	ProtChl	Pha	Phb	Pht	Car
480 nm								■
625 nm				■				
647 nm	■	■	■	■				░
654 nm					■	■	■	
664 nm	■	■	■	■				░
666 nm					■	■	■	

Tab. 6: Formulas used for pigment calculation based on optical density measured at specific wavelengths. *Chl*: chlorophyll, *ProtChl*: protochlorophyllids, *Ph*: pheophytins, *Chlx+c*: carotenoids, *t*: total, A: author, M: (Moran, 1982); W: (Wellburn, 1994). Concentration given in µg·ml^{-1}.

Pigment	A	Formula
Chl a DMF	W	*Chl a* = 11.65*A_{664}-2.96*A_{647}
Chl b DMF	W	*Chl b* = 20.81*A_{647}-4.53*A_{664}
Chl t		*Chl t* = *Chl a* + *Chl b*
ProtChl DMF	M	*P Chl* = -3.49*A_{664}-5.25*A_{647}+28.3*A_{625}
Ph a DMF	M	*C'a* = 23.91*A_{666}-7.22*A_{654}
Ph b DMF	M	*C'b* = -16.38*A_{666}+37.41*A_{654}
Ph t DMF	M	*C't* = 7.53*A_{666}+30.19*A_{654}
Car DMF	W	*C_{x+c}* = (1000*A_{480}-0.89**Chl a*-52.02**Chl b*)/245
Chl a DMSO	W	*Chl a = 12.19*A_{665} – 3.45*A_{649}*
Chl b DMSO	W	*Chl b = 21.99*A_{649} – 11.21*A_{665}*
Car DMSO	W	*C_{x+c} = (1000*A_{470} – 2.14*Chl a-70.16*Chl b)/220*

4.6 Scanning Electron Microscope & Energy Dispersive X-Ray Microanalysis (SEM EDX)

Energy dispersive X-ray analysis (EDX) was conducted to investigate the influence of both the Si and the Cu treatment on the overall content and localization of these elements in the plant, which might link them to the changes in pigment content or reactive oxygen species. Fresh parts of both, gametophores and protonemata, were placed on carbon foil on top of aluminum stubs and gently firmed down to the foil. Plant parts of the repetitions were batched together onto two stubs, one for protonemata, and the other for gametophores. The samples were carbon coated using a Leica EM MED020 and stored in a cabinet with silica gel until use. Twelve measurements were conducted per piece of protonema, while the measurements on gametophores were divided into four measurements per leaflet, with three leaves per single gametophore. Up to three gametophores or protonemata were measured per stub, if there were enough samples. The regions of interest on the leaflet were in a line from the base towards the tip. The settings of the used Jeol IT300 were as follows: 20 kV acceleration voltage, working distance of 11 mm and magnification of about 1500. The probe current was varied as necessary, but remained at about 60-70 nA. Measurements were conducted over a 50 sec. timespan and with live setting using the visible screen as region of interest, and switching to "Free Draw" if too much carbon foil in the background would have impacted the quantification. The EDX system is an EDAX brand setup and operates using TEAM software.

To investigate if a plant is an accumulator or an excluder (Baker, 1981), heavy metal gametophore-protonema ratios (HM G-P ratios) for all treatments were calculated using the averages of element content of the three measured gametophores and protonemata per treatment. To compare for significant differences, a Kruskal-Wallis test and afterwards pairwise comparison with a Mann Whitney W test was conducted. The values used for both tests were produced by pairwise calculation of all possible G-P ratios (9) using the three biological replicates measured per treatment. The data were afterwards transformed using a radian protocol by Sokal and Rohlf (1994), before being analyzed and visualized.

4.7 Cell measurements

The cell shape was analyzed to allow quantification of changes in anatomy induced by the silicon and copper treatments, as well as UV-B irradiation and NaCl treatment. Fresh samples of the plants were mounted on glass slides, covered with 50% glycerol, topped with a cover slip and sealed using transparent nail polish, to preserve the samples until use. Five images per sample were taken, using a Nikon Eclipse Ni light microscope and a Nikon DS-Ri2 camera. Both, length and width, of protonema as well as phylloid cells were measured using Fiji image analysis software. Additionally, in case of protonema cells the surface and volume were calculated using cylindrical approximation, for the copper and salt treated plants, to investigate the increase or decrease of cell wall and inferred buffer potential for cations.

4.8 Harvest

4.8.1 Silicon and copper

The harvest was conducted in a timeframe of eleven hours, sampling pieces of gametophores and protonemata for SEM stubs, ROS staining, pigment extracts and glass slides which were used for further, tissue specific analyses. Additionally, the Cu-2 treated mosses never grew new protonemata and the 1 mM Cu treated *Physcomitrella patens* plants didn't develop gametophores.

4.8.2 Silicon and UV-B

Harvest of the UV-B treatment experiment took seven hours. Samples were used for ROS staining, pigment analysis and cell measurements.

4.8.3 Silicon and NaCl

Harvest of the NaCl experiment took four hours and samples were used for ROS staining, pigment analysis and cell measurements. It should be noted that 0.6 Osm NaCl was too highly concentrated and the explants didn't grow. *P. patens* explants at that concentration seemed to stay green until harvest, but there was no visible increase in biomass.

4.9 Software

Image analysis was conducted using Fiji image analysis software (Rasband, 2015) and the plugin Color-Threshold (Landini et al., 2010). Solution state equilibria were modeled using MINTEQ V 3.1 (Gustafsson, 2016). Microscopic images, especially EDF stacks were created using NIS Basic Research (Laboratory Imaging, 2016). Statistical analysis was conducted using Statgraphics XVI (StatPoint Technologies Inc., 2010). Illustrations and images were produced and edited using Adobe Illustrator CS6 (Adobe Systems Inc., 2012), Adobe Photoshop CS6 (Adobe Systems Inc., 2012) and Adobe Photoshop Elements 5.0 (Adobe Systems Inc., 2006) as well as Paint.NET (Brewster and contributors, 2016). SEM-EDX measurements were conducted and quantified using the Texture and Elemental Analytical Microscopy (TEAM) software (EDAX Inc., 2013). Most data were handled using Microsoft Excel (2010) and Microsoft Excel (2016), the document itself was written using Microsoft Word (2016).

5 Results

5.1 Silicon and copper

5.1.1 Biomass

The cultures with the highest concentration of Cu showed very reduced growth in both species and there was a slight trend in *P. drummondii* that showed, that Si treatment led to better growth under high Cu conditions (1 mM Cu), both for individual explants and for the dishes. Furthermore, Si alone led to similarly high explant biomass in *P. drummondii*, as did the lower concentrated Cu treatment (0.1 mM Cu). In average over the dishes though, both the Si free and the Si spiked 1 mM Cu medium, showed the best results after 7 weeks, with a biomass increase of about 14 cm^2 (Fig. 5 A, Tab. 7).

In *P. patens*, there is less difference between the control and lower concentrated Cu treatments. Only the strong effect of the 1 mM Cu treatments should be noted, which is comparable to the effect in *P. drummondii*, but without detectable Si influence. It should also be noted, that the growth in *P. patens* is generally better than in *P. drummondii* (Fig. 5 B).
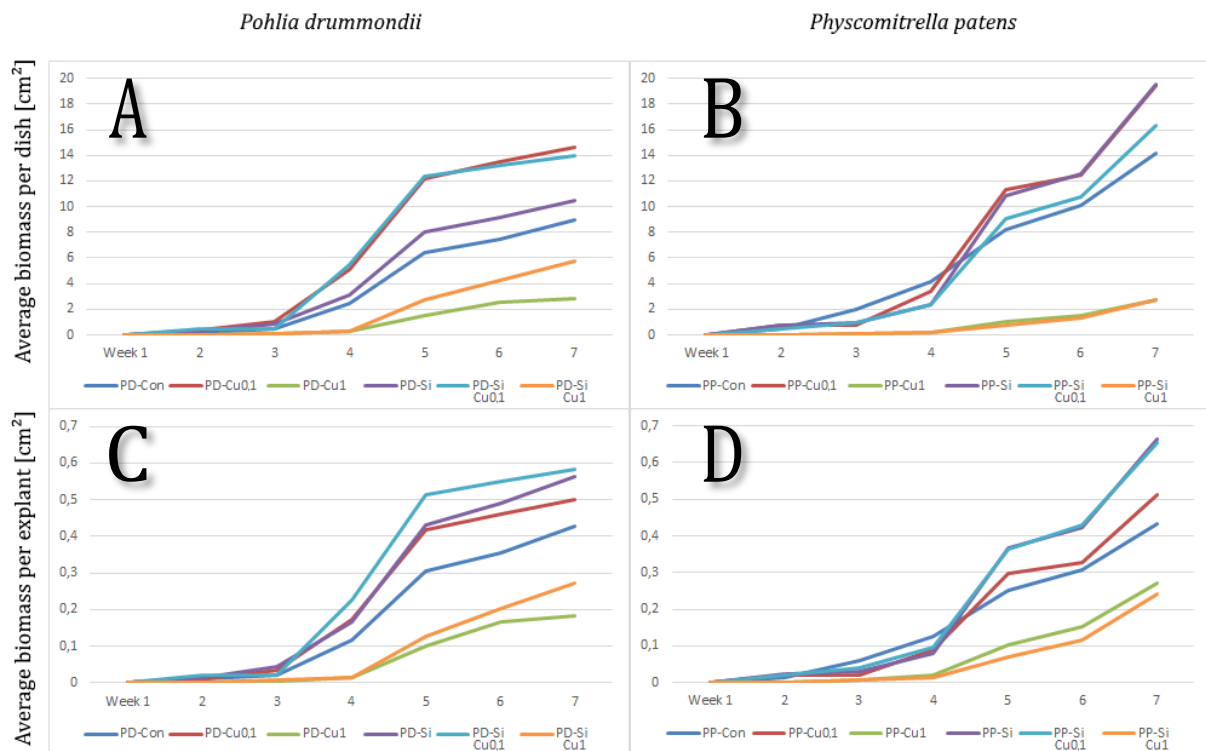
Fig. 5: Biomass increase over time in both mosses, visualized in cm^2, as average over the dishes (A, B; n=1-3) and as average of the individual explants (C, D; n=11-38). Cu concentration given in mM.

Tab. 7: Mean values for biomass in cm^2 for both species, for dishes (n=1-3) and individual explants (n=11-38) ± standard error.

PD	Con	0.1 mM Cu	1 mM Cu	Si	Si 0.1 mM Cu	Si 1 mM Cu
dish	8.98 ± 2.9	14.63 ± 0.49	2.8 ± 1.23	10.51 ± 5.03	14.01 ± 2.14	5.8 ± 0.27
explant	0.43	0.5	0.18	0.56	0.58	0.27
PP						
dish	14.15 ± 3.45	19.45 ± 4.86	2.71 ± 1.21	19.58 ± 2.63	16.35 ± 0.92	2.75 ± 1.26
explant	0.43	0.51	0.27	0.66	0.65	0.24
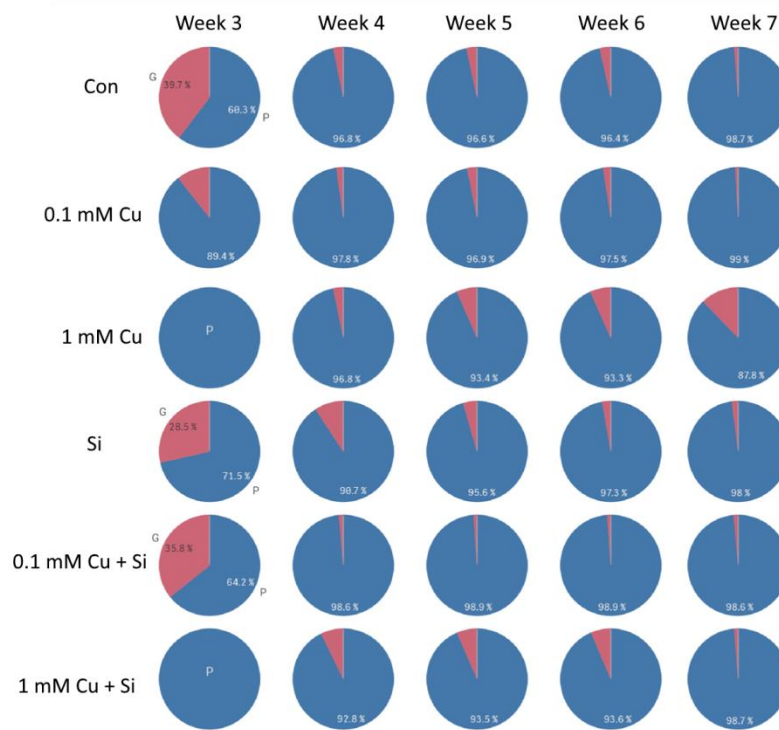
Fig. 6: Pie-charts for Cu/Si treatments and time points of the final 5 weeks of *P. drummondii*, visualizing the ratio between protonemata (P, blue) and gametophores (G, red). Gametophores start developing in week 3 for lower concentrated media and week 4 for higher concentrated media. Due to strong protonemal growth the gametophore portion diminishes over time; n=1-3.

Fig. 7: Pie-charts for Cu/Si treatments and time points of the final 5 weeks of *P. patens*, visualizing the ratio between protonemata (P, blue) and gametophores (G, red). Gametophores start developing in week 3 for lower concentrated media and there is no development in higher concentrated media. Due to strong protonemal growth the gametophore portion diminishes over time; n=1-3.

5.1.2 Gametophore – Protonema ratio

The highest amount of developed gametophores was found after 3 weeks in *P. drummondii* control, Si treatment and the comb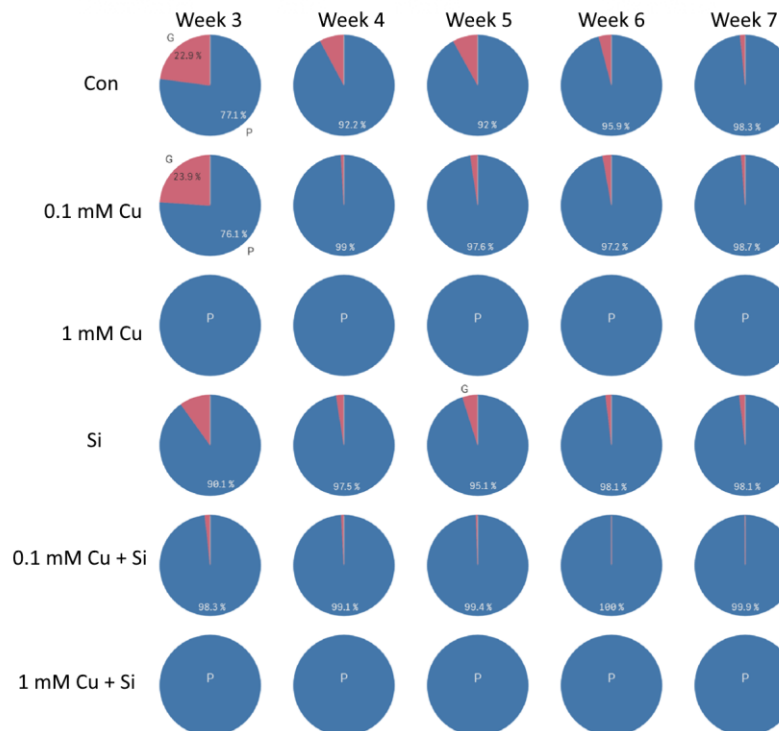ined Si & 1 mM Cu treatment with 39.7%, 28.5% and 35.8% respectively. There was a lower amount of area covered in the Si-free Con 0.1 treatment and both 1 mM Cu treatments showed no gametophore development at that point. The ratio of gametophore coverage declined rapidly in most treatments, only in both 1 mM Cu treatments, where they developed with one week delay, the ratio remained almost unchanged, but below 10%. In the last week, the ratio in the Si & 1 mM Cu treated samples shifted more towards protonemata, while in the Si-free cultures on the other hand the amount of gametophores increased to 12.5% (Fig. 6).

For *P. patens,* the highest gametophore coverage was observed after 3 weeks in control, Si and Con 0.1 treatments with 22.9%, 23.9% and 9.9% respectively. The Si & 1 mM Cu combination showed almost no gametophore development and both 1 mM Cu treatments developed no gametophores for the whole duration of the experiment. The portion of gametophore covered area declined until the last week in all samples (Fig. 7).

5.1.3 Reactive oxygen species (ROS)

5.1.3.1 *Nitrotetrazolium blue chloride (NBT)*

To quantify the oxygen radicals in the plant tissue, we used NBT, which forms blue formazan complexes. Based on Type III Sum of Squares, there is a significant difference in NBT staining based on species ($p<0.001$) and Cu treatment ($p<0.01$). The dependence on Cu treatment is stronger in *Pohlia drummondii* than in *Physcomitrella patens*.

There was significantly more staining in *P. drummondii* 0.1mM Cu than in control ($p<0.001$), staining of the 1mM Cu treatment was significantly lower than in 0.1 mM Cu ($p<0.05$) but not significantly different from the control. No significant difference in staining could be established concerning addition of Si. Generally, *P. patens* was significantly more stained than *P. drummondii* by ~30% independent of treatment (p<0,001, Fig. 8).

In both species NBT staining is significantly correlated with the expected Cu concentration in the media (*P. patens* 0.49, $p<0.01$, n=33; *P. drummondii:* 0.27, $p<0.05$, n=78; Spearman Rank Correlation, Tab. 8 & 9)

5.1.3.2 *3, 3'-diaminobenzidine (DAB)*

DAB on the other hand forms a reddish-brown precipitate with H_2O_2 and was used for quantification thereof. Type III Sum of Squares analysis revealed, that DAB staining is significantly influenced by species ($p<0.01$) and Cu treatment ($p<0.05$), similar to NBT staining.

Overall there is significantly less DAB staining in Si treated *P. patens* plants ($p<0.05$). There also is significantly less DAB staining in 0.1 mM Cu treated *P. patens* plants compared to Cu free treatments ($p<0.05$). Generally, *P. patens* is significantly more DAB stained than *P. drummondii* by ~12%, independent of treatment ($p<0.01$, Fig. 9).

DAB staining of *P. patens* is significantly negatively correlated with Cu treatment (-0.31, $p<0.05$) and Si treatment (-0.31, $p<0.05$, n=54; Spearman Rank correlation, Tab. 11). No significant correlation was found for DAB staining in *P. drummondii* (Tab. 10).
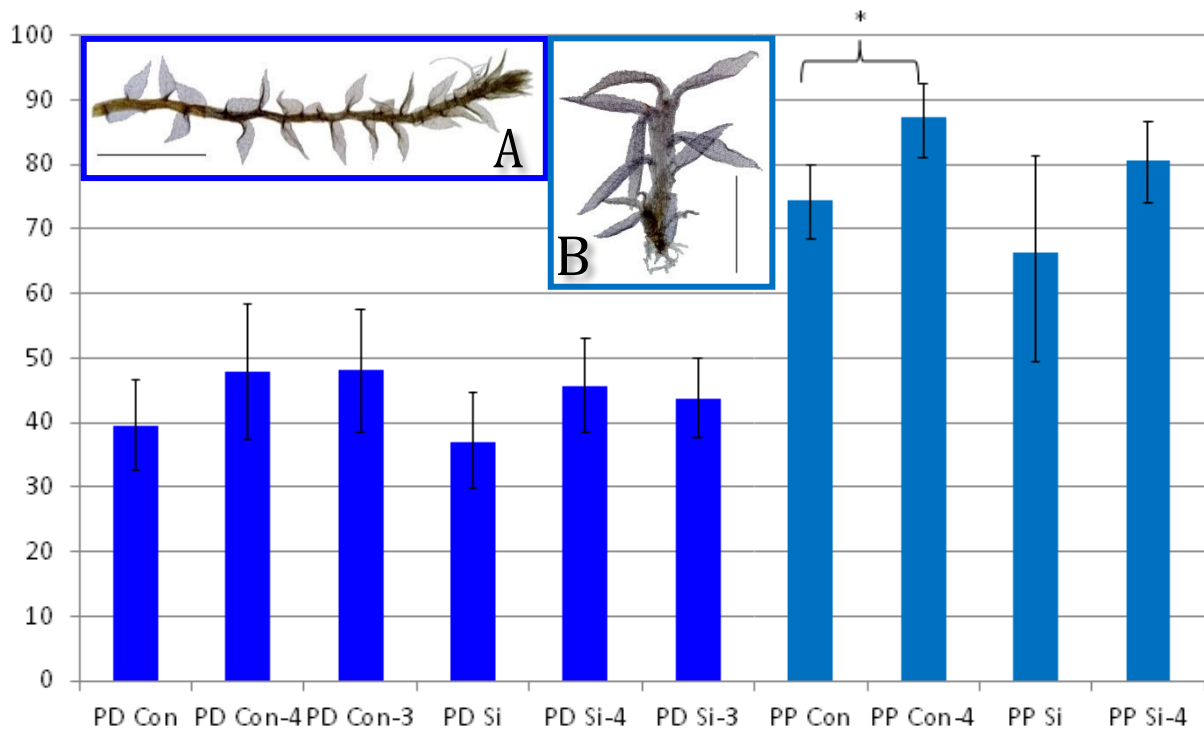
Fig. 8: NBT staining of *P. drummondii* (PD) and *P. patens* (PP) stems, significant difference between the two species (*p*<0. 001) and significantly higher staining in Cu-4 treated *P. patens* plants compared to control, n=5-17; * *p*<0.05, A: *P. drummondii* control, B: *P. patens* 0.1 mM Cu, bar of images: 200 μm.
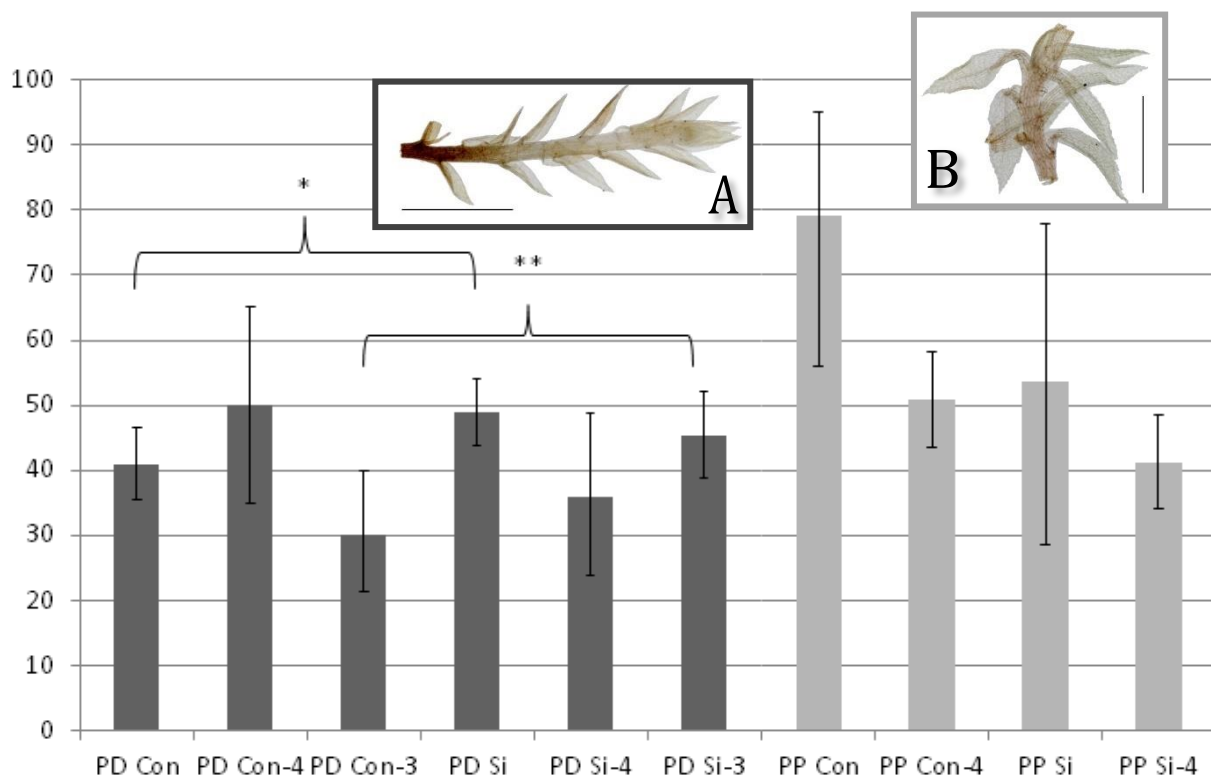

Fig. 9: DAB staining of *P. drummondii* (PD) and *P. patens* (PP) stems, significant difference between the Si treated and untreated counterparts, n=6-20; * *p*<0.05, ** *p*<0.01, A: *P. drummondii* 1 mM Cu, B: *P. patens* control, bar of images 200 μm.

24

Tab. 8: Spearman Rank Correlation of NBT staining in *P. drummondii*. Significant correlation between Cu content in the media and NBT staining (marked as red text, *p*<0.05), n=78.

	Si [mM]	Cu[mM]	NBT
Si [mM]		0.0316	-0.0854
		0.7818	0.4534
Cu[mM]	0.0316		0.2705
	0.7818		0.0176
NBT	-0.0854	0.2705	
	0.4534	0.0176	

Tab. 9: Spearman Rank Correlation of NBT staining in *P. patens*. Significant correlation between Cu content in the media and NBT staining (marked as red text, *p*<0.01), n=33.

	Si [mM]	Cu[mM]	NBT
Si [mM]		0.0575	-0.1654
		0.745	0.3494
Cu[mM]	0.0575		0.4922
	0.745		0.0054
NBT	-0.1654	0.4922	
	0.3494	**0.0054**	

Tab. 10: Spearman Rank Correlation of DAB staining in *P. drummondii*. No significant correlation was found, but there seems to be a trend of positive correlation between Si treatment and DAB staining (marked as blue text), n=64.

	Si [mM]	Cu[mM]	DAB
Si [mM]		0.0727	0.2251
		0.5637	0.0739
Cu[mM]	0.0727		-0.172
	0.5637		0.1723
DAB	0.2251	-0.172	
	0.0739	0.1723	

Tab. 11: Spearman Rank Correlation of DAB staining in *P. patens*. Significant negative correlation between both Cu and Si content in the media and DAB staining (marked as red text, *p*<0.05), n=54.

	Si [mM]	Cu[mM]	DAB
Si [mM]		0.3276	-0.312
		0.0171	0.0231
Cu[mM]	0.3276		-0.307
	0.0171		0.0254
DAB	-0.312	-0.307	
	0.0231	0.0254	

5.1.4 Pigment Analysis

66 extracts were produced and measured alongside seven blanks (only DMF) to adjust for changes during the measuring process. For statistic calculations based on three biological replicates, the data were transformed using log10 to get normal distribution and analyzed with Multifactor ANOVA Type III Sum of Squares as well as Student's t-test.

Overall, the pigment content is significantly influenced by the species ($p<0.001$) and measured tissue (gametophore/protonema; $p<0.001$) with the exception of *ProtChl* ($p<0.05$, $p<0.001$). Pigment content is significantly higher in gametophores of both species, when compared to protonemata ($p<0.001$ all), regardless of treatment.

Additionally, there is a significantly higher Chl a/b ratio in the control than in 0.1 or 1 mM Cu treated protonemata ($p<0.05$ both). The Chl/Ph ratio is significantly higher in 1 mM Cu treated mosses than in the control ($p<0.05$).

When comparing the batched Si treated and Si free protonemata samples of *P. patens*, there are significantly more pigments in Si free samples ($p<0.05$) for all pigments, except for protochlorophylls (Fig. 12). In case of *P. drummondii*, comparison of batched protonema Cu treatments reveals a highly significant increase in pigment content in the highest Cu concentration, when compared to control ($p<0.001$; $p<0.01$ for carotenoids and protochlorophyllids; Fig. 10)

5.1.4.1 *Pohlia drummondii*

In *P. drummondii* the most significantly important factor influencing pigment content is the measured tissue ($p<0.001$). Additionally, Si concentration of the media has significant influence on *Phb*, *ProtChl* and *Chlb* ($p<0.05$ all). *P. drummondii* protonemata are significantly influenced in their *Phb*, *ProtChl* and *Chlb* content by the media Cu concentration ($p<0.05$ all), while in the gametophores Si concentration significantly influences all pigments except *Phb* ($p<0.05$).

In *P. drummondii* protonemata pigment content is significantly higher in 0.1 mM Cu treatments, compared to the control ($p<0.01$ except for *Chla* and *Car*, both $p<0.05$). Also in the 1 mM Cu treated protonemata all pigment content was significantly higher than in the control ($p<0.001$, except for *ProtChl* and *Car*, both $p<0.01$, Fig. 10). In *P. drummondii* gametophores content of all pigment except for *Pha* is significantly lower in Si treated samples than in untreated samples ($p<0.05$). *P. drummondii* gametophores show an inverse trend to *P. drummondii*, with lower pigment content in Si-free samples (Fig. 11).

5.1.4.2 *Physcomitrella patens*

In *P. patens* the only significantly important factor concerning pigment content is the measured tissue ($p<0.001$). The Si concentration of the media alone has significant influence on the content of all pigments in *P. patens* protonemata ($p<0.01$), except for *Car*, which is also significantly influenced by the Cu concentration ($p<0.001$, $p<0.05$ respectively). In gametophores the influence of Si concentration is still significant but weaker for all pigments ($p<0.05$ all) and there is no significant influence of the Cu concentration on *Car* or any other pigments.

In *P. patens* protonemata the pigment content is significantly lower in the Si treated samples than in the untreated samples, except for *ProtChl* ($p<0.01$ all, Fig. 11). The *ProtChl* content in *P. patens* protonemata is significantly higher in the 1 mM Cu treatment than in the control ($p<0.05$). In *P. patens* gametophores the content of all pigments is significantly increased in Si treated samples, compared to untreated samples ($p<0.05$ all). A batched comparison of Si treated and Si-free gametophores shows a slight trend towards higher pigment content under influence of Si (Fig. 13).

26

Fig. 10: Pigment content of protonemata (P) of *Pohlia drummondii* (PD), which were not treated with Cu (Con), was significantly lower than the pigment content of the protonemata that were treated with 1mM $CuCl_2$ (1mM Cu). n=7, 2 SE.

Fig. 11: Pigment content of gametophore (G) of *Pohlia drummondii* (PD). There is a trend towards higher pigment content in Si free samples. n=16, 2SE.
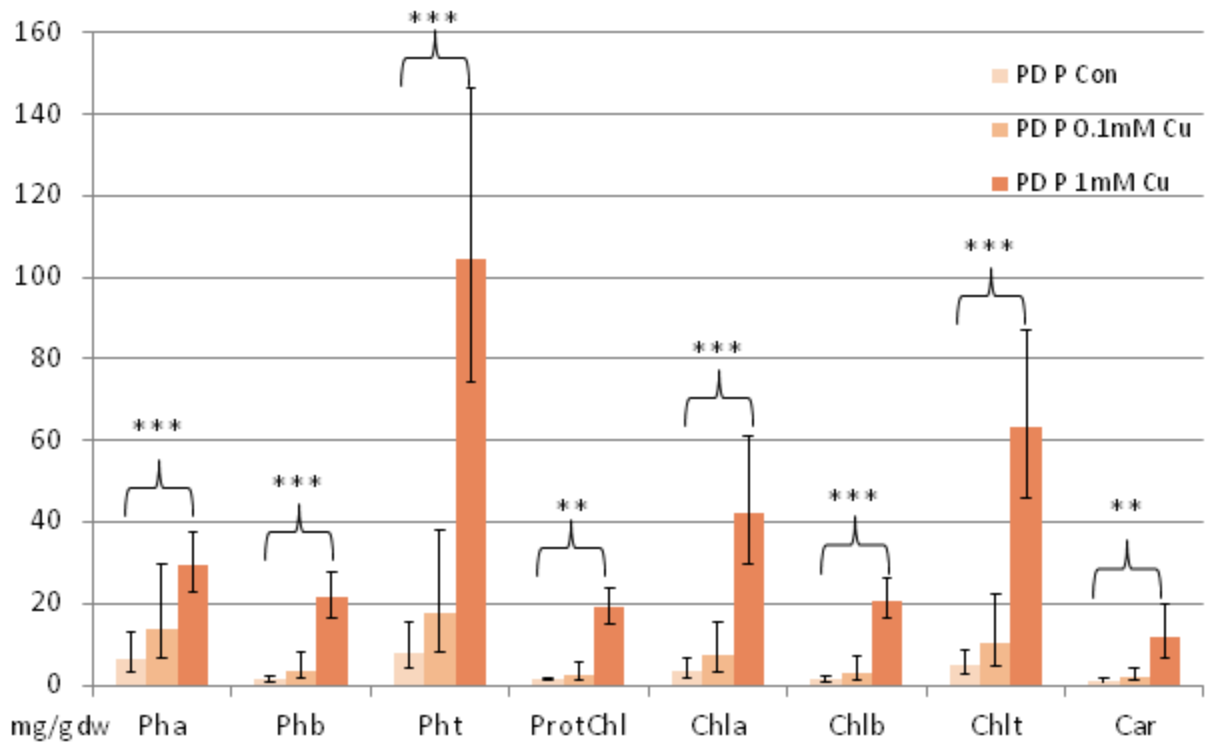
Fig. 12: Pigment content of protonemata (P) of *Physcomitrella patens* (PP), which were not treated with Si (Con), was significantly lower than the pigment content of the protonemata that were treated with Si (Si). n=16, 2SE.
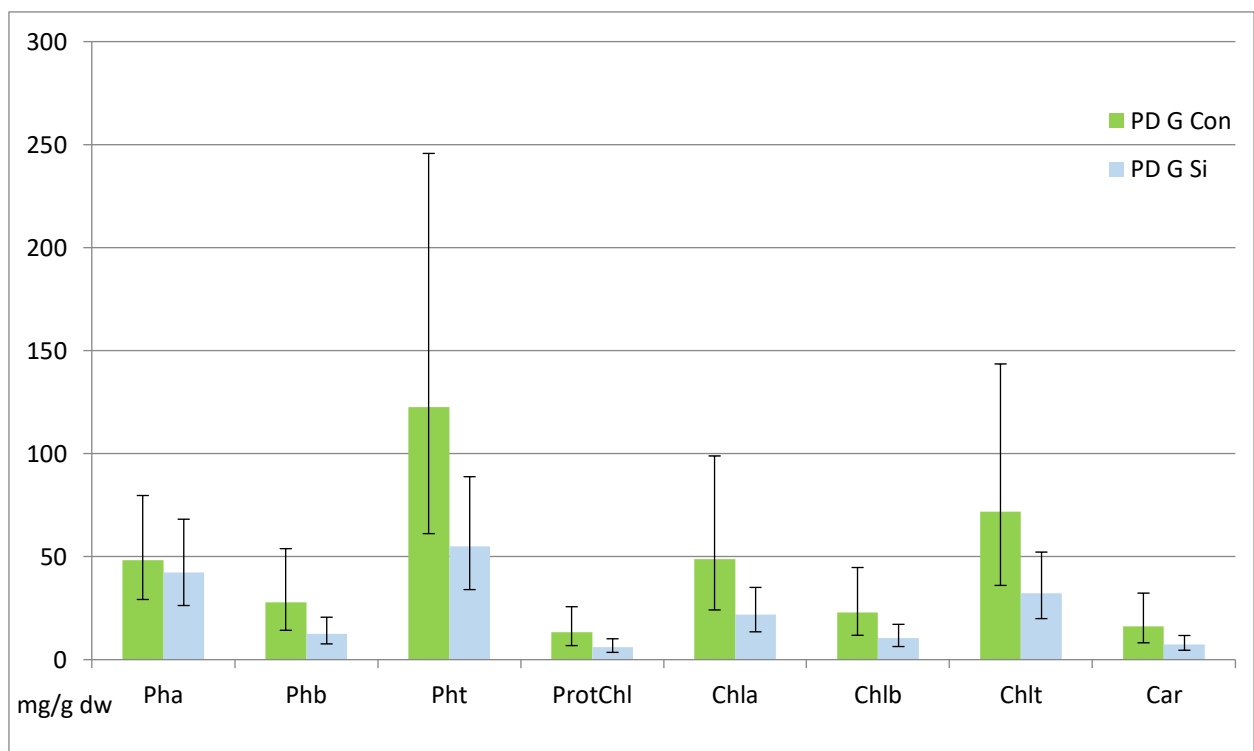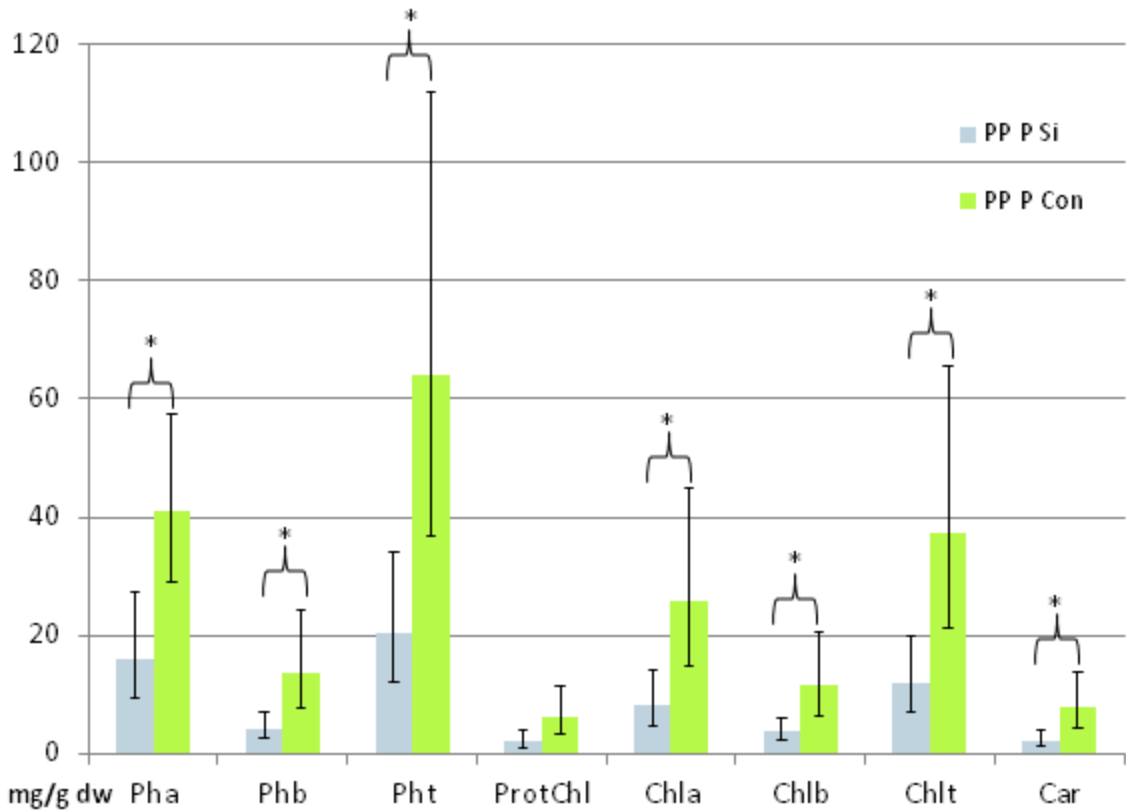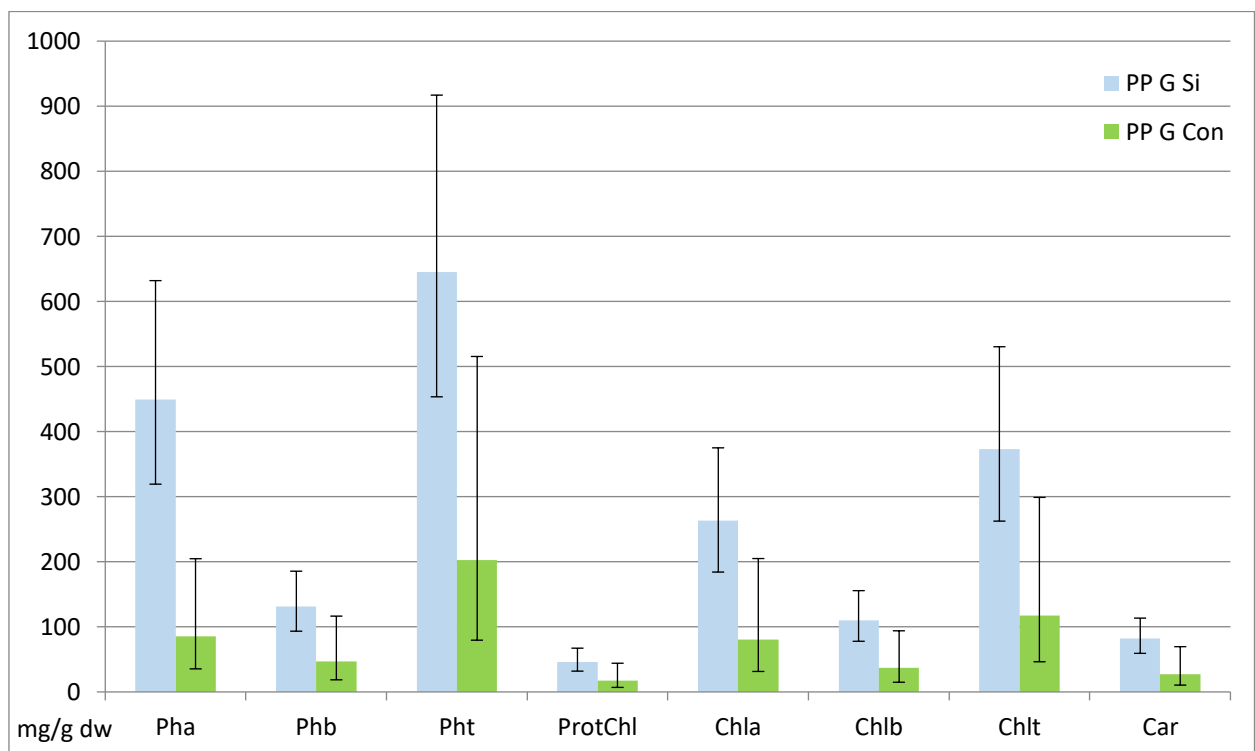

Fig. 13: Pigment content of gametophore (G) of *Physcomitrella patens* (PP). There is a trend towards higher pigment content in Si treated samples. n=10, 2SE.

28

5.1.5 Scanning Electron Microscope & Energy Dispersive X-Ray Microanalysis (SEM EDX)

22 stubs were created and a total of 744 measurements were conducted using SEM EDX. Tab. 13 & 12 summarize the significant differences between the treatments for each species, which are described in detail below.

Tab. 12: Summary of Si and Cu content (wt %) in *Pohlia drummondii*. Con: no added Si, Si: 0.5 mM Si, Cu: $CuCl_2$, G: gametophore, P: protonema. Different letters denote significant difference ($p<0.05$, Tukey HSD).

	Si P	Si G	Si 0.1 mM Cu P	Si 0.1 mM Cu G	Si 1 mM Cu P	Si 1 mM Cu G	Con P	Con G	Con 0.1 mM Cu P	Con 0.1 mM Cu G	Con 1 mM Cu P	Con 1 mM Cu G
Si	0.34 [f]	0.17 [cd]	0.24 [e]	0.22 [de]	0.18 [cde]	0.15 [bc]	0.15 [bc]	0.09 [ab]	0.25 [e]	0.07 [a]	0.15 [bcd]	0.09 [ab]
Cu	0.09 [ab]	0.10 [ab]	0.11 [ab]	0.09 [ab]	0.11 [b]	0.09 [ab]	0.10 [ab]	0.09 [ab]	0.12 [b]	0.11 [b]	0.22 [c]	0.08 [a]

Tab. 13: Summary of Si and Cu content (wt %) in *Physcomitrella patens*. Con: no added Si, Si: 0.5 mM Si, Cu: $CuCl_2$, G: gametophore, P: protonema. Different letters denote significant difference ($p<0.05$, Tukey HSD).

	Si P	Si G	Si 0.1 mM Cu P	Si 0.1 mM Cu G	Si 1 mM Cu P	Con P	Con G	Con 0.1 mM Cu P	Con 0.1 mM Cu G	Con 1 mM Cu P
Si	0.22 [ab]	0.13 [ab]	0.24 [b]	0.11 [ab]	0.14 [abcd]	0.19 [ab]	0.08 [ab]	0.47 [c]	0.07 [a]	0.13 [ab]
Cu	0.13 [a]	0.09 [a]	0.12 [a]	0.11 [a]	0.19 [b]	0.12 [a]	0.10 [a]	0.11 [a]	0.10 [a]	0.21 [b]

Influence of treatment and measured organs on Si and Cu content were analyzed using Type III Sum of Squares in a Multifactor ANOVA setup as well as pairwise comparison of ranked medians using the Mann-Whitney-U test, after an initial Kruskal-Wallis test. Spearman Rank Correlation was also used for data analysis.

5.1.5.1 Si content

EDX-measured Si content in gametophores is significantly influenced by species, Si concentration in the media and measurement site ($p<0.05$, $p<0.001$ and $p<0.05$ respectively; n=363, Fig. 17 & 18). For Si content in protonemata, the only significantly influencing factor is the Cu concentration ($p<0.001$; n=381).

In *P. drummondii* all three factors, measured tissue as well as Si and Cu concentration in the media have significant influence on the Si content of the moss ($p<0.001$ all; n=423). Focusing on the protonemata, both Si and Cu concentration have significant influence on the Si content ($p<0.001$ both; n=205), while only Si concentration remains with significant influence in the gametophores ($p<0.001$; n=218).

There is a significantly higher Si content in *P. drummondii* protonemata, than in gametophores ($p<0.001$; n=223). Si content is significantly lower in 1 mM Cu treated *P. drummondii* protonemata, compared to control and 0.1 mM Cu treated *P. drummondii* protonemata ($p<0.001$; n=133 for both). Si treated protonemata of *P. drummondii* have a significantly higher Si content than untreated samples (p<0.001, Fig. 15). In Si treated *P. drummondii* gametophores, the Si content is significantly higher than in untreated gametophores ($p<0.001$; n=218).

In *P. patens* the factors significantly influencing the Si content are the measured organ and the Cu concentration in the media ($p<0.001$ both; n=321). In *P. patens* protonemata both Si and Cu concentration are still of significant influence on Si content ($p<0.05$, $p<0.001$; n=176), while they have no significant influence in the gametophores.

There is a significantly lower Si content overall in 1 mM Cu treated *P. patens* protonemata, compared to control and 0.1 mM Cu treated *P. patens* protonemata ($p<0.001$; n=104 for both, Fig. 16).

5.1.5.2 *Cu content*

Overall, only Cu concentration in the media has influence on the Cu content in the gametophores ($p< 0.01$; n=363). In protonemata, the species, as well as Si and Cu concentration of the media, have significant influence on the Cu content ($p<0.001$ all; n=381).

In *P. drummondii* all three factors, tissue type, as well as Si and Cu concentration in the media significantly influence the Cu content ($p<0.001$, $p<0.001$, $p<0.01$ respectively; n=423). In *P. drummondii* protonemata, both Si and Cu concentration have significant influence on the Cu content ($p<0.001$ both; n=205; Fig. 14), while in the gametophores only the Cu concentration has significant influence ($p<0.05$; n=218). *P. drummondii* protonemata have a significantly higher Cu content than the gametophores ($p<0.001$; n=223). Concerning protonemata, there also is a significantly lower Cu content in Si treated samples, compared to untreated samples ($p<0.01$; n=205). Focusing on the Cu treatments, the Cu content *of P. drummondii* protonemata is significantly higher in 0.1 mM and 1 mM Cu treated samples, than in the control ($p<0.001$ both; n=144 & n=133 respectively). Additionally, it is significantly higher in 1 mM Cu treated samples compared to the 0.1 mM Cu treated samples ($p<0.01$; n=133). In 1 mM Cu treated *P. drummondii* gametophores the Cu content is significantly lower than in the control or in 0.1 mM Cu treated samples ($p<0.001$; n=146 both).

When comparing the average Si content between the top and bottom measurements on individual phylloids, there is significantly more Si in the top portion than in the base of the phylloids in *P. patens* control samples ($p<0.05$, n=18; Fig. 17). The Cu content, on the other hand, is significantly higher in the base than in the tip in the same samples ($p<0.05$, n=18; Fig. 18).

In *P. patens* Cu content is significantly influenced by the measured organ and the Cu concentration of the media ($p<0.01$, $p<0.001$ respectively; n=321). In *P. patens* protonemata only Cu concentration has significant influence on the Cu content ($p<0.001$; n=176), while in the gametophores no factor has significant influence.

In general, there is a significantly higher Cu content in *P. patens* protonemata, compared to the gametophores ($p<0.001$; n=321). The Cu content in 1 mM Cu treated *P. patens* protonemata is significantly higher than in 0.1 mM Cu treated or control protonemata ($p<0.001$; n=104 for both, Fig. 16).
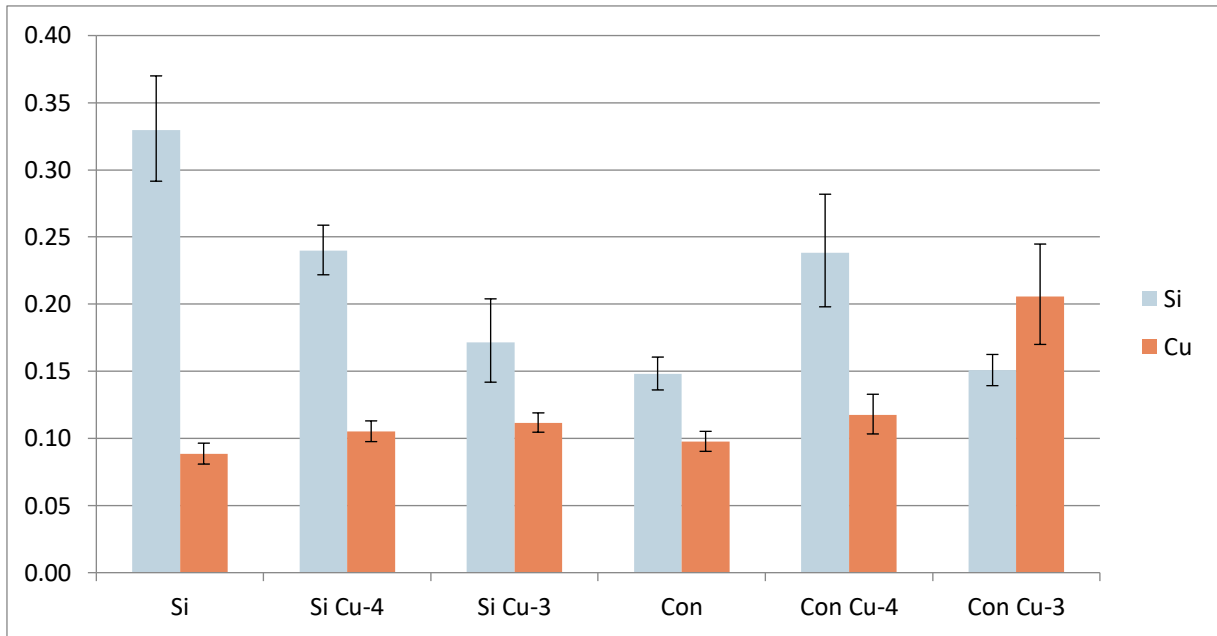
Fig. 14: Si and Cu content (wt %) of *P. drummondii* protonemata. 95% confidence, n=203.
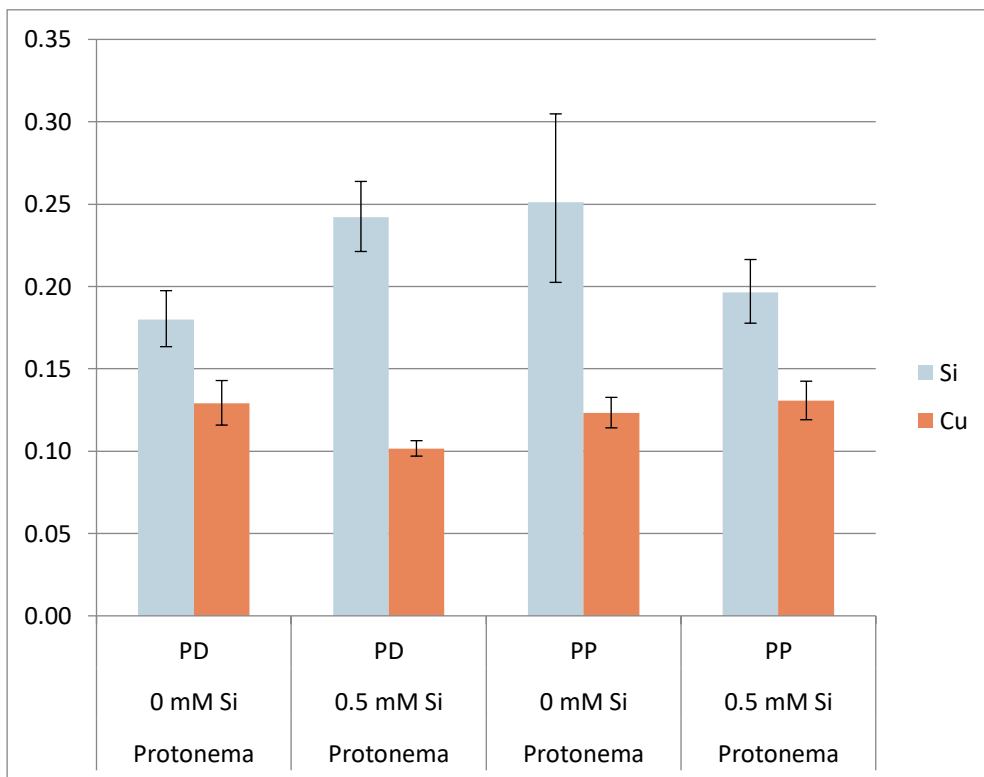

Fig. 15: Si and Cu content in (wt %) of *Pohlia drummondii* (PD) and *Physcomitrella patens* (PP) protonemata, batched by Si concentration in the media. There is a significant difference between Si treated and untreated *P. drummondii* cultures, 95% confidence, n=381.
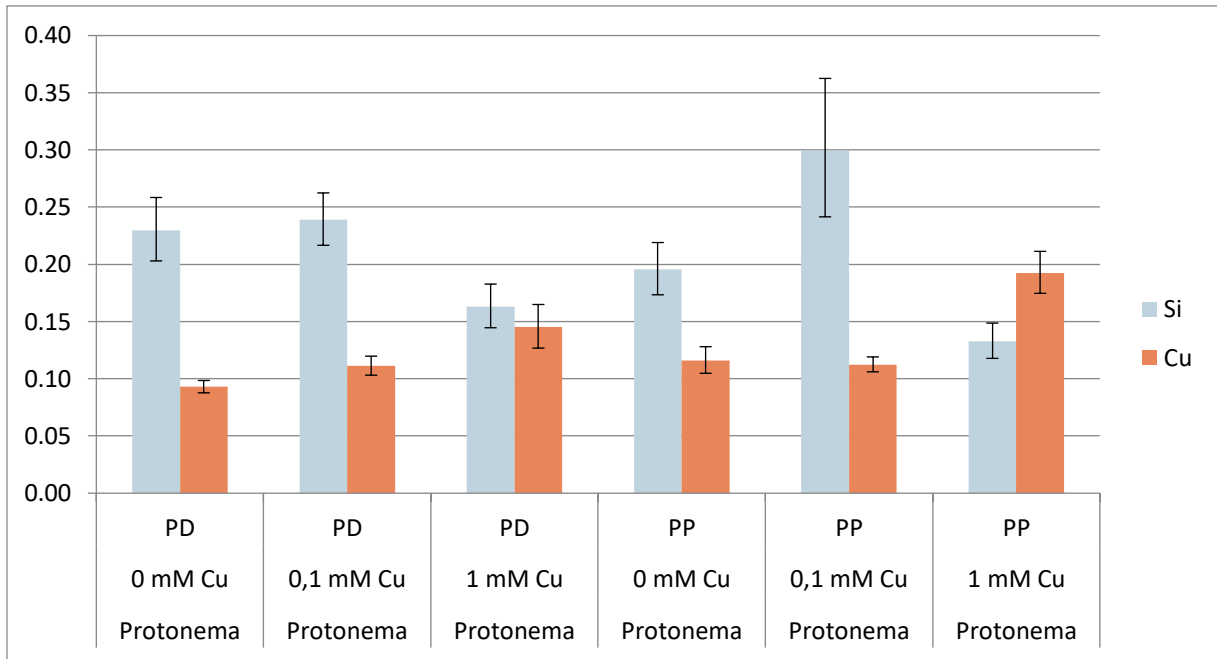
Fig. 16: Si and Cu content (wt %) of *Pohlia drummondii* (PD) and *Physcomitrella patens* (PP) batched by Cu treatment, 95% confidence, n=379.

5.1.5.3 Correlation

There is a significant negative correlation between Cu and Si content in *P. drummondii* protonemata (-0.25; p<0.001). There also is a significant negative correlation between Cu concentration in the media and Si content in protonemata and Si concentration in the media and Cu content in protonemata (-0.25; -0.20; p<0.001 respectively; Tab. 14). Sample size for this setup was 205.

Tab. 14: Spearman Rank Correlation of Si and Cu concentration in the media and measured Si and Cu content in *P. drummondii* protonemata (wt %). P-values are in the white cells, significant values are red; n=205.

	Si [mM]	Cu [mM]	Si_wt%	Cu_wt%
Si [mM]		0.0821	0.3177	-0.1999
		0.2410	0.0000	0.0043
Cu [mM]	0.0821		-0.2595	0.4462
	0.2410		0.0002	0.0000
Si_wt%	0.3177	-0.2595		-0.2541
	0.0000	0.0002		0.0003
Cu_wt%	-0.1999	0.4462	-0.2541	
	0.0043	0.0000	0.0003	

5.1.5.4 Heavy metal Gametophore-Protonema ratio (HM G-P ratio)

The Heavy Metal Gametophore-Protonema ratio (HM G-P ratio) describes the difference in heavy metal content between protonema and gametophore as quotient. A number below 1 suggests excluder behavior and a number above 1 suggests accumulator behavior. The number 1 describes an equal distribution, akin to indicator plant behavior. The average HM G-P ratio for Si in *P. patens* is at 0.38, while for *P. drummondii* it is at 0.56. Most interestingly there were two cases where the Si content differed by a factor of over three. In *P. patens* samples of the 0.1 mM Cu treatment the Si content was almost 6 times higher in the protonemata than in the gametophores. The G-P ratio of this treatment also is significantly lower than in the other treatments (p<0.05; n=36).

Fig. 17: Comparison of Si (wt %) in tip and base of phylloids of both species in Si free treatments. Only in *P. patens* control there is significantly more Si in the top of the phylloid, compared to the bottom. 95% confidence, n=18.
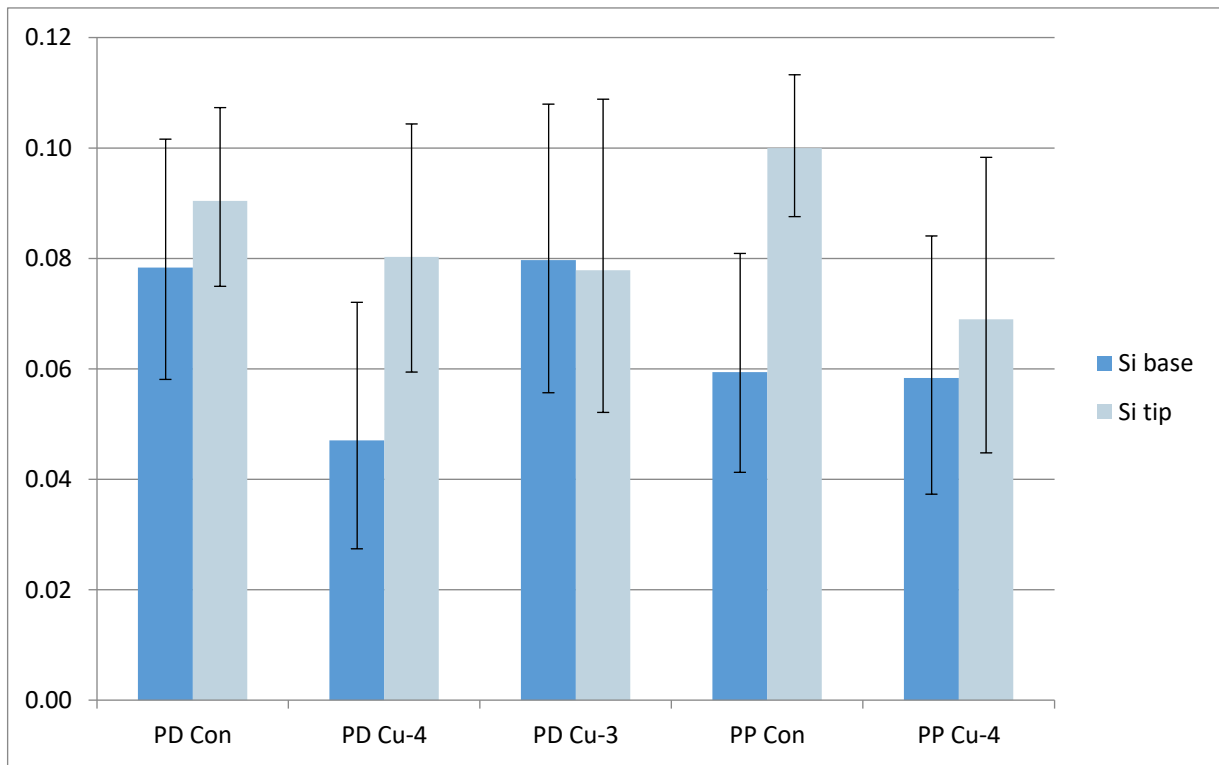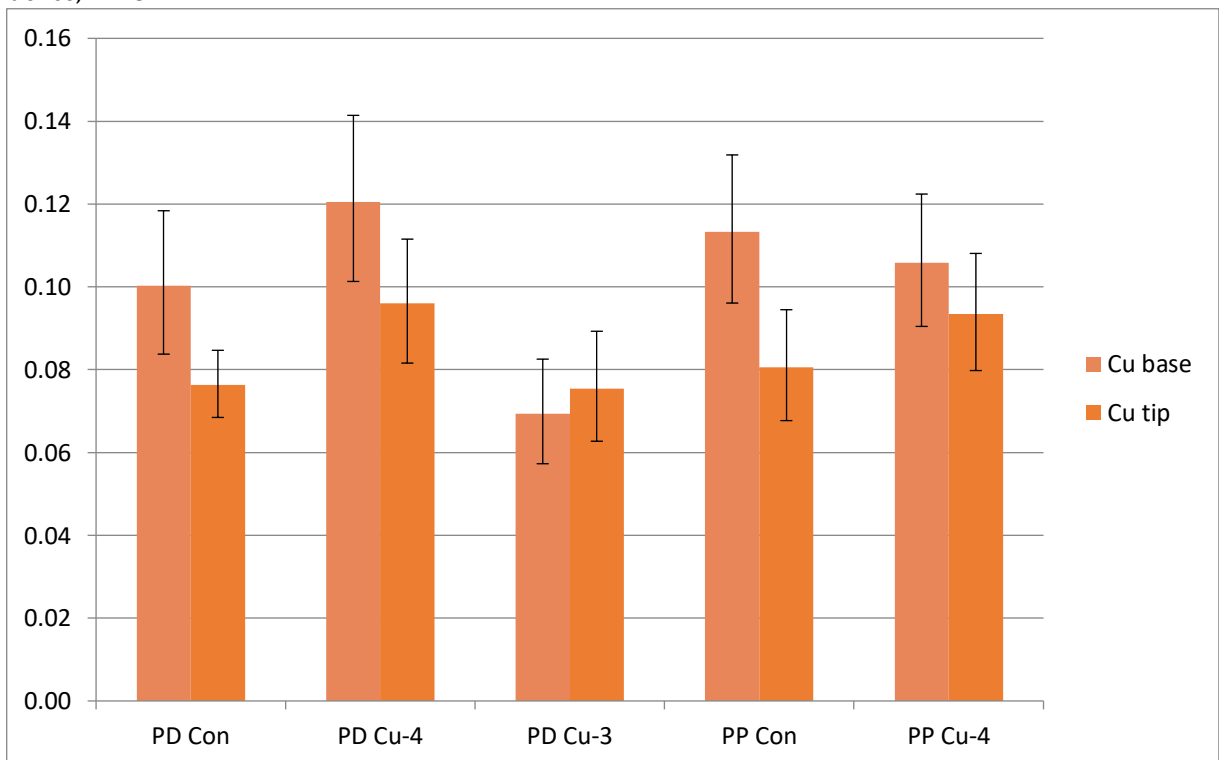

Fig. 18: Comparison of Cu (wt %) in tip and base of phylloids of both species in Si free treatments. Only in *P. patens* control there is significantly more Cu in the bottom than in the top of the phylloid. 95% confidence, n=18

Similarly, the Si content was almost 4 times higher in the protonemata of *P. drummondii* in the Cu-4 treatment and the G-P ratio was significantly lower than in the control ($p<0.001$; n=18). The G-P ratio for Si is significantly higher in Si and Cu treated samples compared to only Cu treated samples, only Si treated samples and the control ($p<0.001$; n=51).

The average G-P ratio for Cu *in P. patens* is 0.86, while in *P. drummondii* it is 0.8. There is only a single case, Con-3, where the Cu content in the protonemata is almost three times as high as in the gametophores. The G-P ratio of Con-3 for Cu in *P. drummondii* is significantly lower, than in the control ($p<0.01$). More details can be found in Tab. 15.

Tab. 15: Average G-P ratios for Si and Cu (wt %) in both species. Low values refer to higher accumulation in protonemata compared to the gametophores. PP: *P. patens*, PD: *P. drummondii*.

PP Treatment	Si	Cu	PD Treatment	Si	Cu
Con	0.41	0.83	Con	0.57	0.90
Si	0.47	0.77	Si	0.46	1.09
0.1 mM Cu	0.17	0.92	0.1 mM Cu	0.26	0.90
Si 0.1 mM Cu	0.47	0.91	Si 0.1 mM Cu	0.82	0.84
			1 mM Cu	0.52	0.35
			Si 1 mM Cu	0.71	0.71

5.1.5.5 Minteq simulation

According to a simulation using the Minteq software, with the calculated ion contents of the media and the pH of 5.8, 18.6% of the Cu (~18.6 µM) were plant available in the 0.1 mM $CuCl_2$ media. 1% was bound as $CuSO_4$ and 80.3% as Cu-tartrate. For the 1 mM $CuCl_2$ media, the amount of free Cu ions was estimated to be 23.4% (~234.2 µM), while 1.3% were bound as $CuSO_4$ and 75.3% as Cu-tartrate. Addition of sodium orthosilicate did not influence the Cu-ion balance.

5.1.6 Cell measurements

5.1.6.1 Protonema

In general *P. patens* protonema cells were both significantly longer and wider than *P. drummondii* protonema cells ($p<0.001$ both).

Average cell length in protonemata of *P. drummondii* varied a lot, ranging from 49.8 µm in combined 1 mM Cu and Si treatment to 92.3 µm in the Si treatment. It decreased significantly with increase of Cu concentration ($p<0.001$ all), except when comparing the Si treatment and the combined 0.1 mM Cu-Si treatment. Si treatment led to significantly longer cells in both Cu-free ($p<0.01$) and 0.1 mM Cu treatment ($p<0.001$). Average cell width in *P. drummondii* protonemata ranged from 12.8 µm in Si free 1 mM Cu treatment, to 17.5 µm in Si treatment. The Cell width of the protonema cells was significantly lower in combined 0.1 mM Cu-Si treatment ($p<0.05$) compared to Si free 0.1 mM Cu treatment. On the other hand, it was significantly higher in combined 1 mM Cu-Si treatment ($p<0.001$) compared to the Si free version (Fig. 20). The average cell surface in *P. drummondii* varied between 2277 µm^2 in the combined 1 mM Cu and Si treatment and 5644 µm^2 in the Si treatment. The surface of *P. drummondii* protonema cells was significantly higher in samples of the Si treatment, compared to the control ($p<0.001$). Similarly cells of the combined 0.1 mM Cu and Si treatment had significantly higher surface area than the ones treated only with 0.1 mM Cu ($p<0.001$). Concerning Cu treatment, the 1 mM Cu treated *P. drummondii*

protonema cells had significantly smaller cell surface area than the 0.1 mM Cu treatment and control ($p<0.001$ both). In combination with Si, *P. drummondii* protonema cells without additional Cu were significantly bigger in cell surface area than both 0.1 mM and 1 mM Cu treated samples ($p<0.001$ both) and the 0.1 mM Cu treated ones were also significantly bigger than the combined 1 mM Cu and Si treatment ($p<0.001$).

In *P. patens* cell length was more stable, ranging between 93.2 µm in the combined 1 mM Cu and Si treatment and 105.6 µm in the combined 0.1 mM Cu and Si treatment. Cell width varied between 18.0 µm in combined 1 mM Cu and Si treatment and 22.7 µm in Si treatment. Si treatment led to significantly wider protonema cells in both species, if no Cu was involved ($p<0.001$), while in combination with 1 mM Cu it led to significantly shorter cells in *P. patens* protonemata ($p<0.01$). For *P. patens*, the average cell surface ranged from 6583 µm² in the combined 1 mM Cu and Si treatment and 8179 µm² in the Si treatment. The cell surface area of Si treated cells was significantly bigger than the surface of the control group ($p<0.001$). The opposite was the case at a Cu concentration of 1 mM ($p<0.01$). The combined treatment of 1 mM Cu and Si also had a significantly lower cell surface area than both the combination of 0.1 mM Cu and Si and Si treatment alone ($p<0.001$ both). In 0.1 mM Cu the cell surface area was significantly bigger than in the 1 mM Cu treatment ($p<0.01$). A summary using interaction plots can be found in Fig. 19, a summary in numbers in Tab. 16.
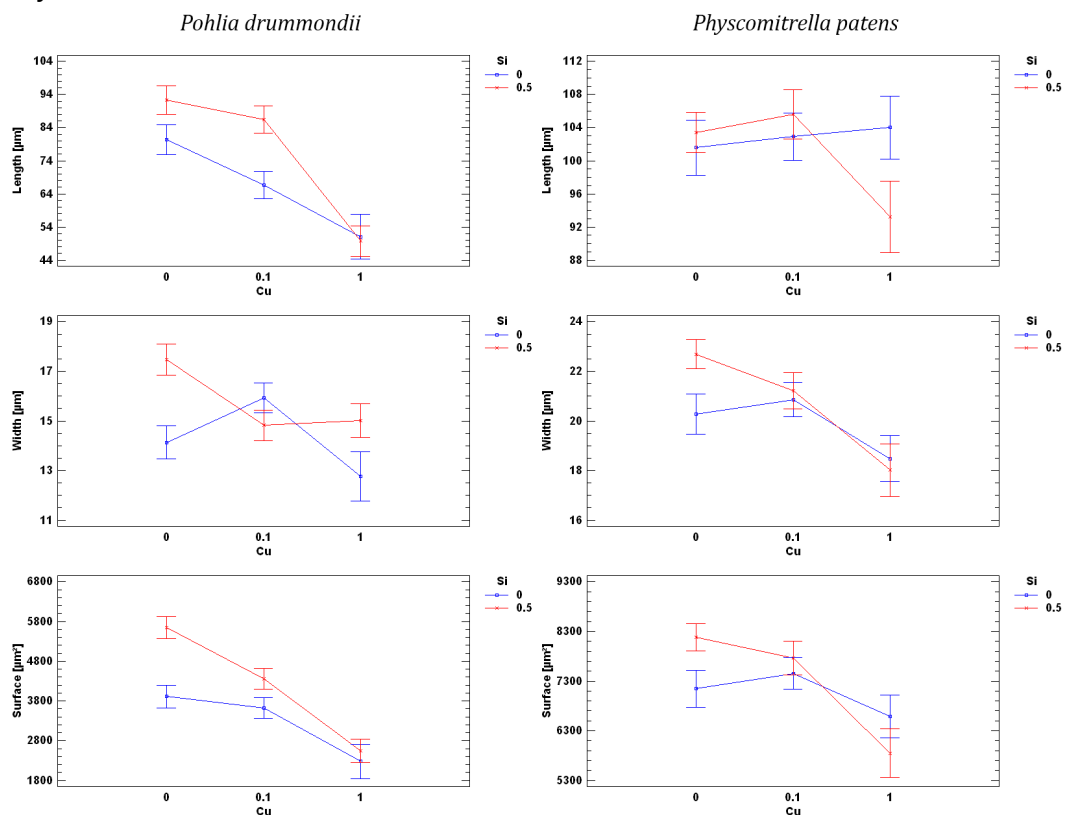
Fig. 19: Interaction plots for Si and Cu concentration (mM) in the media and cell length, width and surface for *P. drummondii* and *P. patens* protonemata, n= 670 and n=806 respectively, 95% confidence Tukey HSD.
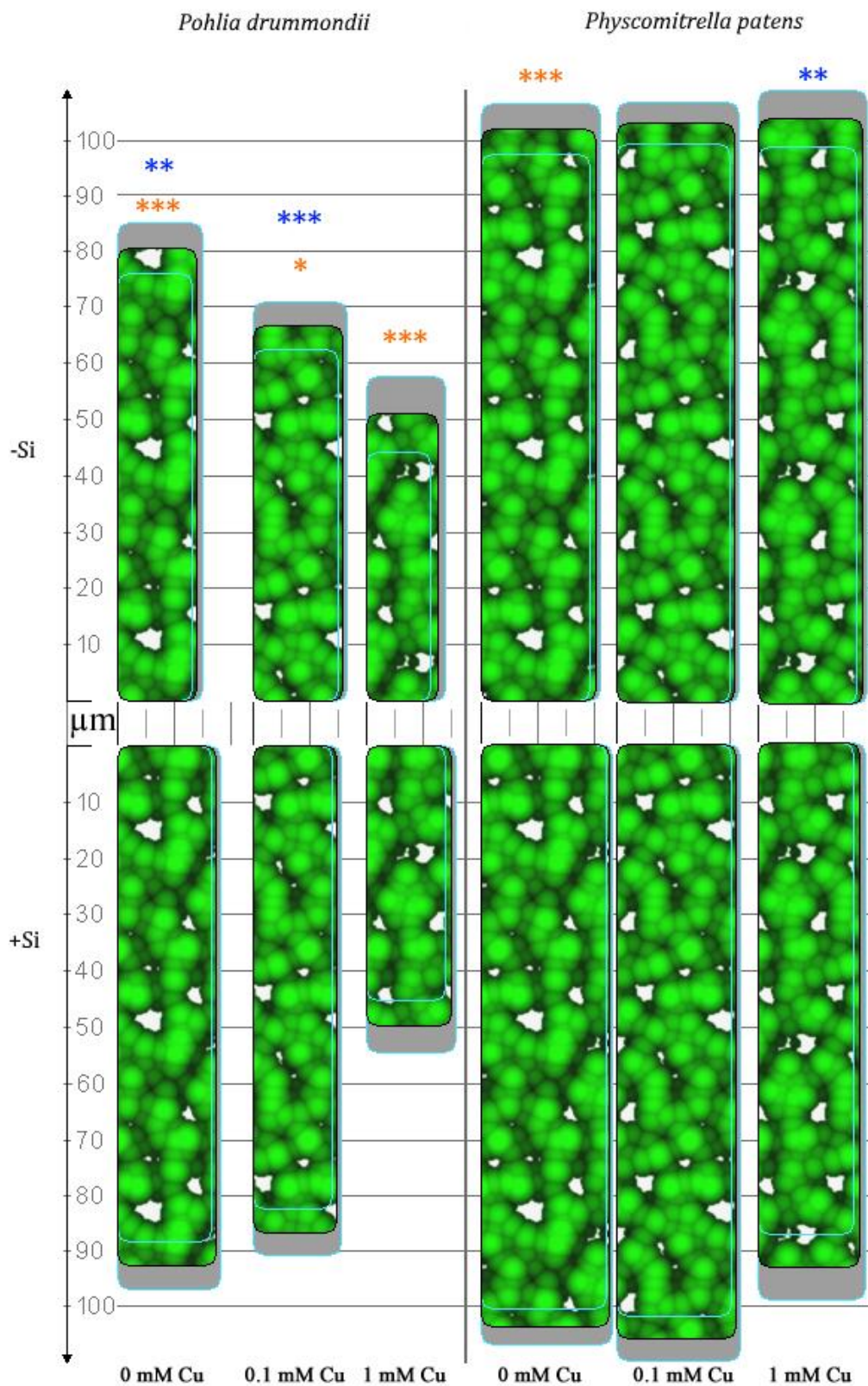
Fig. 20: Comparison of protonema cell size. Blue asterisks denote significant difference in length, orange asterisks denote significant difference in width when comparing medians (Mann Whitney U test) between Si treated and not Si treated counterparts, Cyan frames visualize 95% interval. n>60.

Tab. 16: Average of length, width, surface and volume (µm, µm² and µm³ cylindrical approximation) of protonema cells of both species. Con: no added Cu or Si, Si: 0.5 mM sodium-orthosilicate, Cu: CuCl$_2$, PD: *Pohlia drummondii*, PP: *Physcomitrella patens*. Different letters denote significant difference over both species ($p<0.05$, Tukey HSD).

	PD Si	PD Si 0.1 mM Cu	PD Si 1 mM Cu	PD Con	PD 0.1 mM Cu	PD 1 mM Cu
Length	92.3[d]	86.5[cd]	49.8[a]	80.4[c]	66.7[b]	51.1[a]
Width	17.5[de]	14.8[abc]	15.0[bc]	14.1[ab]	15.9[cd]	12.8[a]
Surface	5644[d]	4365[c]	2547[a]	3910[bc]	3615[b]	2277[a]
Volume	23705[c]	15708[b]	7962[a]	13210[ab]	12740[ab]	6475[a]
	PP Si	PP Si 0.1 mM Cu	PP Si 1 mM Cu	PP Con	PP 0.1 mM Cu	PP 1 mM Cu
Length	103.4[f]	105.6[f]	93.2[de]	101.6[ef]	102.9[ef]	104.0[ef]
Width	22.7[h]	21.2[g]	18.0[e]	20.3[fg]	20.9[g]	18.5[ef]
Surface	8179[h]	7767[gh]	5848[de]	7147[fg]	7456[g]	6583[ef]
Volume	43215[f]	38832[ef]	25081[c]	34307[de]	36842[e]	28457[cd]

Tab. 17: Spearman Rank Correlation of Si and Cu concentration in the media and measured protonema cell length and width in *P. drummondii*. P-values are in the white cells; significant values are red; n=806.

|	Si	Cu	Length [µm]	Width [µm]
Si		-0.1829	-0.0003	0.1558
		0	0.9937	0
Cu	-0.1829		-0.0097	-0.2612
	0		0.7824	0
Length [µm]	-0.0003	-0.0097		-0.0112
	0.9937	0.7824		0.7498
Width [µm]	0.1558	-0.2612	-0.0112	
	0	0	0.7498	

Tab. 18: Spearman Rank Correlation of Si and Cu concentration in the media and measured protonema cell length and width in *P. patens*. P-values are in the white cells; significant values are red; n=670.

	Si	Cu	Length [µm]	Width [µm]
Si		0.1012	0.1591	0.1565
		0.0089	0	0.0001
Cu	0.1012		-0.4472	-0.1502
	0.0089		0	0.0001
Length [µm]	0.1591	-0.4472		-0.1015
	0	0		0.0087
Width [µm]	0.1565	-0.1502	-0.1015	
	0.0001	0.0001	0.0087	

Additionally, cell width and cell length were correlated to Si and Cu concentration in the media using Spearman Rank Correlation, separately for both species (Tab. 17 & 18). In *P. drummondii* protonemata, cell width was significantly correlated with Si concentration (0.16, $p<0.001$), but significantly negative correlated with Cu (-0.26, $p<0.001$). In *P. patens* both length and width of the protonema cells are significantly positive correlated with the Si concentration of the media (0.16, $p<0.001$ both). Cell length and width also are significantly negative correlated with the Cu concentration (-0.45 and -0.15 respectively, both $p<0.001$).

5.1.6.2 Gametophore

Generally, *P. patens* gametophore cells were wider than the ones of *P. drummondii*, when comparing the same treatments, but for cell length the opposite was true ($p<0.001$ all; with exception of length in control: $p< 0.01$).

The length for gametophore cells in *P. drummondii* varied between 41.6 µm in the control group and 72.9 µm in the Si treated samples. The cell width in *P. drummondii* ranged from 11 µm in control samples to 17.8 µm in 0.1 mM Cu treated samples. Both treatment with Si and Cu individually increased the cell length in *P. drummondii* significantly ($p<0.001$ all). Combined Si and Cu treatment, on the other hand, led to slightly shorter cells than Si alone ($p<0.01$ for 1 mM Cu and $p<0.001$ for 0.1 mM Cu). The Si treatment also led to a significant increase in cell width, compared to the control ($p<0.001$). Similarly, the 0.1 mM Cu treatment led to a significant increase in cell width compared to control ($p<0.001$).

For *P. patens* cell length ranged from 46.6 µm in control to 56.6 µm in 0.1 mM Cu treatment.

Cell width in *P. patens* it was rather stable with 18.9 µm in both Si and combined Si and 0.1 mM Cu treatment and 20.2 µm in the control. Since the 1 mM Cu concentration inhibited the moss from developing gametophores, there is no data on those cells.

In *P. patens* both Cu and Si treatment increased the cell length, similar to *P. drummondii* ($p< 0.001$ and $p<0.01$ respectively) and there is no significant difference from the combined treatment to the individual treatments, except when comparing to the significantly shorter control cells ($p<0.001$). The only significant difference in cell width is between control and Si treatment, where control cells are significantly wider ($p<0.01$).

Since gametophore cells cannot be described geometrically as easily as protonema cells, there is no data on surface and volume. Fig. 21 describes the data as interaction plot, while Fig. 22 illustrates the average cell size for comparison. Tab. 19 summarizes the data numerically.
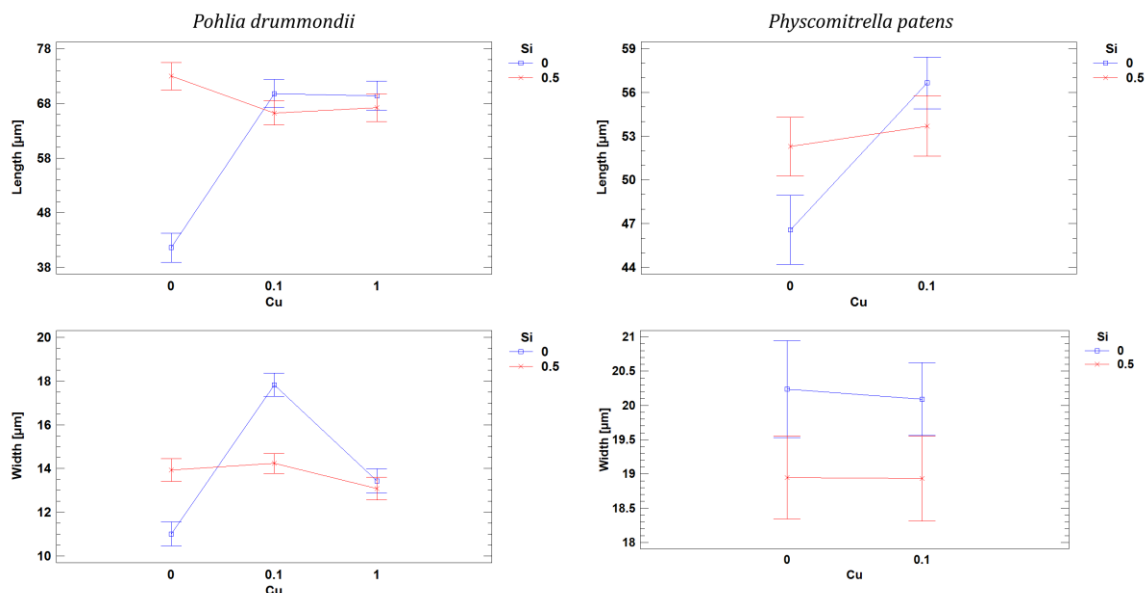
Fig. 21: Interaction plots for Si and Cu concentration (mM) in the media and cell length and width for *P. drummondii* and *P. patens* gametophore, n= 1066 and n=636 respectively, 95% confidence Tukey HSD.
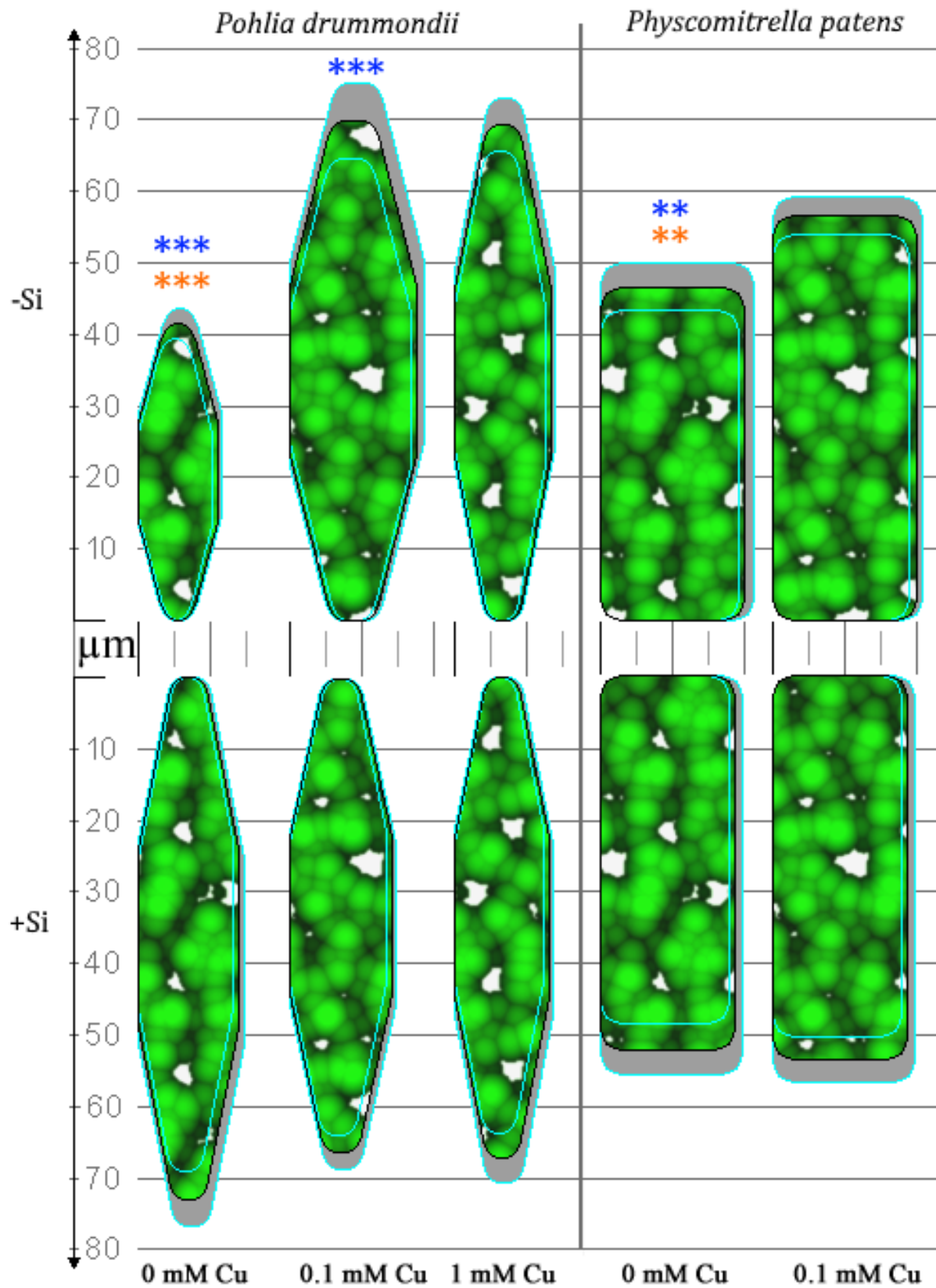
Fig. 22: Comparison of gametophore cell size. Blue asterisks denote significant difference in length, orange asterisks denote significant difference in width when comparing medians (Mann Whitney U test) between Si treated and not Si treated counterpart, Cyan frames visualize 95% interval. n>116.

Tab. 19: Average of length and width (μm) in gametophore cells of both species. Con: no added Si, Si: 0.5 mM Si, Cu-4: 0.1 mM CuCl$_2$, Cu-3: 1 mM CuCl$_2$, PD: *Pohlia drummondii*, PP: *Physcomitrella patens*. Different letters denote significant difference ($p<0.05$, Tukey HSD).

	PD Si	PD Si Cu-4	PD Si Cu-3	PD Con	PD Con Cu-4	PD Con Cu-3
Length	72.9[e]	66.2[d]	67.2[d]	41.6[a]	69.8[de]	69.3[de]
Width	13.9[b]	14.2[b]	13.1[b]	11.0[a]	17.8[c]	13.4[b]
	PP Si	PP Si Cu-4	PP Si Cu-3	PP Con	PP Con Cu-4	PP Con Cu-3
Length	52.3[bc]	53.7[c]		46.6[ab]	56.6[c]	
Width	18.9[cd]	18.9[cd]		20.2[d]	20.1[d]	

Tab. 20: Spearman Rank Correlation of Si and Cu concentration in the media and measured gametophore cell length and width in *P. drummondii*. P-values are in the white cells; significant values are red; n=1066.

	Si	Cu	Length [μm]	Width [μm]
Si		0,004	0,2534	-0,0247
		0,8966	0	0,42
Cu	0,004		0,2333	0,0854
	0,8966		0	0,0053
Length [μm]	0,2534	0,2333		0,25
	0	0		0
Width [μm]	-0,0247	0,0854	0,25	
	0,42	0,0053	0	

Tab. 21: Spearman Rank Correlation of Si and Cu concentration in the media and measured gametophore cell length and width in *P. patens*. P-values are in the white cells; significant values are red; n=636.

	Si	Cu	Length [μm]	Width [μm]
Si		-0,1534	-0,0121	-0,1245
		0,0001	0,7604	0,0017
Cu	-0,1534		0,208	0,0024
	0,0001		0	0,951
Length [μm]	-0,0121	0,208		0,0665
	0,7604	0		0,0936
Width [μm]	-0,1245	0,0024	0,0665	
	0,0017	0,951	0,0936	

In *P. drummondii* both Si and Cu are significantly correlated with cell length (0.25 and 0.23 respectively, both *p*<0.001) and cell length and cell width are also correlated (0.25, *p*<0.001; Tab. 20). In general, the influence on the gametophore cell length is stronger, than on the protonema cells and for the cell length/width correlation it is inverted from negative to positive. Also, there is no influence on the cell width by Si, compared to the protonema cells.

In *P. patens* there is a slight negative correlation between Si and gametophore cell width (-0.12, *p*<0.01) and a positive correlation between Cu and cell length (0.21, *p*<0.001; Tab. 21). In this case the correlative influence of Cu on cell length and Si on cell width was inverted, when comparing the different tissues.

5.2 Silicon and UV-B

5.2.1 Biomass

The highest gain in biomass for *P. drummondii* occurs in the combined Si and UV treated samples, both for dishes and individual explants. The control on the other hand gained the least biomass for this species and did way worse than the control plants in the previous, heavy metal focused, experiment. They also lacked gametophores, the reasons for this will be discussed later. In *P. patens* control and combined Si and UV treatment are at about the same level, with a high gain of biomass, while UV or Si treatment on their own led to comparably little growth. More details can be found in Fig. 23 & Tab. 22.
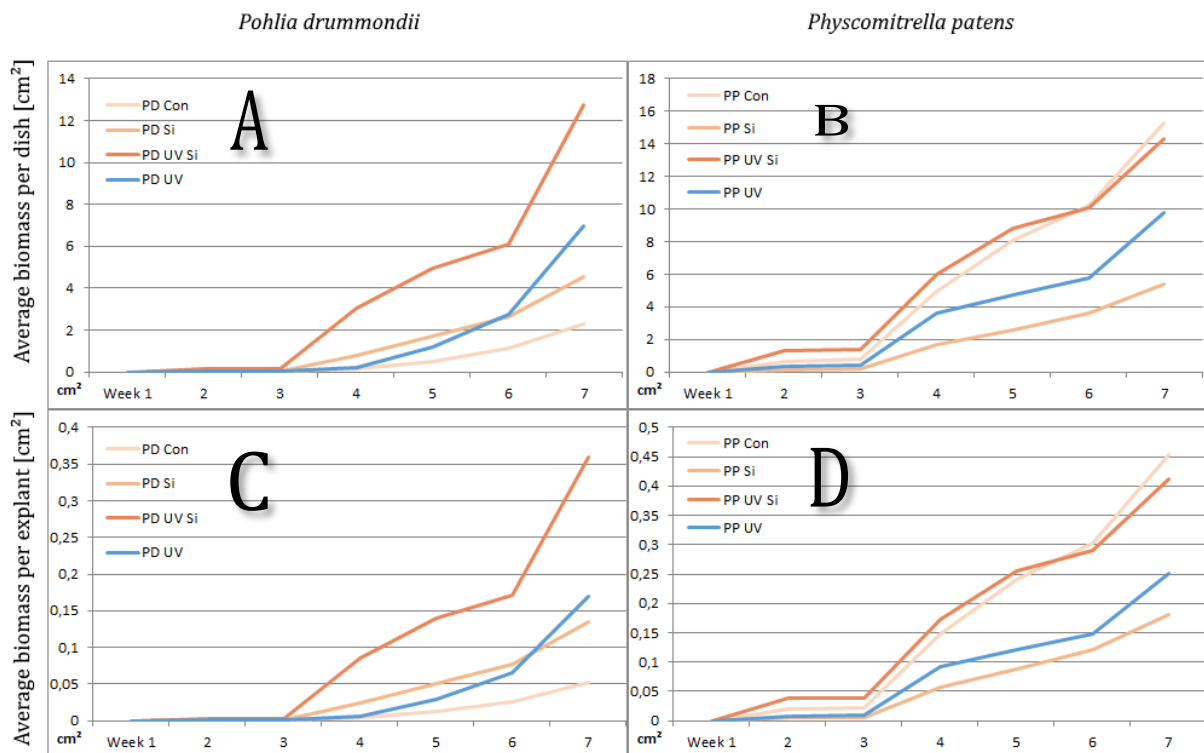
Fig. 23: Biomass increase over time in both mosses, visualized in cm^2, as average over the dishes (A, B; n=1-3) and as average of the individual explants (C, D; n=29-43).

Tab. 22: Mean values for biomass in cm^2 for both species, for dishes and individual cultures ± Standard error; n=1-3, n=29-43.

	PD Con	PD Si	PD UV Si	PD UV	PP Con	PP Si	PP UV Si	PP UV
dish	2.27 ± 0.63	4.53 ± 0.57	12.75 ± 2.54	6.98 ± 0.26	15.28 ± 4.05	5.39 ± 1.05	14.31 ± 3.45	9.80
culture	0.05	0.13	0.36	0.17	0.45	0.18	0.41	0.25
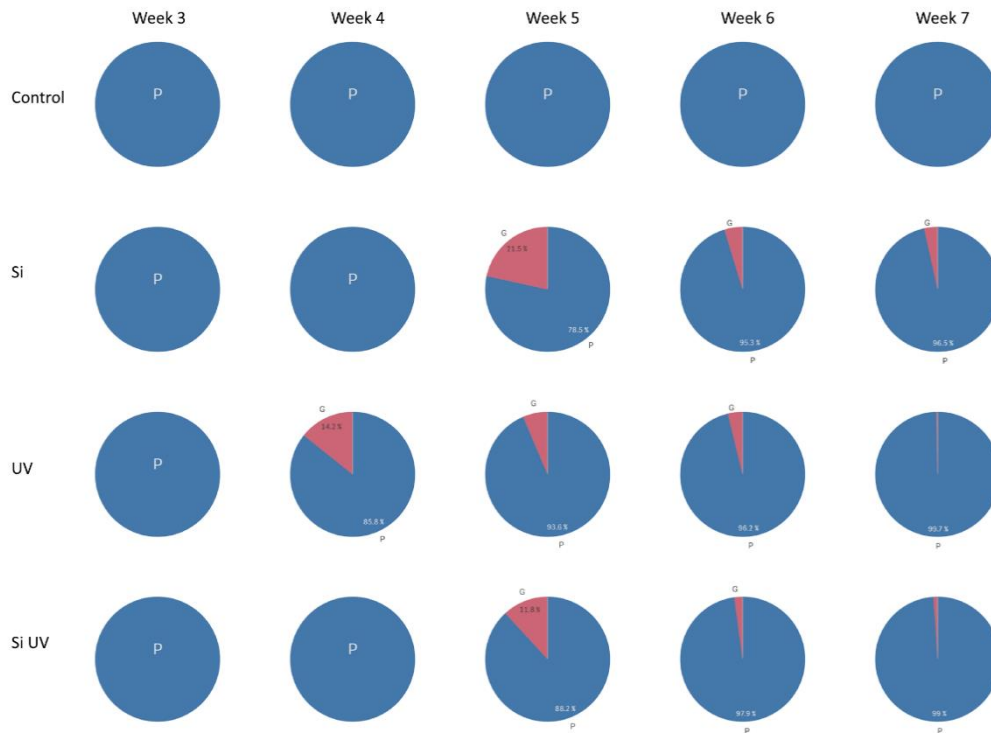
Fig. 24: Pie-charts for all treatments and time points of *P. drummondii*, visualizing the ratio between protonemata (P, blue) and gametophores (G, red). Gametophores start developing in week 4, before UV treatment actually started and week 5 for the other samples with exception of the control treatment. Due to strong protonemal growth the gametophore portion diminishes over time; n=1-3.
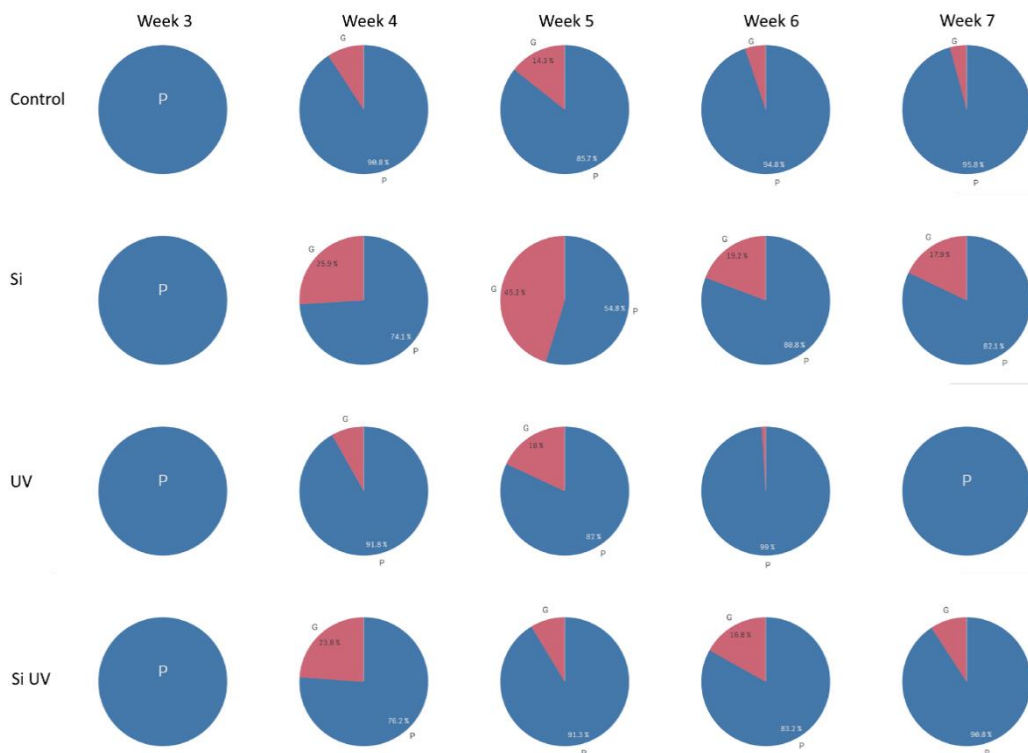
Fig. 25: Pie-charts for all treatments and time points of *P. patens*, visualizing the ratio between protonemata (P, blue) and gametophores (G, red). Gametophores start developing in week 4, especially strong in the two Si treatments. Due to strong protonemal growth the gametophore portion diminishes over time; n=1-3.

5.2.2 Gametophore – Protonema Ratio

The highest amount of developed gametophores was found after 5 weeks in *P. drummondii* Si treatment with 21.5% coverage. The samples of the UV and Si UV treatment also developed gametophores, but only 14.2% (week 4) and 13.8% (week 5) respectively. The ratio declined till the end of the experiment and the control plants never developed gametophores (Fig. 24).

In case of *P. patens* all cultures developed gametophores starting from week 4 onwards. The highest coverage by far was observed in the Si treatment at week 5 with 45.2%. Generally, the Si treated plants showed higher coverage with 25.9% and 23.8%. Also, their coverage ratio didn't decline as much as for the other treatments, still reaching 10% at the end of the experiment. Compared with the not UV treated counterparts the UV treated samples have developed less gametophores (Fig. 25).

5.2.3 Reactive oxygen species (ROS)

5.2.3.1 *Nitrotetrazolium blue chloride (NBT)*

NBT staining, which visualizes on oxygen radicals, did not reveal any measurable staining in *P. patens*, as only the very tips were blue and there was hardly any staining in the *P. drummondii* treatments with exception of control and silicon treatment (Fig. 26).

5.2.3.2 *3, 3'-diaminobenzidine (DAB)*

Compared to the NBT staining, DAB staining detects H_2O_2 for ROS quantification. In general, *P. patens* was more stained with DAB than *P. drummondii* (p<0.001). According to Type III Sum of Squares, there is a significant influence of the UV treatment (p<0.01, n=57) leading to lower staining in *P. drummondii*, independent from silicon treatment (Fig. 27). No similar effect was found in *P. patens*.
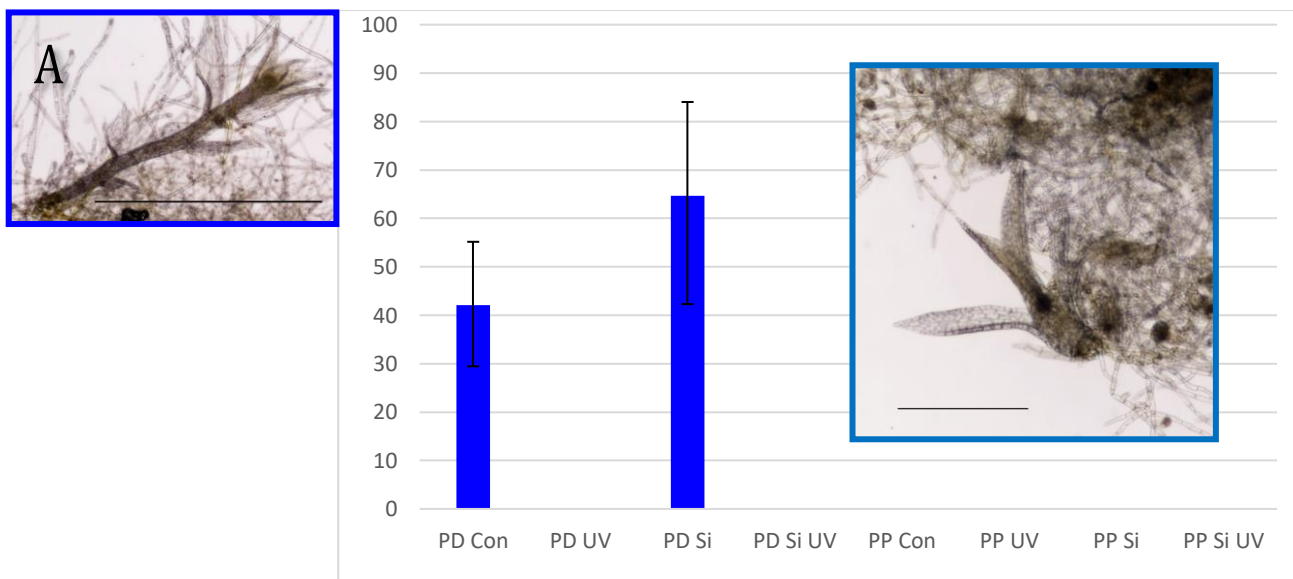
Fig. 26: Summary of NBT staining, almost no staining at all, especially in *P. patens*, no significant difference between *P. drummondii* control and Si treatment. n=4-20, A: *P. drummondii* Si, B: *P. patens* Si, bar of images: 200 μm.
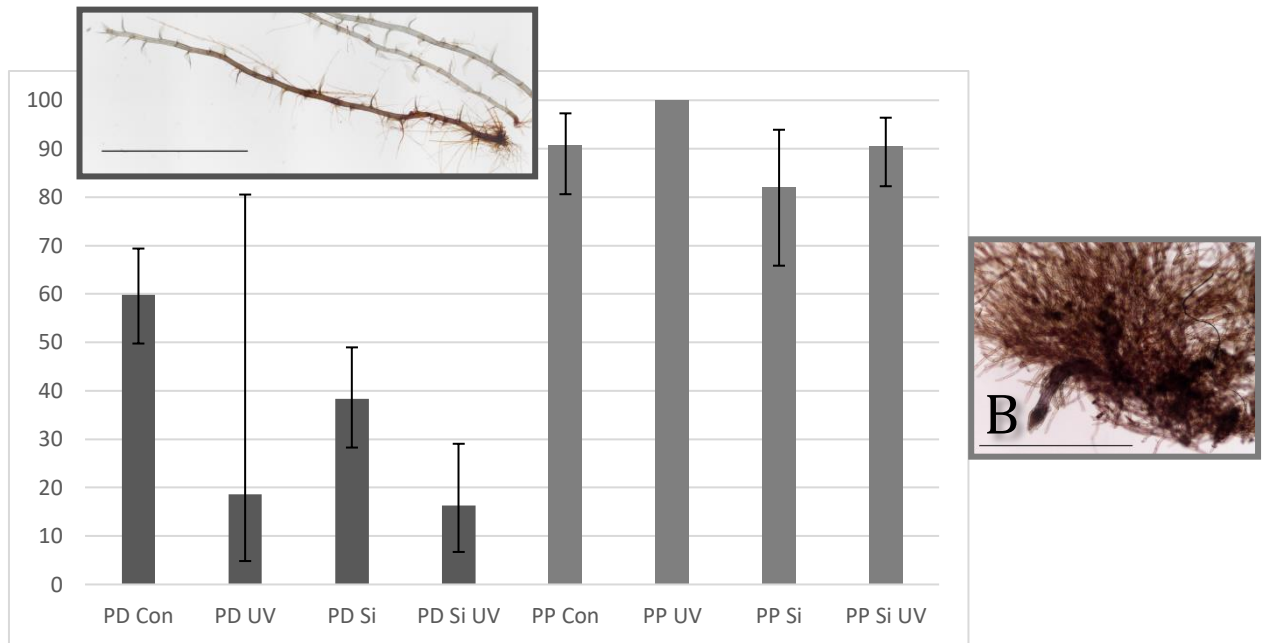
Fig. 27: Summary of DAB staining, no significant difference between the Si treated and untreated counterparts n=2-36, A: *P. drummondii* Si UV, B: *P. patens* UV, bar of images: 800 and 200 μm.
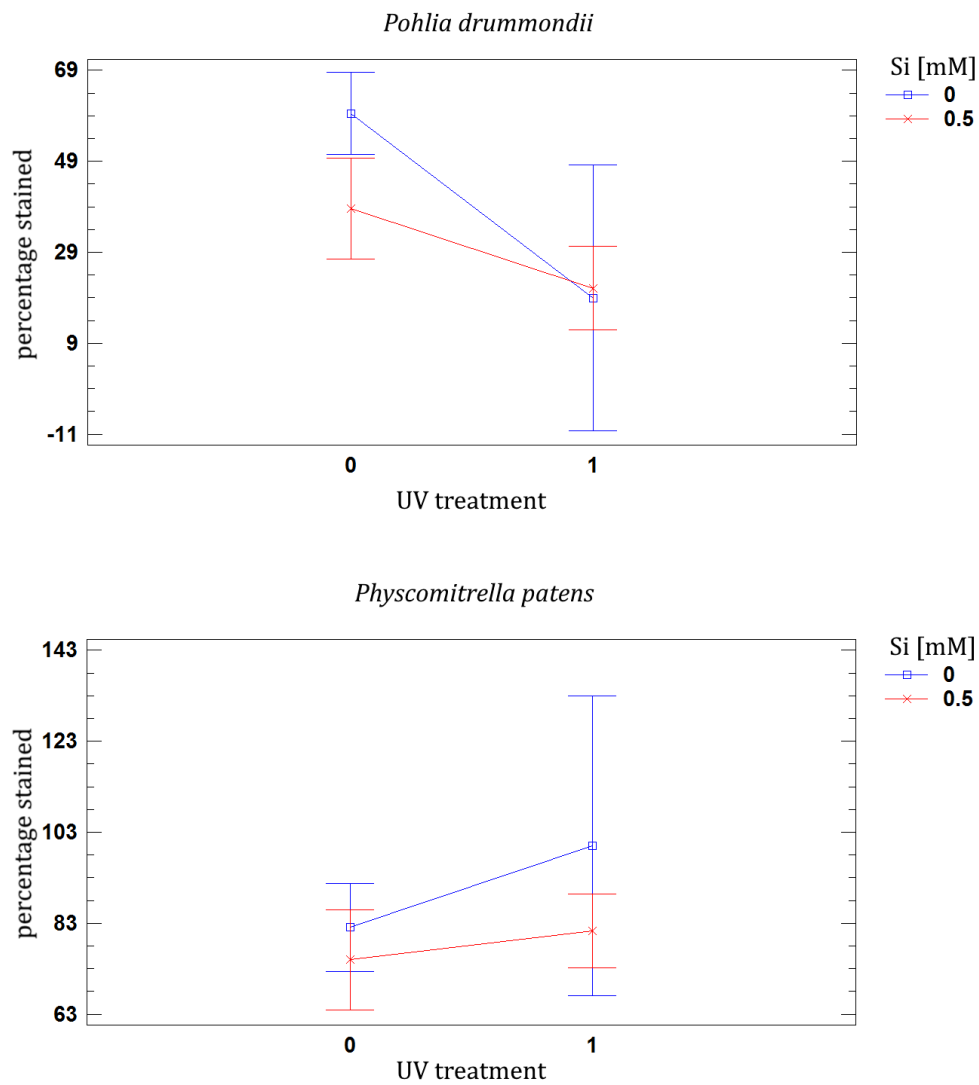
Fig. 28: Interaction plot with 95% Tukey-HSD-Intervals, illustrating the difference of DAB staining in the different treatments as connected data points; for *P. drummondii* n=57, *for P. patens* n=76.

44

5.2.4 Pigment analysis

The content of *pheophytin a & b*, *total pheophytin*, *protochlorophyll*, *chlorophyll a & b, total chlorophyll*, as well as *carotenoids* was spectrophotometrically measured to investigate plant health. Due to lack of formulae for *pheophytin* and *protochlorophyll* content in DMSO, only *chlorophylls* and *carotenoid* contents were calculated. A total of 72 extracts were produced, half using DMF and the other half using DMSO as solvents. They were measured alongside multiple blanks of pure solvent, to adjust for changes during the 105-minute procedure. Due to the low amount of sample material and resulting error, no statistical analysis was performed.

While *P. drummondii* DMF extracts only allowed for analysis of control and UV treated protonemata, the UV treated sample contained about as much of the respective pigments, as the best *P. patens* sample (Fig. 29 A, C, E-H) or even more, like in case *pheophytin b* and *protochlorophyll* (Fig. 29 B & D). The difference in pigment content in the DMSO extracts of the differently treated samples was minute, but Si treated protonemata always had the lowest and Si & UV treated samples the highest pigment content (Fig. 30 A-D).

The highest average content of many pigments in *P. patens* was found in the control samples of gametophores in both solvents (Fig. 29 A, C, E-H, Fig. 30 A-D). For *pheophytin b* and *protochlorophyll* the highest content was calculated for the Si and UV treated protonemata (Fig. 29 B & D). In some cases, there was a higher pigment content in the DMSO extracts, than in the DMF extracts. In the few measurements of DMF extracts the content of pigments was higher in the UV treated protonemata samples of *P. drummondii*, compared to *P. patens*, the opposite was true in the DMSO extracts for *chlorophylls* and *carotenoids*.

Calculation of phaeophytinisation quotient, based on DMF extracts, showed, that despite the difference in treatments, there was no significant difference in phaeophytinisation with a value of about 1.45 overall (Tab. 23). According to the standard table presented by Ronen and Galun (1984, Tab. 3), there was no acidification of pigments.

Tab. 23: Average phaeophytinisation quotient of the different pigment extracts of the UV treatment experiment. G: gametophore, P: protonemata, n=3.

	Con G	Con P	UV G	UV P	Si G	Si P	Si UV G	Si UV P
PP	1.46	1.43		1.45	1.44	1.45	1.47	1.42
PD		1.46		1.47	1.44	1.44	1.43	1.44
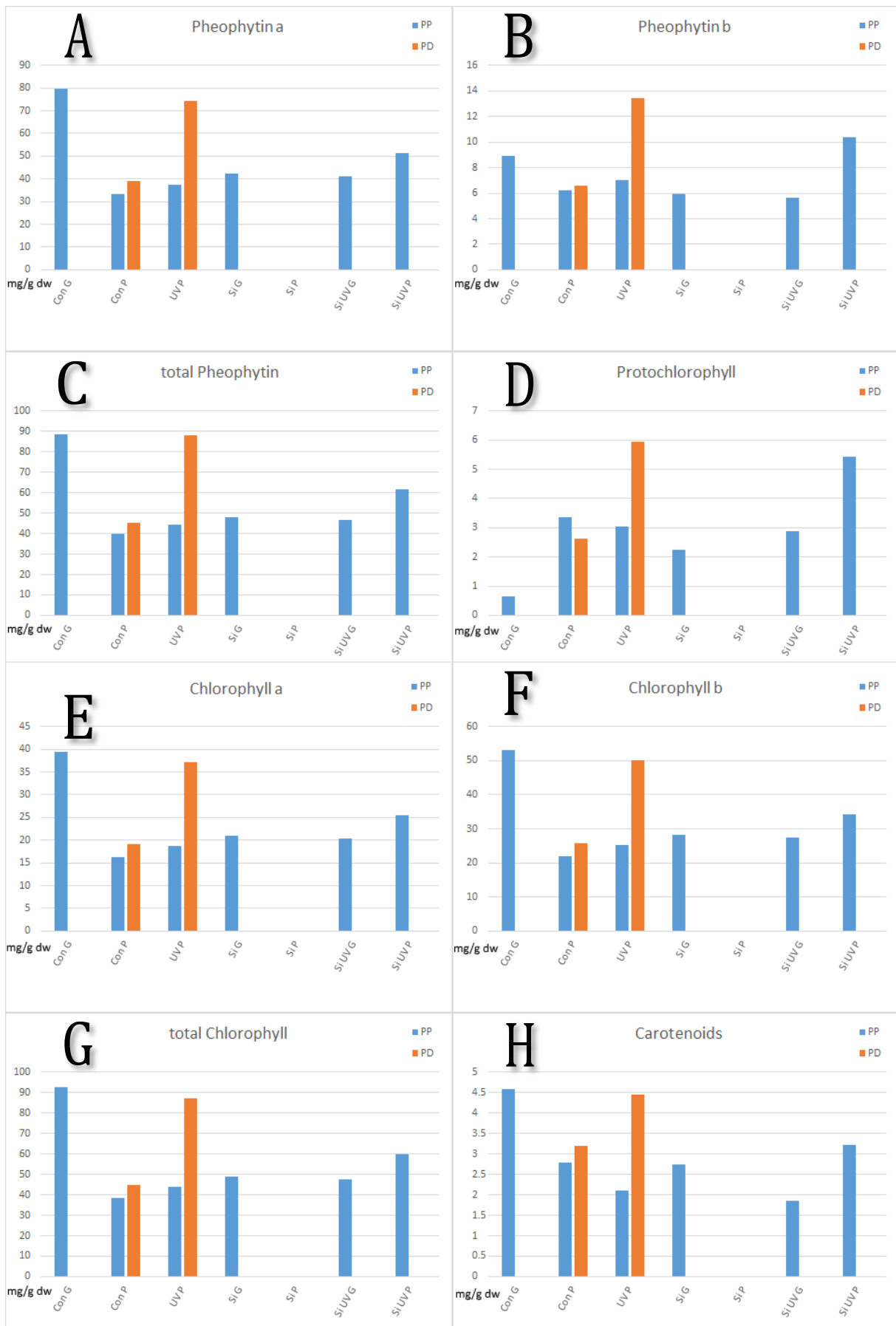
Fig. 29: Pigment content of protonemata (P) and gametophores (G) of *Physcomitrella patens* (PP, blue) and *Pohlia drummondii* (PD, orange) in DMF extracts. Higher pigment content was found in control *P. patens* gametophore; n=1-3.
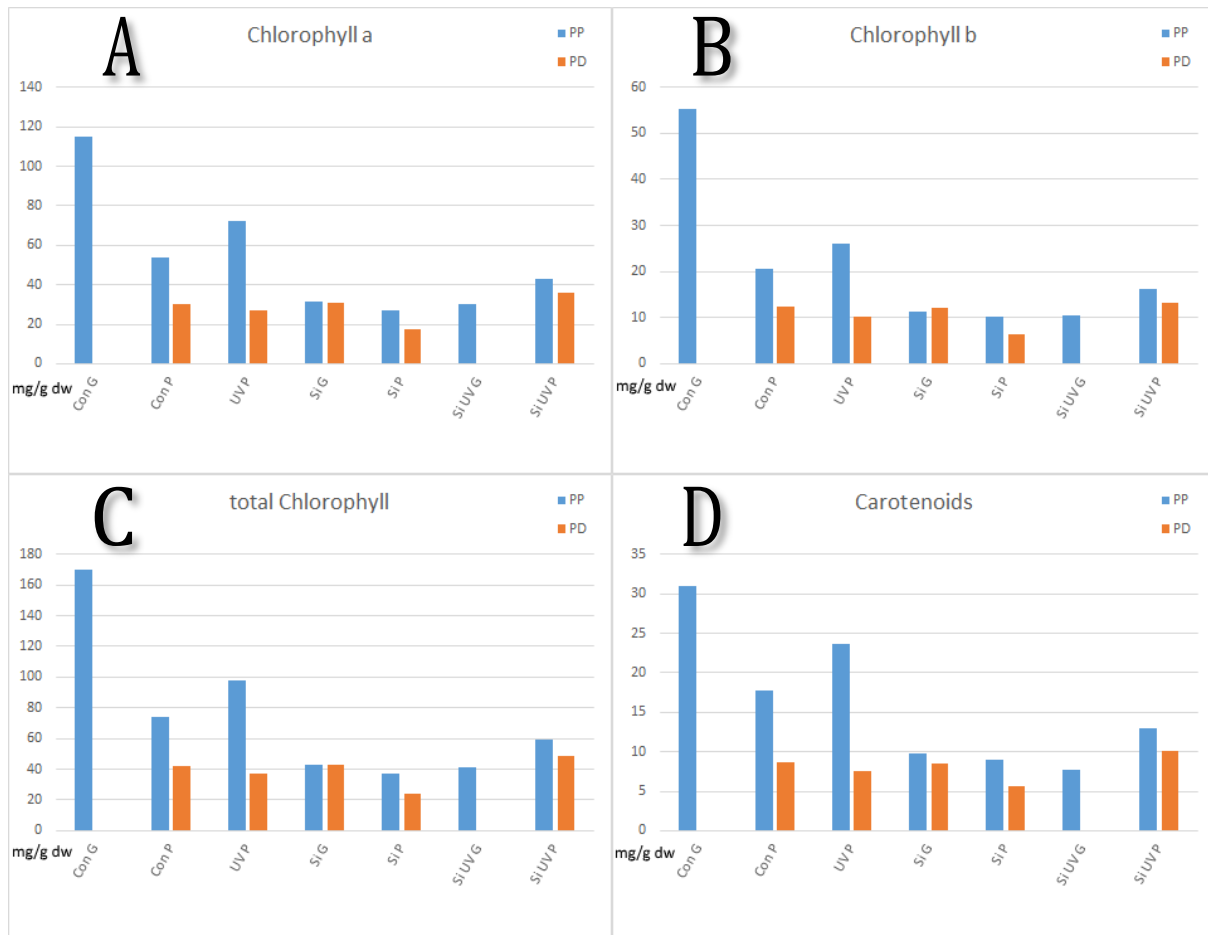
Fig. 30: Pigment content of protonemata (P) and gametophores (G) of *Physcomitrella patens* (PP, blue) and *Pohlia drummondii* (PD, orange) in DMSO extracts. There seems to be a trend towards higher pigment content in control *P. patens* gametophores; n=1-3.

5.2.5 Cell measurements

5.2.5.1 Protonema

Control cells of *P. drummondii* were significantly shorter and thinner than the ones of *P. patens* ($p<0.001$ both; n=100 both). Average protonema cell length in *P. drummondii* varied between 79.6 µm in control and 98.8 µm in the combined Si UV treated samples. Variation of average cell width in *P. drummondii* ranged from 12.1 µm in the UV treated samples to 14.8 µm in the control. Control protonemata cells were both longer and wider in *P. patens* than in *P. drummondii* ($p<0.001$ both, n=100). *P. drummondii* cells were significantly wider in the control than in the Si treatment ($p<0.001$, n=100). For combined Si UV treatment and UV treatment it was the other way round, with Si UV treated protonema cells being significantly wider ($p<0.001$, n=100).

Average *P. patens* cell length varied between 81.5 µm in the Si treatment and 106.4 µm in the UV treatment. The cells of *P. patens* control were significantly longer than the ones treated with silicon ($p<0.001$, n=129). Similarly, the UV treated cells were significantly longer than the ones in the combined Si UV treatment ($p<0.001$, n=115). Cell width ranged from 19.3 µm in the control to 22 µm in the combined Si UV treatment. UV treated protonema cells on the other hand were significantly longer then not UV treated cells ($p<0.001$ all, n=100). A summary using interaction plots can be found in Fig. 31 and graphical summary in Fig. 32. Numerical details can be found in Tab. 24.
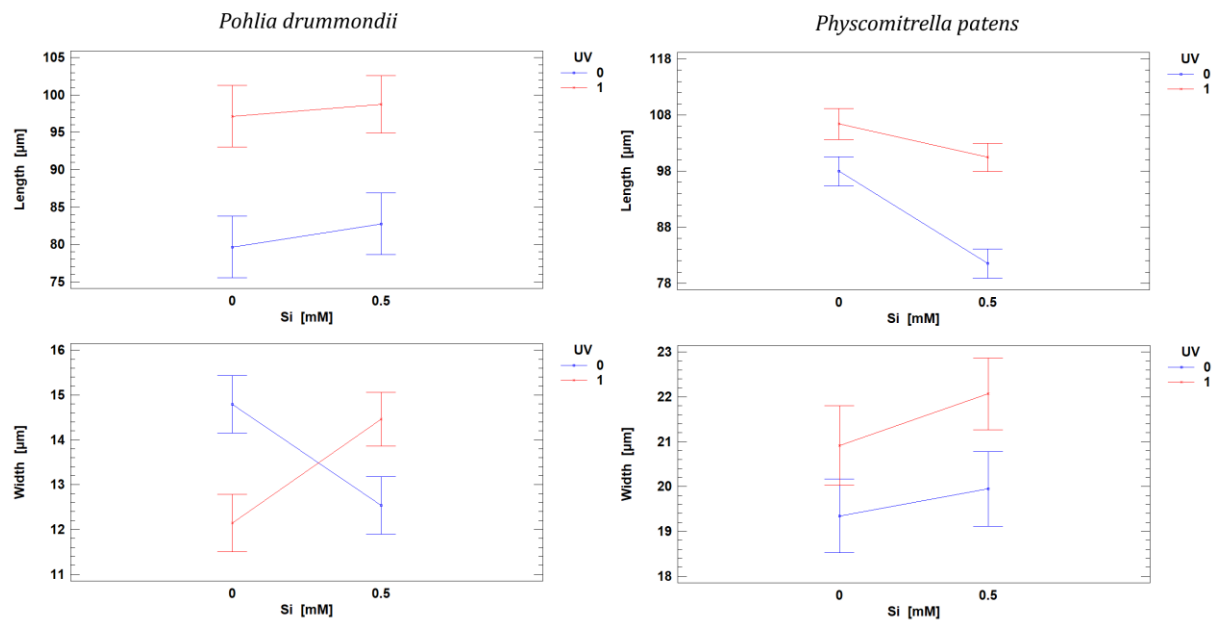
Fig. 31: Interaction plots for Si concentration (mM) in the media, UV treatment (binary) and cell length and width for *P. drummondii* and *P. patens* protonemata, n= 415 and n=515 respectively, 95% confidence Tukey HSD.

Tab. 24: Average of length and width (µm) of protonema cells of both species. Con: no added Si or UV trreatment, Si: 0.5 mM sodium-orthosilicate, UV: additional 4 week UV treatment, PD: *Pohlia drummondii*, PP: *Physcomitrella patens*. Different letters denote significant difference (*p*<0.05, Tukey HSD).

	PD Con	PD Si	PD UV	PD Si UV	PP Con	PP Si	PP UV	PP Si UV
Length	79.6[a]	82.8[a]	97.2[b]	98.8[bc]	98.0[b]	81.5[a]	106.4[c]	100.4[bc]
Width	14.8[b]	12.5[a]	12.1[a]	14.5[b]	19.3[c]	19.9[c]	20.9[cd]	22.0[d]
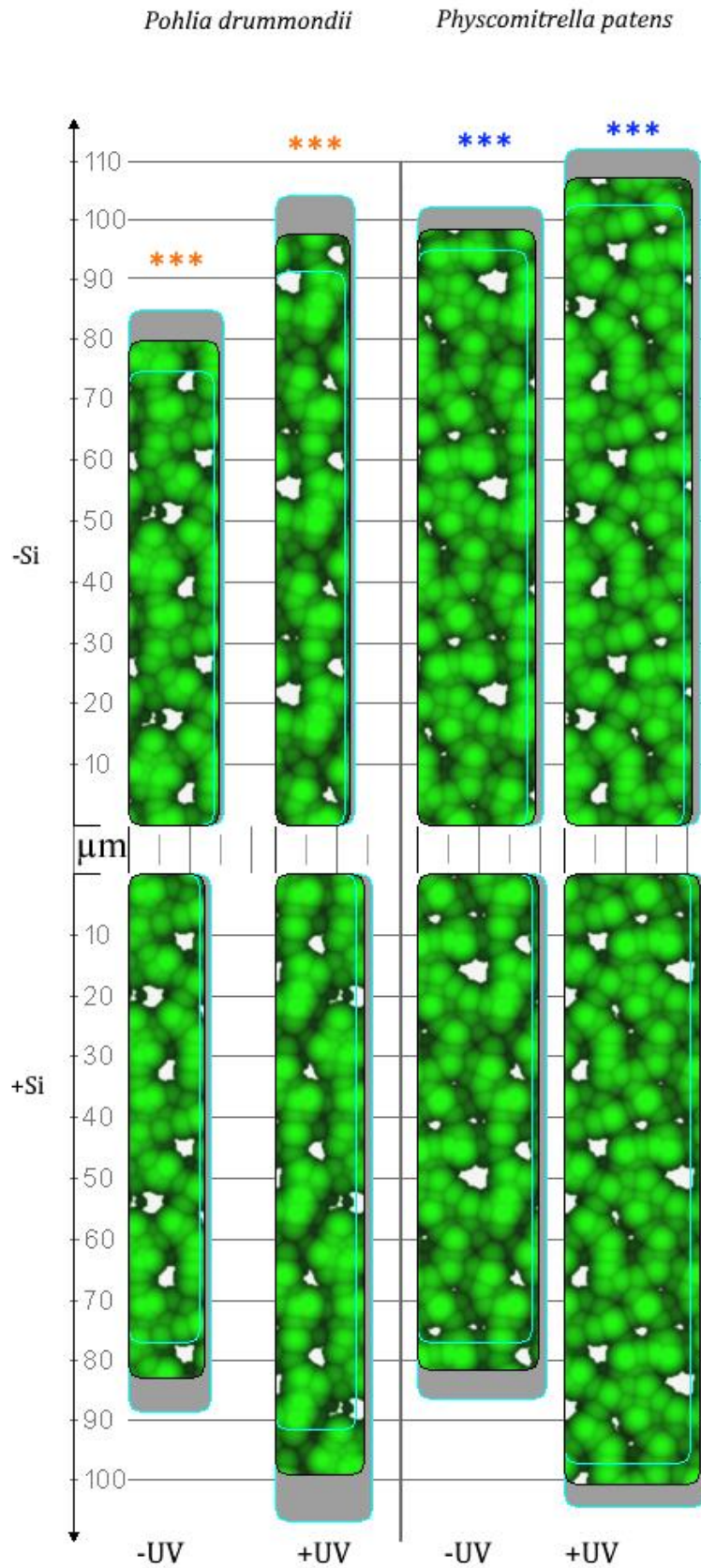
Fig. 32: Comparison of protonema cell size. Blue asterisks denote significant difference in length, orange asterisks denote significant difference in width when comparing medians (Mann Whitney U test) between Si treated and not Si treated counterpart, Cyan frames visualize 95% interval. n>100.

5.2.5.2 Gametophore

There was not enough material for *P. drummondii* control or *P. patens* Si treated gametophores to perform cell measurements, so not all planned comparisons could be performed. Average gametophore cell length in *P. drummondii* varied between 66.6 μm in the combined Si UV treatment and 75.1 μm in the Si treatment. The cell length of *P. drummondii* gametophore cells was significantly higher in UV treated samples than in the combined Si UV treatment ($p<0.01$, n=88). Average cell width in *P. drummondii* ranged between 12.2 μm in the UV treatment and 16.9 μm in the Si treatment and was significantly higher in the combined Si UV treatment, than in the UV treatment alone ($p<0.001$, n=88).

Average gametophore cell length in *P. patens* ranged from 41.5 μm in the combined Si UV treatment to 55.5 μm in the UV treatment. Similar to *P. drummondii*, UV treatment lead to significantly longer cells than the combined Si UV treatment ($p<0.001$, n=128). Average cell width for *P. patens* ranged from 17.2 μm in the combined Si UV treatment to 19.6 μm in the control. *P. patens* cell width is significantly higher in UV treated samples, compared to combined Si UV treatment ($p<0.001$, n=128). Graphical and numerical summaries can be found in Fig. 33 and Tab. 25.

Tab. 25: Average of length and width (μm) in gametophore cells of both species. Con: no added Si, Si: 0.5 mM Si, UV: additional 4 week UV treatment, PD: *Pohlia drummondii*, PP: *Physcomitrella patens*. Different letters denote significant difference ($p<0.05$, Tukey HSD).

	PD Si	PD UV	PD Si UV	PP Con	PP UV	PP Si UV
Length	75.1[d]	74.7[d]	66.6[c]	51.6[b]	55.5[b]	41.5[a]
Width	16.9[c]	12.2[a]	14.5[b]	19.6[d]	21.1[e]	17.3[c]
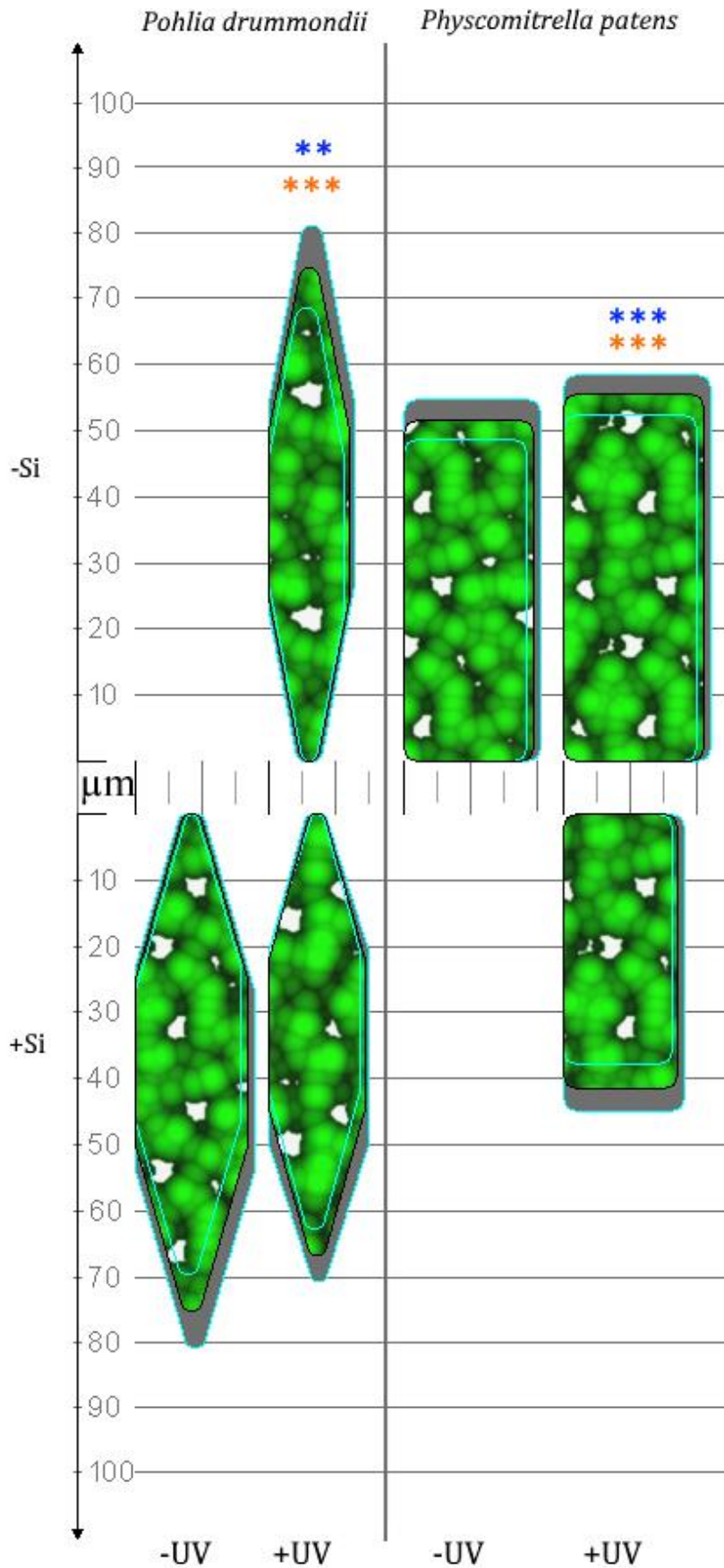
Fig. 33: Comparison of protonema cell size. Blue asterisks denote significant difference in length, orange asterisks denote significant difference in width when comparing medians (Mann Whitney U test) between Si treated and not Si treated counterpart, Cyan frames visualize 95% intervlal. n>100.

5.3 Silicon and Salinity

5.3.1 Biomass

The highest gain in biomass for *P. patens* was observed in Si treatment, 0.2 Osm NaCl and the combined 0.2 Osm and Si treatment with an average of about 25cm² per dish each. For *P. drummondii* the maximum size per dish was at about 34 cm² in the Si treated samples. NaCl treated samples for 0.2 Osm were at about the same niveau as in *P. patens*, but the higher concentrated ones were less developed in comparison. For 0.6 Osm, both with and without Si, there was no development at all and most cultures were deemed dead, except for individual cultures that retained their green color, without visible growth, even after six weeks of cultivation in single dishes of combined 0.6 Osm NaCl and Si treatment for both species.

Recalculated for individual cultures it seems that Si treatment led to the biggest individuals in *P. drummondii*, right before both 0.2 Osm NaCl treatments, while in *P. patens* it was the combined Si and 0.2 Osm NaCl treatment, that led to development of the biggest individuals. Fig. 34 displays the development of the cultures over time and Tab. 26 summarizes the measurements of Week 7 numerically. During the experiment, only individual gametophores developed, so there were no Gametophore: Protonema ratio calculations possible.
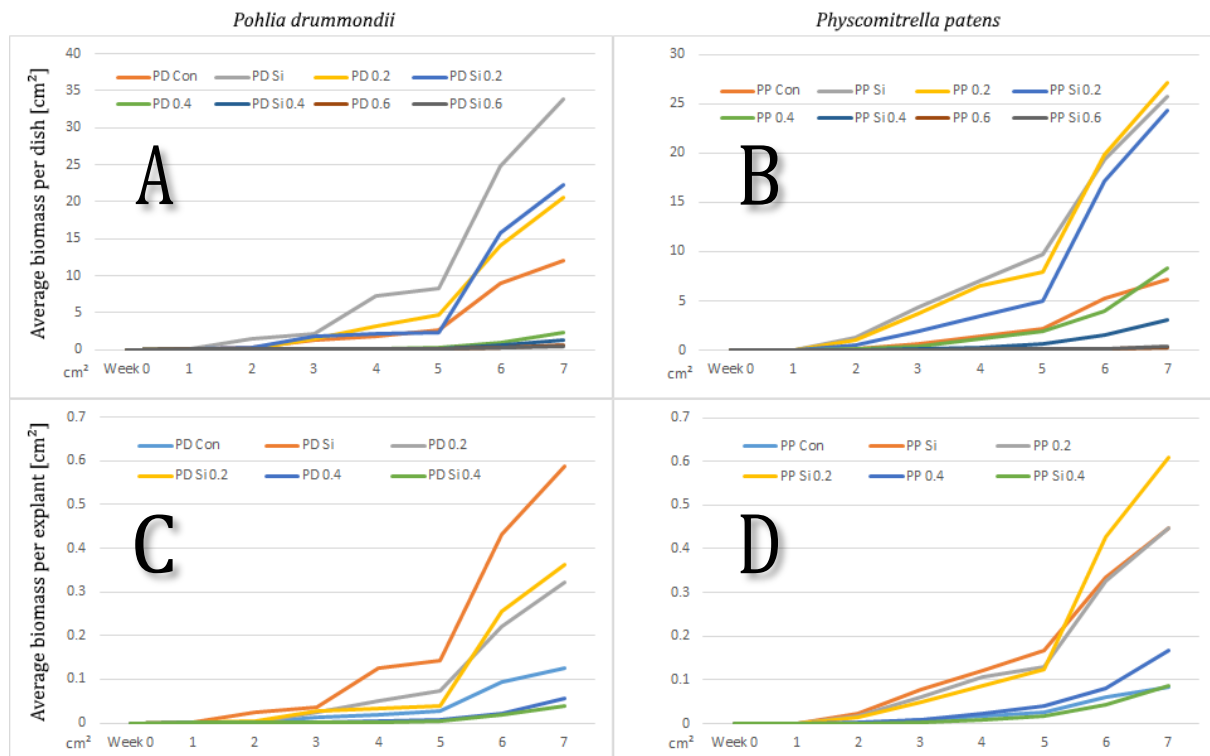
Fig. 34: Biomass increase over time in both mosses, visualized in cm², as average over the dishes (A, B; n=2-3) and as average of the individual explants (C, D; n=33-85). Because of the high lethality of the 0.6 Osm NaCl concentration, the data was omitted.

Tab. 26: Mean values for biomass in cm² for both species, for dishes and individual cultures ± Standard error; n=2-3, n=33-85

	Con	Si	0.2	Si 0.2	0.4	Si 0.4	0.6	Si 0.6
PD dishes	12.05 ± 2.45	33.82 ± 15.68	20.63 ± 0.66	22.25 ± 10.06	2.25 ± 1.94	1.33 ± 0.06	0.66 ± 0.16	0.49 ± 0.34
PD cultures	0.13	0.59	0.32	0.36	0.06	0.04		
PP dishes	7.17 ± 6.49	25.75 ± 4.94	27.18 ± 2.35	24.39 ± 1.66	8.32 ± 6.85	3.04 ±1.79	0.25 ± 0.14	0.37 ± 0.05
PP cultures	0.08	0.45	0.45	0.61	0.17	0.09		

52

5.3.2 Reactive oxygen species (ROS)

Because there were not enough gametophores developed to assess ROS staining like in previous experiments, a different method was devised to quantify NBT and DAB staining. The images were analyzed using a freeform selection and blue and red histograms for NBT and DAB staining, respectively. in Fiji image analysis software. The measured mean values of three dishes were used to calculate the staining intensity by subtraction from 255, the maximal possible value, because lighter areas would contain more red or blue (white background) than stained areas that appeared darker, sometimes tending towards black.

5.3.2.1 NBT

The highest staining intensity was found in the 0.2 Osm NaCl treatment of *P. patens* and the Si treatment of *P. drummondii* protonemata. The lowest intensity was found in 0.4 Osm NaCl treated *P. patens* and the Si treated *P. patens* samples. Staining of Si treatments appears to be slightly stronger than in the Si free variants for *P. drummondii*, while for *P. patens* it's about the same, or weaker (Fig. 35).
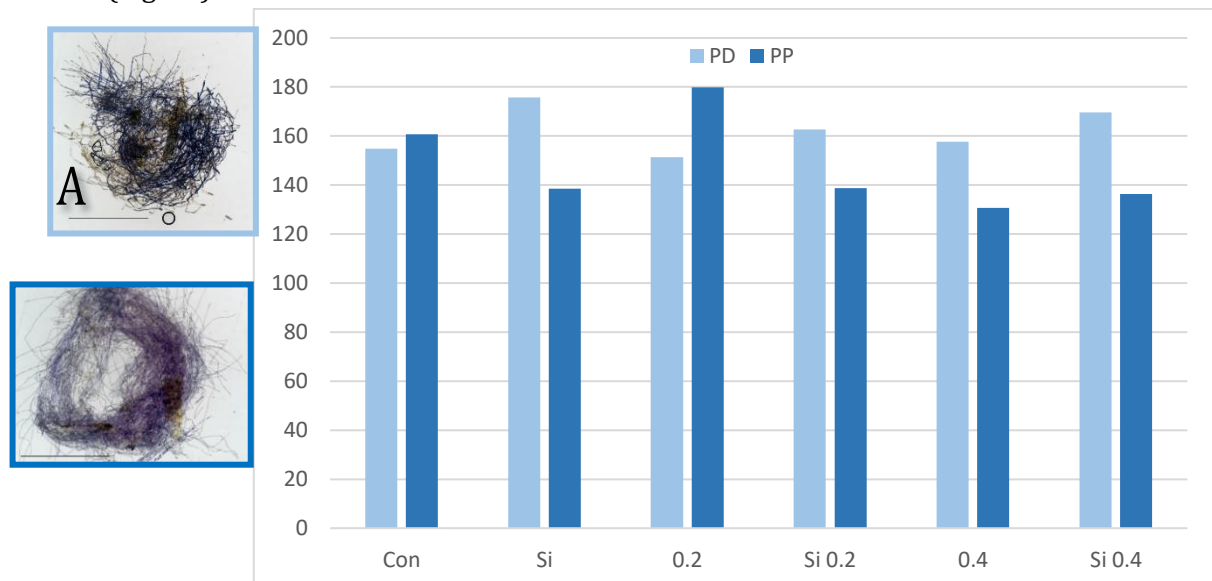
Fig. 35: NBT staining of protonemata as intensity (range 1-255, inverted from blue histogram) in *P. drummondii* the Si treated samples are always slightly more stained than the Si free samples; n=3, A: *P. drummondii* 0.4 Osm, B: *P. patens* 0.4 Osm, bar of images: 400 μm.

5.3.2.2 DAB

For DAB, staining is generally stronger in *P. drummondii* than in *P. patens*. The highest staining intensity was found in *P. drummondii* control and combined Si and 0.4 Osm NaCl treatment. The lowest staining intensity was measured in the Si treatment of *P. patens*. *P. patens* shows a similar trend to the NBT staining with lower staining, in Si treatments, compared to Si free treatments, while *P. drummondii* shows slightly stronger staining, if Si is involved, except for the control – Si pair, where it's the opposite (Fig. 36).
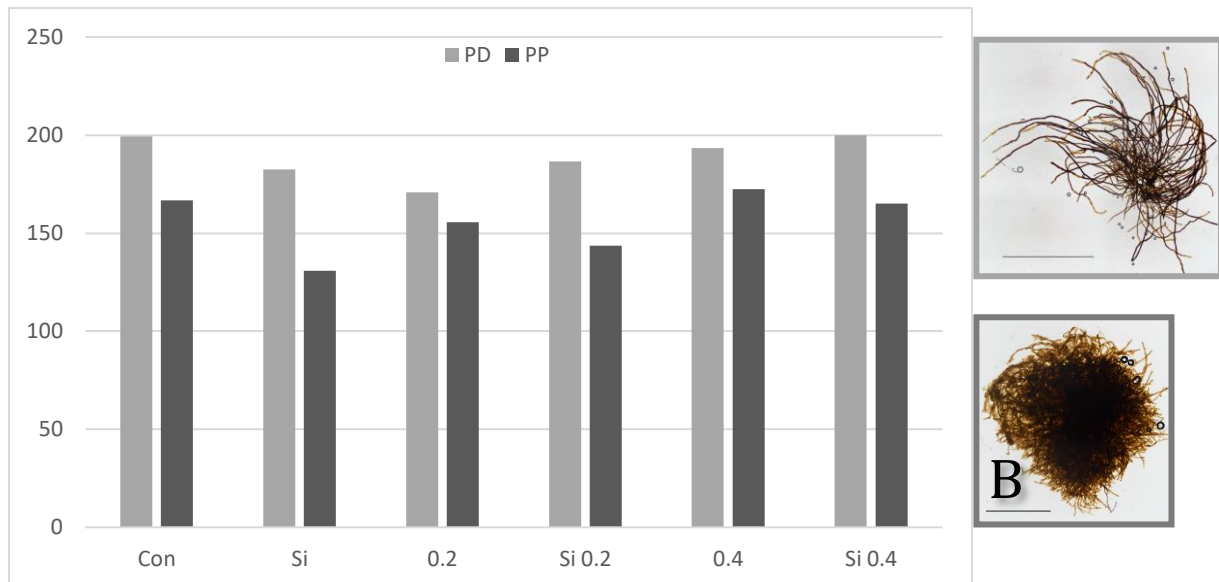
Fig. 36: DAB staining of protonemata as intensity (range 1-255, inverted from red histogram) staining is always stronger in *P. drummondii* than in *P. patens*; n=3, A: *P. drummondii* 0.4 Osm, B: *P. patens* 0.4 Osm & Si, bar of images: 800 and 400 μm respectively.

5.3.3 Pigment analysis

A total of 64 extracts were produced, in the same way as samples from the UV-B experiment pigment analysis.

In the DMF extracts the highest content of *pheophytin a* was found in the Si and 0.2 Osm NaCl treatments of both species. In a combined treatment, the content is slightly lower, especially in *P. drummondii*. All 3 treatments lead to higher *pheophytin a* content than the control for *P. patens*, while *P. drummondii* control had about the same level as the combined 0.2 Osm NaCl and Si treatment. The lowest content was found in the combined 0.4 Osm NaCl and Si treatment of *P. drummondii* (Fig. 37 A). *Pheophytin b* content in the DMF extracts was highest in *P. drummondii* samples, which were treated with a combination of 0.2 Osm NaCl and Si, while all other values were lower than half that amount. Also, *pheophytin b* content in *P. patens* was always lower than in *P. drummondii*. The lowest measured content was found in the Si and combined 0.4 Osm NaCl and Si treatments of *P. patens* (Fig. 37 B). The highest values for *total pheophytin* content were found in the control, Si and 0.2 Osm NaCl treatments of *P. drummondii*. For *P. patens,* the highest content was measured in the 0.2 Osm NaCl treatment. Similar to *pheophytin b*, the lowest content was found in the 0.4 Osm NaCl, Si combination treatment and the pure Si treatment of *P. patens* (Fig. 37 C). Most *protochlorophyll* was found in the *P. drummondii* extracts, especially in the combined 0.2 Osm NaCl and Si treatment. The highest content in *P. patens* was found in control and 0.2 Osm NaCl treatment (Fig. 37 D). The same goes also for *chlorophyll a*, *chlorophyll b* and *total chlorophyll*, as well as *carotenoids*. The lowest measured values were found in *P. patens*, in both the pure Si treatment and the combined 0.4 Osm NaCl and Si treatment (Fig. 37 E-H).

The measured *chlorophyll* contents in the DMSO extracts were partially very variable and lower than in the DMF extracts. The highest content of *chlorophylls* and *carotenoids* was found in *P. patens* 0.2 Osm NaCl and *P. drummondii* 0.2 Osm NaCl combined with Si. Lowest content for all 4 pigments was found in *P. drummondii* samples treated with a combination of 0.4 Osm NaCl and Si. All other measured values didn't differ much from each other (Fig. 38 A-D).
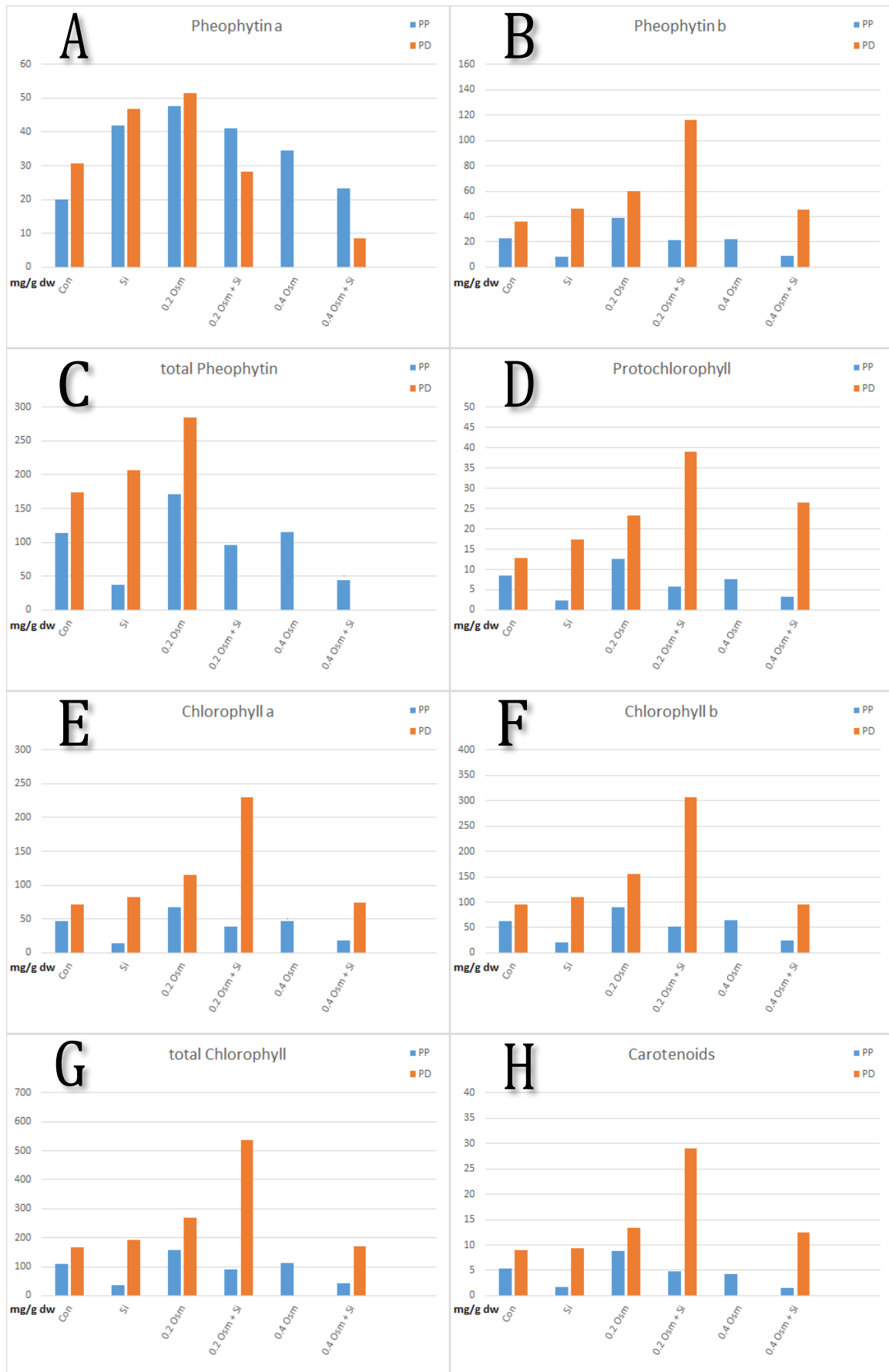
Fig. 37: Pigment content of *Physcomitrella patens* (PP, blue) and *Pohlia drummondii* (PD, orange) in DMF extracts. There is a trend towards higher pigment content in 0.2 Osm & Si treated *P. drummondii* (B, D-H); n=1-3.
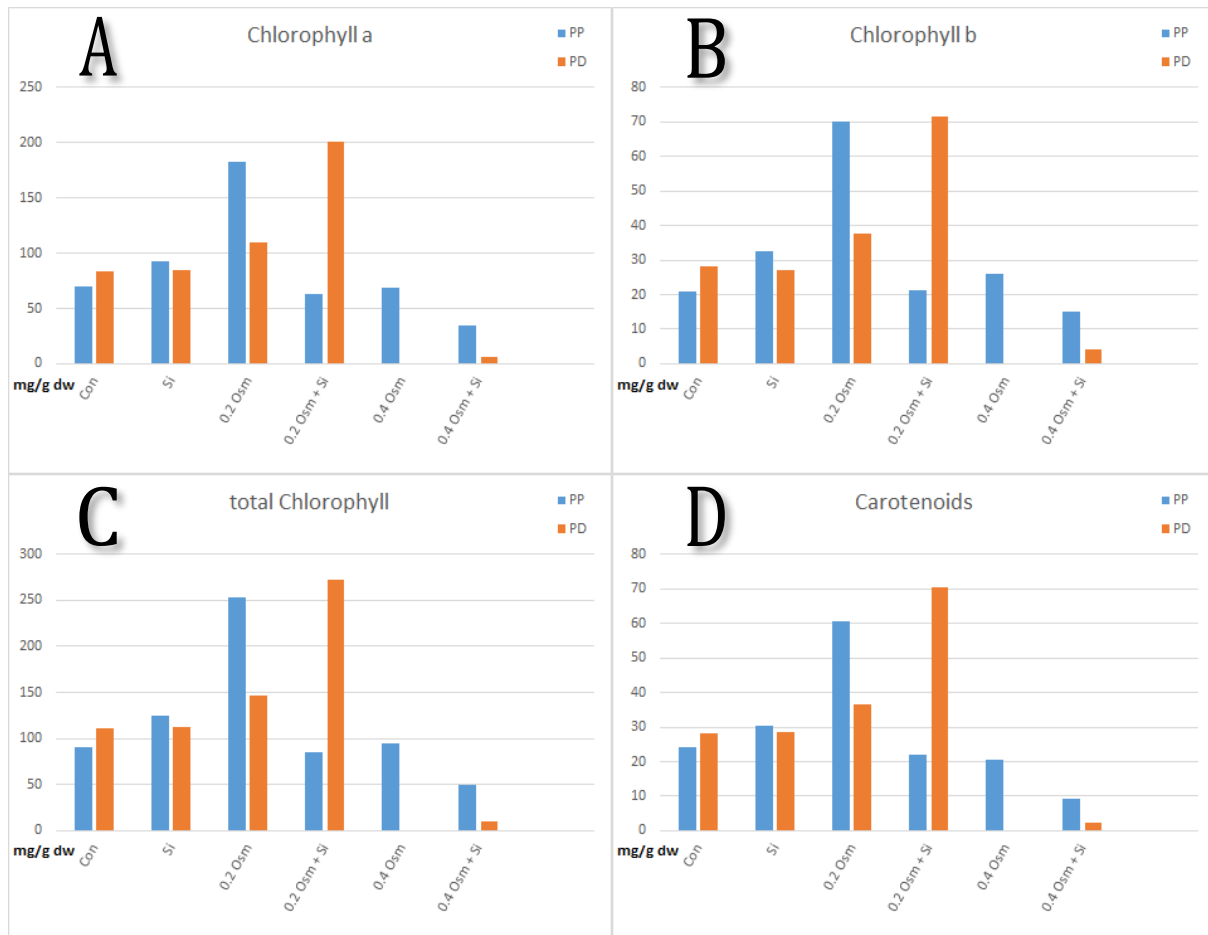
Fig. 38: Pigment content of *Physcomitrella patens* (PP, blue) and *Pohlia drummondii* (PD, orange) in DMSO extracts; n=1-3.

The average value for the phaeophytinisation quotient, based on DMF extracts, was 1.45 and despite the difference in treatments, there was no significant difference in phaeophytinisation, between most treatments (Tab. 27). Only the quotient of the 0.4 Osm NaCl treatment of *P. patens* and the control samples of *P. drummondii* were low enough (1.41 both) to estimate an acidification of about 3-5% according to the standard table of Ronen and Galun (1984, Tab. 3).

Tab. 27: Average phaeophytinisation quotient of the different pigment extracts of the salinity treatment experiment. G: gametophore, P: protonemata, n=3.

	Con	Si	0.2 Osm	0.2 Osm + Si	0.4 Osm	0.4 Osm + Si
PD	1.41	1.45	1.49	1.47	1.47	1.44
PP	1.50	1.48	1.45	1.47	1.41	1.44

5.3.4 Cell measurements

Generally, *P. patens* cells are significantly longer and wider than *P. drummondii* cells, except in the 0.4 Osm NaCl treatment, where they are significantly slimmer and the 0.4 Osm NaCl/Si combination, where they are both significantly shorter and slimmer (all *p*<0.001, n=150)
In *P. drummondii* cell length ranged from 12.0 µm in 0.4 Osm NaCl to 267.3 µm in the combined 0.2 Osm NaCl and Si treatment. Cell width varied from 5.7 µm in the control to 61.2 µm in the combined 0.4 Osm NaCl and Si treatment.

P. patens cell length had its minimum with 25.7 μm in the 0.4 Osm NaCl treatment and its maximum with 184.4 μm in the control group. For cell width the minimum was observed with 8.8 μm in the control and the maximum was found with 50.6 μm in in the 0.4 Osm NaCl treatment.

P. drummondii control cells are significantly shorter than the ones treated with 0.4 Osm NaCl, or any of the Si treated ones ($p<0.05$ and $p<0.001$ respectively, n=150). The combined treatments of 0.2 and 0.4 Osm NaCl with Si also led to significantly longer cells when compared to the Si free equivalents ($p<0.001$ both, n=150). Treatment with Si alone led to significantly longer cells, than in 0.2 or 0.4 Osm NaCl, or the combination of 0.4 Osm NaCl with Si ($p<0.001$, $p<0.05$, $p<0.01$ respectively, n=150). Cells treated with the combination of 0.4 Osm NaCl and Si also developed significantly longer cells than 0.4 Osm NaCl alone or the combination of 0.2 Osm NaCl and Si ($p<0.001$ and $p<0.01$ respectively, n=150).

In terms of cell width, *P. drummondii* control cells are significantly slimmer than most other treatments ($p<0.001$, n=150), except for Si treated cells, compared to which they are significantly wider ($p<0.01$, n=150). For the samples of the treatments with Si, 0.2 Osm NaCl, 0.4 Osm NaCl and the 0.4 Osm NaCl/Si combination it can be said that they form a row of ascending significantly different width (Si < 0.2 Osm NaCl < 0.4 Osm NaCl/Si < 0.4 Osm NaCl, $p<0.001$ all, n=150 all, also see Tab. 28 and Fig. 40). When comparing the combined 0.4 Osm NaCl and Si treatment, the cell width is significantly higher than in the other two Si treatments ($p<0.001$ all, n=150).

In *P. drummondii* Si treatment led to a strong increase in cell length (15-25%), while cell width was only marginally increased in the samples cultivated on media with higher NaCl concentration (Fig. 39 A). NaCl treatment on the other hand increased cell width by a lot (about 100%) between the 0.2 and 0.4 Osm concentration in the media, while the difference was not significant for cell length (Fig. 39 C). The surface calculations show a similar pattern to the cell width diagram, with the Si treated samples being slightly offset towards positive X (Fig. 39 E).

P. patens cells of the Si treatment were significantly longer than the cells of any other treatment ($p<0.001$ all, n=150 all). Control cells were the second longest, significantly different from all other samples ($p<0.001$ all, n=150 all). There was no significant difference between the 0.4 Osm NaCl treated cells and both 0.2 Osm NaCl treated cells and the 0.2 Osm NaCl/Si combination, but there was a difference between the latter two, with longer cells being found in the 0.2 Osm NaCl/Si treatment ($p<0.001$, n=150). At the lower end, there were cells of the 0.4 Osm NaCl/Si treatment, which were significantly smaller than cells from all other treatments ($p<0.001$ all, n=150 all).

Concerning cell width, *P. patens* cells of the control group rank second after the 0.4 Osm NaCl samples ($p<0.001$, n=150), tied with 0.4 Osm NaCl/Si treated cells. Significantly slimmer than those are the samples of the 0.2 Osm NaCl ($p<0.01$ and $p<0.001$ respectively, n=150, also see Tab. 28 and Fig. 40) and 0.2 Osm NaCl/Si treatments ($p<0.01$ compared to 0.4 Osm NaCl/Si, n=150). The slimmest cells were found in samples of the Si treatment, which were significantly slimmer than cells from Control, 0.2 Osm NaCl/Si, 0.4 Osm NaCl and 0.4 Osm NaCl/Si treatments ($p< 0.01$, $p<0.05$, $p<0.001$ and $p<0.001$ respectively, n=150 all).

Overall, Si treatment in *P. patens* led to an increase in cell length (<10%), with exception for the highest NaCl treatment, where the cells were significantly smaller, as the Si free treatments broke with a downward trend (Fig. 39 B). Similarly, the Si treated samples keep an upward trend in cell width over the increasing NaCl concentrations, but with lower values than the samples from Si free treatments. Interestingly the cell width of 0.2 Osm NaCl treated samples was lower than on both control and 0.4 Osm NaCl (Fig. 39 D). Cell surface calculations for Si free samples were similar to the cell width diagram, but the Si treated samples showed a downward trend similar to the cell length diagram (Fig. 39 F).

Pohlia drummondii   *Physcomitrella patens*
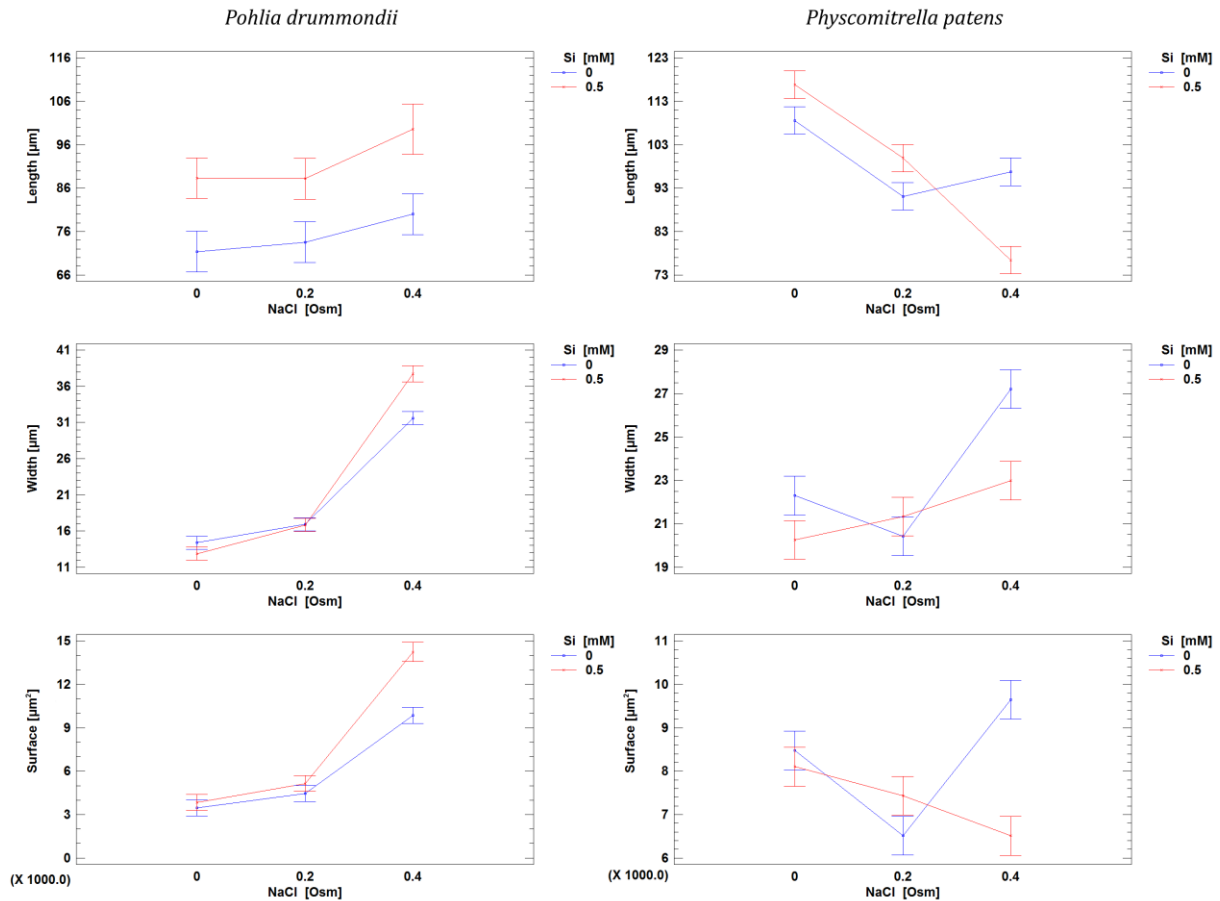
Tab. 28: Average of length, width, surface and volume (μm, μm^2 and μm^3 cylindrical approximation) of protonema cells of both species. Con: no added Si, Si: 0.5 mM sodium-orthosilicate and different concentrations of NaCl (Osm), PD: *Pohlia drummondii*, PP: *Physcomitrella patens*. Different letters denote significant difference also when comparing between species (*p*<0.05, n=150, Tukey HSD).

	PD Si	PD Si NaCl 0.2	PD Si NaCl 0.4	PD Con	PD NaCl 0.2	PD NaCl 0.4
Length	88.3[b]	88.2[b]	99.6[c]	71.4[a]	73.5[a]	80.0[ab]
Width	12.9[a]	16.8[b]	37.7[d]	14.4[a]	16.9[b]	31.6[c]
Surface	3836[a]	5154[b]	14246[d]	3468[a]	4456[ab]	9861[c]
Volume	1780[a]	2343[b]	5953[d]	1557[a]	1991[ab]	4095[c]
	PP Si	PP Si NaCl 0.2	PP Si NaCl 0.4	PP Con	PP NaCl 0.2	PP NaCl 0.4
Length	116.8[e]	100.0[c]	76.4[a]	108.6[d]	91.1[b]	96.8[bc]
Width	20.2[a]	21.3[ab]	23.0[b]	22.3[b]	20.4[a]	27.2[c]
Surface	8104[bc]	7436[b]	6511[a]	8475[c]	6513[a]	9647[d]
Volume	3718[bc]	3348[b]	2822[a]	3818[cd]	2917[a]	4189[d]

Fig. 39: Interaction plots for Si concentration (mM) in the media, NaCl concentration (Osm), cell length, cell width and cell surface for *P. drummondii* and *P. patens* protonemata, n= 850 and n=900 respectively, 95% confidence Tukey HSD.
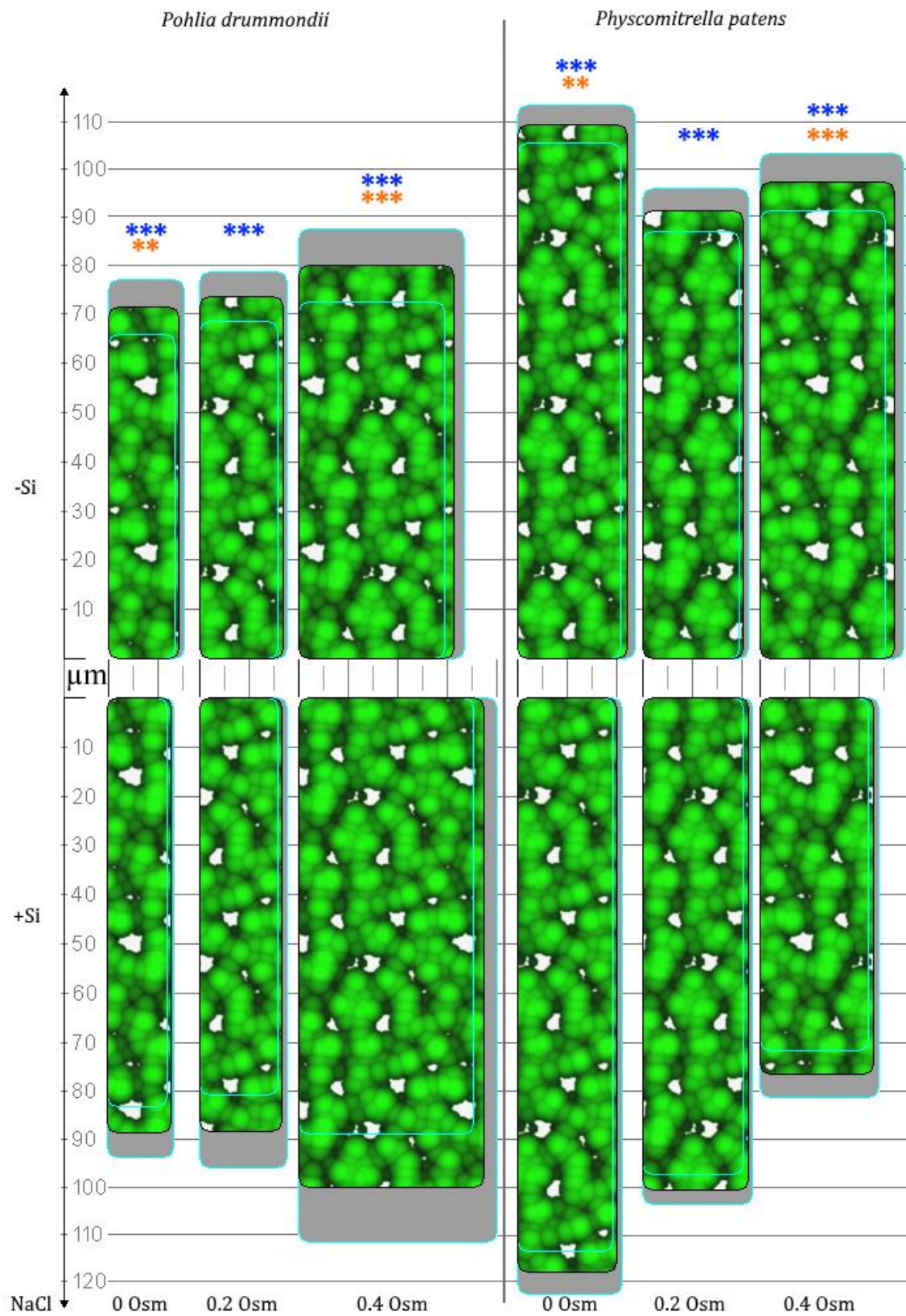
Fig. 40: Comparison of protonema cell size. Blue asterisks denote significant difference in length, orange asterisks denote significant difference in width when comparing medians (Mann Whitney U test) between Si treated and not Si treated counterpart, Cyan frames visualize 95% interval. N=150.

6 Discussion

All experiments were designed to investigate the influence of Si on the two moss species *P. drummondii* and *P. patens*, under abiotic stress caused by copper, UV-B radiation and salinity. We hypothesized that Si might have alleviating effects, like those reported for some species of higher plants (Malčovská et al., 2014a; Pascual et al., 2016). On the other hand we expected a shift towards a higher development of protonemata, instead of gametophores as the plant attempts to evade detrimental conditions, if no Si is available, similar to reports by Sassmann et al. (2015a). Another hypothesis dealt with the question, if Si would alleviate the effects of UV radiation, by physical filtering or scattering the incoming radiation and protecting pigments, like chlorophyll and carotenes. We also expected different results depending on species, because the chosen species are adapted to different environmental conditions (Frahm and Frey, 2004; Frank et al., 2005; Wernitznig, 2009).

6.1 Silicon and Copper

Given the acquired data for *P. drummondii*, the Si treatment had a positive effect, when comparing the biomass gain over the duration of the experiment. Since the number of samples was very low, a significant difference could not be established. For *P. patens,* the only thing that could be verified is, that the higher Cu treatment (1 mM $CuCl_2$) led to significantly reduced biomass in comparison to the other treatments. That can be explained with the high toxicity of Cu, leading to an increase in reactive oxygen species (Antreich et al., 2016). Those are harmful for cell components like the cell membrane and will increase the amount of energy that is needed for repair mechanisms (Prasad, 2004). This is especially apparent in the NBT staining of *P. patens*, which was stronger and comprised of relatively more stained tissue than in *P. drummondii*. Hydrogen peroxides, as detected by DAB, led to slightly less staining and there was less difference between the species. Just the *P. patens* control plants showed more staining, than the other treatments.

According to Yamasaki et al. (2008), Cu free media can cause stress by Cu deficiency, since Cu is involved in the formation of certain enzymes, like Cu/Zn superoxide dismutase, which would be downregulated when Cu is unavailable. An indirect way to remobilize extra-cellular Cu that previously was bound to the low-methyl-esterified pectins of the cell wall, would be endocytosis (Krzesłowska, 2011). This happens when the cell undergoes division (Kasprowicz et al., 2009) or is starving (Baluška et al., 2006). Si has no alleviating effect in that context, as the only significant differences in ROS staining are found between the DAB staining of control and Si, and 0.1 mM Cu and 0.1 mM Cu/Si treatment respectively for *P. drummondii*. In both cases the Si treated samples were more stained.

There was no significant influence of Si on Cu content of the gametophores. In the protonemata the Cu content was significantly reduced by Si in the 1 mM Cu treatments. According to He et al. (2015) Si increases cell wall regeneration in rice. A similar effect might have been at work here, additionally increasing callose synthesis to exclude Cu (Fahr et al., 2013), but examination of cell wall composition is necessary to further our understanding. Cells of *P. drummondii* protonemata in higher Cu concentrations were shorter, despite the lower cell wall rigidity caused by the Cu-ions (Fry, 1998). Furthermore, the additional Si treatment reversed the effect in the 0.1 mM Cu-Si combination. No similar effect was found for *P. patens*. Si also increased both cell length and cell width in protonema cells of both species, without additional Cu, while Cu decreased both parameters. There are still exceptions, like Si-free *P. patens* samples, where the cell length was rather stable or the cell width of Si-free *P. drummondii*, which increased in the 0.1 mM $CuCl_2$ treatment. Si treatment also led to significant increases in cell width and length in *P. drummondii*

gametophore cells, compared to the control. The gametophore cells *of P. patens* behaved differently though, with slimmer phylloid cells being found in the control group, while the Cu treated cells were still longer than the untreated ones. We also observed that the high Cu concentration led to a change of habitus of the moss. *P. patens* protonemata started to grow as a mound of sorts, on top of the cellophane and some of the *P. drummondii* protonemata branches grew up rather than spreading horizontally. Measurement of the adsorbed ions of the cell wall fraction would help increasing our understanding of the mechanisms at work.

The amount of pigments was significantly decreased by Si treatment for *P. patens* protonemata, while it increased significantly with the Cu concentration in *P. drummondii* protonemata. For gametophores it increased in Si treated *P. patens* samples, but decreased in Si treated *P. drummondii* samples. In both cases the difference was not significant. Because of the small sample size and the possible inaccuracies of the measurement method it was hard to find conclusive evidence of a positive or negative effect of the Si treatment in that respect. According to Pavlović et al. (2014) a positive effect of Cu on the Cu adapted species *P. drummondii* can be ascertained because of the increased pigment content we found in the protonemata.

The gametophyte to protonema ratio (as defined by Sassmann et al. (2015a)) of *P. patens* was the lowest in the combined treatment with 0.1 mM $CuCl_2$ and Si, and the Cu-free Si treatment. In the Si-free 0.1 mM $CuCl_2$ treatment, it was initially about equal to the control, but declined faster afterwards. In *P. drummondii* the lowest ratio was found in the 0.1 mM $CuCl_2$ treatment and the highest ratio besides the control was found in the combination of 0.1 mM $CuCl_2$ and Si. Our explanation for this effect is a visible alleviating effect of Cu toxicity by Si, but as a Cu tolerant species we initially expected a lower gametophore ratio in the control in comparison. However, it cannot be completely ruled out that hypoxia caused by moisture that condensed inside the dish had a negative influence on the gametophore development (Fukao and Bailey-Serres, 2004).

While both moss species generally show excluder behavior for Si, 0.1 mM $CuCl_2$ treated plants of *P. patens* and *P. drummondii* show the highest difference between protonema and gametophore. For Cu, the strongest excluder behavior was found in 1 mM $CuCl_2$ treated *P. drummondii*. The only case of slight Cu accumulation was found in the Si treatment of *P. drummondii*.

6.2 Silicon and UV-B

In terms of biomass accumulation, the *P. drummondii* didn't grow as good in the control, as in all other treatments. A reason for that could be the lack of Cu in the used media (Yamasaki et al., 2008) as well as changed climate conditions in the cultivation cabinet because of increased temperatures during summer (Glime, 2017), when comparing it to the copper experiment. The treatment that caused the most accumulation of biomass for this species was the UV Si combination, which also worked very well for *P. patens*, where it is equal in size with the control group. In both species those samples performed better than the UV treatment or Si treatment alone. This suggests a positive effect of Si under additional UV-B stress. On its own, Si caused opposite effects in *P. patens* and slightly positive effects in *P. drummondii* in context of biomass. Part of the experimental effect of UV-B is comparable to what Ruplitsch (2011) observed with *P. patens* cultivated from individual leaves under similar conditions (culture from single leaf, as opposed to whole gametophore). It initially increased development of gametophores, but reduced growth of protonemata in the samples of this species.

The analysis of ROS staining with the NBT dye stained only the *P. drummondii* control and Si treatment. DAB staining showed very high hydrogen peroxide levels in *P. patens*, while they were lower in *P. drummondii*. Also in *P. drummondii,* the staining was generally lower when the plant was treated with UV-B, which can be explained by a higher level of antioxidants being produced to cope with the UV irradiation (Wolf et al., 2010), which was excluded during the staining process. The difference between Si treated and not Si treated mosses was not significant.

Although a lot of pigment data was excluded due to low sample size and infected dishes, the UV treatment increased the pigment content *in P. drummondii* protonemata, when compared to the control protonemata, in DMF extracts. In DMSO extracts, we found no difference between the *P. drummondii* treatments, except in the Si and Si/UV treated protonemata, where the additional UV-B irradiation led to a higher pigment content. For *P. patens* the highest pigment content in both solvents was found in the control gametophore, except for *protochlorophylls*. The combined Si/UV treatment led to high pigment content in DMF extracts of *P. patens* protonemata, which was also higher than in the samples only treated with Si. UV treatment also led to increased pigment content in protonemata of both species, while Si alone led to lower pigment content in the protonemata of both species (DMSO extracts), similar to the Cu stress experiment. This is the opposite of what was reported by Kakani et al. (2003) for crops. His review showed almost without exception a reduction of photosynthetic pigments after UV-B treatment. Either a reduced synthesis, or an increased degradation of the pigment were held responsible. For future investigation, a better method, like measurement of chlorophyll fluorescence adapted to moss in petri dishes, might improve data acquisition.

The gametophore to protonema ratio for *P. drummondii* was the highest in the Si treatment. In both UV and Si UV treatment it was about the same at its peak, but the UV treated samples developed gametophores earlier than the other samples. The control plants didn't develop any gametophores, probably because of the increased temperature (Glime, 2017). Under the given conditions, Si didn't alleviate the UV induced stress but rather increased it slightly, which is not supported by the ROS staining. For *P. patens,* there is not much difference between the control and the UV treated samples, but the highest gametophore to protonema ratio was observed in the Si treatment. The combined Si and UV treatment also had a rather high G/P ratio, leading to the conclusion that for *P. patens* Si indeed has a positive effect, but since there is not much difference between UV and control it is most likely not alleviating in nature.

UV treatment clearly increased the protonemal cell length in both species and the cell width in *P. patens* protonemata, but while it had the same effect in Si treated *P. drummondii* cells, it was the opposite in the Si-free cells, which were slimmer than in the control. Since in *P. drummondii* control and in Si treated *P. patens* no gametophores developed, the only conclusions that can be drawn from the data are, that a combination of UV and Si leads to shorter and slimmer cells in *P. patens* gametophores and shorter, but wider cells in *P. drummondii* gametophores. So almost the opposite effect as on the protonema cells. According to Gall et al. (2015) UV-B irradiation increases cell wall rigidity because it cross-links the polysaccharides in the cell wall. This only explains part of the cases of smaller cell size.

6.3   Silicon and Salinity

In the salinity experiment the highest gain of biomass was measured in both species, if treated solely with Si. Control samples of both species stayed small in comparison, both on a per dish and per culture basis for calculation. The lower temperatures after summer also have taken some influence on this (Glime, 2017). In *P. drummondii* both 0.2 Osm NaCl and the 0.2 Osm

NaCl/Si treatments came in second, while the control took the third place. In *P. patens,* the difference between the Si and both 0.2 Osm NaCl and 0.2 Osm NaCl/Si treatments was very small, while the biomass gain in the control samples was much lower and about the same as in *P. drummondii*. This would support Frank et al. (2005) and Possnig (2011), who proposed that *P. patens* is more resistant to salt/osmotic stress, than some other moss species. Because of the lack of gametophores, the *modus operandi* for quantifying ROS staining had to be changed to an intensity based quantification, which made the data incomparable to the other experiments and because of the low number of samples the results were limited. There was a slightly increased NBT staining in all three Si treated samples of *P. drummondii* compared to the Si- free treatments. NBT staining for Si treated *P. patens* samples decreased compared to the Si-free samples, except in the 0.4 Osm NaCl & 0.4 Osm NaCl/Si treated pair. DAB staining was overall slightly higher in *P. drummondii* compared to *P. patens.* It was also slightly increased in all salt and Si treated samples of *P. drummondii*, while it decreased in Si treated *P. patens* samples. A higher number of samples would have been needed to do statistical analysis with this method of quantification. In terms of extracted pigments Si and 0.2 Osm NaCl both increased the amount of *pheophytin a* in both species. For *pheophytin b* Si reduced the amount in *P. patens* though. The chlorophylls and carotenoids had their maximum in the 0.2 Osm NaCl treatment of *P. patens* and the combined Si/NaCl treatment of *P. drummondii* in both extracts. This hints both at the salt tolerance of *P. patens* (Frank et al., 2005; Pavlović et al., 2014) and an additional positive effect of Si that comes into play for *P. drummondii*.

Cell length was slightly positively influenced both by raising NaCl concentration and there was a significant, positive influence by Si availability in *P. drummondii*. In *P. patens,* it was negatively influenced by NaCl concentration, especially with additional Si treatment in the 0.4 Osm NaCl/Si treatment. Cell width of *P. drummondii* was positively influenced by the NaCl concentration and only at 0.4 Osm additional Si also influenced it positively. In case of *P. patens,* the cell width increased slightly with the NaCl concentration, more so without additional Si. The lower concentration (0.2 Osm) led to lower cell width at first though. In general, the surface area of the cells increased with the salt concentration in *P. drummondii*, and at 0.4 Osm, it increased even more with additional Si treatment. For Si treated *P. patens* cells on the other hand the surface area decreased with the concentration, while without Si it followed a pattern, similar to the cell width, with a minimum at 0.2 Osm and a maximum at 0.4 Osm NaCl. So, Si has a more positive influence on cell size in *P. drummondii* than in *P. patens*. This stands in contrast to reports in maize (Zörb et al., 2015) and *Cornus stolonifer*a (Mustard and Renault, 2004), where NaCl treatment had a cell wall stiffening impact, or only influenced the cell wall composition. A more detailed investigation of cell wall composition is needed.

7 Conclusion

The first aspect, the increase of vitality, growth and reduction of ROS as alleviating effect of Si treatment can be dismissed for the Cu experiment. In terms of biomass *P. drummondii* was growing only marginally better with Si than without Si and even though the biggest differences were between control and Si as well as the highest Cu concentration and its comparison treatment with Si, the experiment ended before the difference was significant. In *P. patens,* the difference was even smaller, therefore there was no evidence of a significant positive effect of Si on the gain of biomass under Cu stress. DAB staining even showed an increase of ROS in the Si treatments, the opposite of the expected effect (Malčovská et al., 2014b).

In case of the UV-B experiment the UV/Si treated samples of *P. drummondii* both gained more biomass compared to UV treated samples. Similarly, *P. patens* gained more biomass under influence of the Si/UV treatment. The ROS data showed no significant difference. It still can be said, that Si treatment had a positive effect on both, at least concerning biomass.

The salinity experiment showed, that *P. drummondii* did not grow as well with higher concentrations of salt, as it did with Si or in the control medium. The Si treated samples gained way more biomass than even the control, but beyond that, there was no more than a marginal positive effect of Si on biomass. Taking ROS staining into account, NBT staining of all and DAB staining of the salt treatments showed higher staining in Si treated samples. For *P. patens,* the difference in biomass between the pairs of different salt concentration is again marginal, except for control and Si treatment. The ROS staining on the other hand showed a reduction in Si treated samples, with exception of NBT staining in the 0.4 Osm NaCl and 0.4 Osm NaCl/Si pair. This is evidence for a positive effect of Si in dealing with salinity in *P. patens*, which, according to Rios et al. (2017), is caused by Si-mediated regulation of aquaporins.

The second hypothesis focused on the protonema-gametophore ratio (G-P ratio) as defined by Sassmann et al. (2015a). Like expected, the portion of protonemata developed was higher in the Cu treated samples. The higher concentrated Cu treatments led to slightly more gametophores in *P. drummondii* towards the end of the experiment, probably, because the plant is adapted to heavy metals (Antreich et al., 2016). Also, the higher Cu concentration completely suppressed gametophore development in *P. patens*.

In context of the UV-B experiment, the G-P ratio was shifted towards protonemata in the *P. drummondii* samples not treated with Si, which can be interpreted as a positive effect of Si in this regard (Sassmann et al., 2015a). For *P. patens,* the situation is less clear, since the control samples never developed gametophores. Because the highest ratio of gametophores developed in Si treated samples and the UV treated samples only varied in timing of gametophore development, most likely related to temperature differences (Glime, 2017), no positive effect of Si on G-P ratio was evident. Since the salinity experiments didn't lead to gametophore development for the duration of 7 weeks, no G-P ratio could be calculated.

The hypothesis that Si treatment reduces the amount of mobile heavy metal ions (Cu), like reported in higher plants (Adrees et al., 2015), at this point, cannot be fully discarded, nor do we have decisive evidence. While the Minteq simulation showed no influence of Si on the Cu-ion balance of the media, the decrease of Cu content in the *P. drummondii* protonemata, cultivated on the two higher concentrated Cu media, points towards an immobilization of Cu or a well working exclusion mechanism, like increased callose or pectin synthesis (Fahr et al., 2013;

Krzesłowska et al., 2009), that is supported by Si. In context of lowering the Cu mobility within the plant by Si treatment, only in the *P. drummondii* 0.1 mM Cu - 0.1 mM Cu/Si and *P. patens* control - Si pairs, a slight decrease of heavy metal gametophore-protonema ratio was observed, which was not enough to support the hypothesis.

Concerning the hypothesis of alleviation of UV-B damage on plants and pigments by Si treatment (Malčovská et al., 2014a; Shen et al., 2014), an increase of all pigments in the UV/Si treated protonemata of *P. patens* (DMF extracts) provided some evidence. In *P. drummondii* the increase in the same treatments (DMSO extracts) was not as big and for *P. patens* DMSO extracts the situation was inversed. A bigger experimental setup or another set of methods is needed to clarify the situation.

Numerous differences between the two species and their reactions in the experiments support the hypothesis, that the stress reaction is species-dependent (Antreich et al., 2016; Frank et al., 2005; Sassmann et al., 2015a; Sassmann et al., 2015b; Url, 1956), both for the abiotic stress applied and for the applied Si treatment. For generalizing our findings many more species need to be tested under similar conditions.

8 Future aspects

To get a better understanding of the influence of Si, a transcriptomic analysis is needed (Bokor et al., 2017; Imadi et al., 2015). Metabolomics is a very important tool that can be used to investigate the influence of Si in all three experimental setups, concerning the synthesis of proteins, transporter proteins, pigments and antioxidants (Arbona et al., 2013). An analysis of cell wall components could shed more light on the question, if the cell shape is more influenced by changed composition, or by bivalent/trivalent cations, like Cu^{2+} in the Cu treatment, crosslinking the pectins (Obel et al., 2009). Using 2'7'-dichloroflourescein (H2DCF) and dihydroethidium (DHE), staining of reactive oxygen species (ROS) is possible in *vivo* using a confocal laser scanning microscope (CLSM) and it enables pinpointing of affected cells (Wojtala et al., 2014). It should be noted, that the throughput using this method is rather low, so the culture schedule needs to be adjusted accordingly. Concerning further investigation of chlorophyll, it would be of advantage to investigate chlorophyll fluorescence/photo quenching (Fv/Fm, PEA; Liepiņa and Ievinsh (2016)) and the chlorophyll content (SPAD; Netto et al. (2005)), since the spectrophotometric measurement alone was unreliable and is too dependent on accuracy of the dry weight measurement. It is necessary to establish a measurement protocol, since common methods are not adequate or impossible without contaminating the samples. It also would be advantageous to investigate changes over time of cultivation. A more detailed investigation into salinity/osmolarity influencing the cultivated mosses is necessary to differentiate both stress factors. For example, a non-toxic and non-metabolizable compound (e.g. D-mannose; polyethylen glycol (PEG), used by Saglam et al. (2014)) could be used to enable investigation of osmotic/drought stress alone.

Focusing on single aspects of the previous experiments enables the introduction of more species in a broader approach, or a more detailed investigation by increasing the number of repetitions.

9   References

Adobe Systems Inc., 2006, Adobe Photoshop Elements 5.0 v5.0.2.

Adobe Systems Inc., 2012, Adobe Creative Suite 6.

Adrees, M., Ali, S., Rizwan, M., Zia-ur-Rehman, M., Ibrahim, M., Abbas, F., Farid, M., Qayyum, M.F., Irshad, M.K., 2015. Mechanisms of Silicon-Mediated Alleviation of Heavy Metal Toxicity in Plants: A Review. Ecotoxicology and Environmental Safety 119, 186-197.

Antreich, S., Sassmann, S., Lang, I., 2016. Limited Accumulation of Copper in Heavy Metal Adapted Mosses. Plant Physiology and Biochemistry 101, 141-148.

Appenroth, K.-J., 2010. Definition of "Heavy Metals" and Their Role in Biological Systems, in: Sherameti, I., Varma, A. (Eds.), Soil Heavy Metals. Springer-Verlag, Berlin Heidelberg, pp. 19-29.

Arbona, V., Manzi, M., de Ollas, C., Gómez-Cadenas, A., 2013. Metabolomics as a Tool to Investigate Abiotic Stress Tolerance in Plants. International Journal of Molecular Sciences 14, 4885-4911.

Baker, A.J.M., 1981. Accumulators and Excluders-Strategies in the Response of Plants to Heavy Metals. Journal of Plant Nutrition (United States) 3, 643-654.

Baluška, F., Baroja-Fernandez, E., Pozueta-Romero, J., Hlavacka, A., Etxeberria, E., Šamaj, J., 2006. Endocytic Uptake of Nutrients, Cell Wall Molecules and Fluidized Cell Wall Portions into Heterotrophic Plant Cells, in: Šamaj, J., Baluška, F., Menzel, D. (Eds.), Plant Endocytosis. Springer Berlin Heidelberg, Berlin, Heidelberg, pp. 19-35.

Benvenuto, L.M., Honaine, M.F., Osterrieth, M.L., 2013. Amorphous Silica Biomineralizations Inpolytrichum Strictummenzies Ex Brid. (Bryophyta). Journal of Bryology 35, 112-118.

Bokor, B., Ondoš, S., Vaculík, M., Bokorová, S., Weidinger, M., Lichtscheidl, I., Turňa, J., Lux, A., 2017. Expression of Genes for Si Uptake, Accumulation, and Correlation of Si with Other Elements in Ionome of Maize Kernel. Frontiers in Plant Science 8, 1063.

Brewster, R., contributors, 2016, Paint.Net v4.0.13, dotPDN LLC.

Cowen, R., manuscript, 2004. Exploiting the Earth. Johns Hopkins University Press.

Daudi, A., O'Brien, J.A., 2012. Detection of Hydrogen Peroxide by Dab Staining in Arabidopsis Leaves. Bio-protocol 2, e263.

Decreux, A., Messiaen, J., 2005. Wall-Associated Kinase Wak1 Interacts with Cell Wall Pectins in a Calcium-Induced Conformation. Plant and Cell Physiology 46, 268-278.

DIN 5031, 1984. Deutsches Institut Für Normung (Hrsg.): Strahlungsphysik Im Optischen Bereich Und Lichttechnik; Benennung Der Wellenlängenbereiche. Din 5031 Teil 7, Januar 1984.

Dragisic Maksimovic, J., Mojovic, M., Maksimovic, V., Romheld, V., Nikolic, M., 2012. Silicon Ameliorates Manganese Toxicity in Cucumber by Decreasing Hydroxyl Radical Accumulation in the Leaf Apoplast. J Exp Bot 63, 2411-2420.

EDAX Inc., 2013, Team Eds Software Suite Enhanced 4.3-Released.

Ernst, W.H.O., 1972. Ecophysiological Studies on Heavy Metal Plants in South Central Africa. Kirkia, pp. 125-145.

Fahr, M., Laplaze, L., Bendaou, N., Hocher, V., Mzibri, M.E., Bogusz, D., Smouni, A., 2013. Effect of Lead on Root Growth. Frontiers in Plant Science 4, 175.

Feller, U., 2016. Drought Stress and Carbon Assimilation in a Warming Climate: Reversible and Irreversible Impacts. Journal of Plant Physiology 203, 69-79.

Frahm, J.-P., Frey, W., 2004. Moosflora, 4 ed. UTB, Stuttgart.

Frank, W., Ratnadewi, D., Reski, R., 2005. Physcomitrella Patens Is Highly Tolerant against Drought, Salt and Osmotic Stress. Planta 220, 384-394.

Fry, S.C., 1998. Oxidative Scission of Plant Cell Wall Polysaccharides by Ascorbate-Induced Hydroxyl Radicals. Biochemical Journal 332, 507-515.

Fukao, T., Bailey-Serres, J., 2004. Plant Responses to Hypoxia – Is Survival a Balancing Act? Trends in Plant Science 9, 449-456.

Gall, H.L., Philippe, F., Domon, J.-M., Gillet, F., Pelloux, J., Rayon, C., 2015. Cell Wall Metabolism in Response to Abiotic Stress. Plants 4, 112-166.

Glime, J.M., 2017. Bryophyte Ecology.

Greger, M., 2004. Metal Availability, Uptake, Transport and Accumulation in Plants, in: Prasad, M.N.V. (Ed.), Heavy Metal Stress in Plants: From Biomolecules to Ecosystems. Springer Berlin Heidelberg, Berlin, Heidelberg, pp. 1-27.

Gregory, R.P.G., Bradshaw, A.D., 1965. Heavy Metal Tolerance in Populations of Agrostis Tenuis Sibth. And Other Grasses, New Phytologist, pp. 131-143.

Gustafsson, J.P., 2016, Visual Minteq 3.1.

He, C., Ma, J., Wang, L., 2015. A Hemicellulose-Bound Form of Silicon with Potential to Improve the Mechanical Properties and Regeneration of the Cell Wall of Rice. New Phytologist 206, 1051-1062.

Hollosy, F., 2002. Effects of Ultraviolet Radiation on Plant Cells. Micron 33, 179-197.

Hou, X.W., Tong, H.Y., Selby, J., DeWitt, J., Peng, X.X., He, Z.H., 2005. Involvement of a Cell Wall-Associated Kinase, Wakl4, in Arabidopsis Mineral Responses. Plant Physiology 139, 1704-1716.

Imadi, S.R., Kazi, A.G., Ahanger, M.A., Gucel, S., Ahmad, P., 2015. Plant Transcriptomics and Responses to Environmental Stress: An Overview. J Genet 94, 525-537.

Jacobsen, T., Adams, R.M., 1958. Salt and Silt in Ancient Mesopotamian Agriculture. Progressive changes in soil salinity and sedimentation contributed to the breakup of past civilizations 128, 1251-1258.

Kakani, V.G., Reddy, K.R., Zhao, D., Sailaja, K., 2003. Field Crop Responses to Ultraviolet-B Radiation: A Review. Agricultural and Forest Meteorology 120, 191-218.

Kasprowicz, A., Michalak, M., Wierzchowiecka, M., Maruniewicz, M., Wojtaszek, P., 2009. Endocytosis and Actin-Dependent Transport of Plant Cell Wall Components. Postepy Biochem 55, 181-186.

Kim, Y.H., Khan, A.L., Lee, I.J., 2016. Silicon: A Duo Synergy for Regulating Crop Growth and Hormonal Signaling under Abiotic Stress Conditions. Critical Reviews in Biotechnology 36, 1099-1109.

Klemm, P., 1895. Desorganisationserscheinungen Der Zellen. Jahrbücher für wissenschaftliche Botanik 28, 627-700.

Knight, C., Cove, D.J., Boyd, P.J., Ashton, N.W., 1988. The Isolation of Biochemical and Developmental Mutants in Physcomitrella Patens., in: Glime JM. (Ed.), Methods in Bryology. Hattori Botanical Laboratory, Nichinan, Japan, pp. 47-58.

Kreeb, K., 1974. Ökophysiologie Der Pflanzen. VEB Gustav Fischer Verlag, Jena.

Kroemer, K., Reski, R., Frank, W., 2004. Abiotic Stress Response in the Moss Physcomitrella Patens: Evidence for an Evolutionary Alteration in Signaling Pathways in Land Plants. Plant Cell Reports 22, 864-870.

Krzesłowska, M., 2011. The Cell Wall in Plant Cell Response to Trace Metals: Polysaccharide Remodeling and Its Role in Defense Strategy. Acta Physiologiae Plantarum 33, 35-51.

Krzesłowska, M., Lenartowska, M., Mellerowicz, E.J., Samardakiewicz, S., Woźny, A., 2009. Pectinous Cell Wall Thickenings Formation—a Response of Moss Protonemata Cells to Lead. Environmental and Experimental Botany 65, 119-131.

Küntzel, A., Dröscher, T., 1940. The Developing Copper Colour Complexes of the Biuret Reaction with Albumen Bodies and Albumen Decomposition Products. Biochemische Zeitschrift 306, 177-204.

Laboratory Imaging, 2016, Nis Elements Basic Research 4.60.00 64 bit, Nikon.

Landini, G., Dougherty, B., Rasband, W., 2010, Threshold_Colour Plugin for Fiji V1.15.

Lepeschkin, W., 1924. Kolloidchemie Des Protoplasmas. Von Prof. Dr. W. Lepeschkin. Mit 22 Abbildungen. Berlin 1924, Verlag Von Julyus Springer. 228 Seiten. Preis Geb. 9,90 Mark. Berichterstatter: Siedler-Zehlendorf. Archiv der Pharmazie 262, 544-545.

Levitt, J., 1980. Responses of Plants to Environmental Stress: Chilling, Freezing and High Temperature Stresses., 2nd ed. Academic Press, New York.

Libbert, E., 1987. Lehrbuch Der Pflanzenphysiologie, 4. erw. neugest. Aufl. ed. VEB Gustav Fischer Verlag Jena, pp. 151-153.

Lichtenthaler, H.K., 1998. The Stress Concept in Plants: An Introduction. Annals of the New York Academy of Sciences 851, 187-198.

Liepiņa, L., Ievinsh, G., 2016. Potential for Fast Chlorophyll a Fluorescence Measurement in Bryophyte Ecophysiology. Estonian Journal of Ecology 63, 137–149.

Lindsay, W.L., 1979. Chemical Equilibria in Soils. Wiley-Interscience Publication.

Liu, H., Able, A.J., Able, J.A., 2016. Smarter De-Stressed Cereal Breeding. Trends in Plant Science 21, 909-925.

Lutgens, F.K., Tarbuck, E.J., 2000. Essentials of Geology, 7th ed. Prentice Hall.

Ma, J.F., Miyake, Y., Takahashi, E., 2001. Chapter 2 Silicon as a Beneficial Element for Crop Plants. Studies in Plant Science 8, 17-39.

Malčovská, M.S., Dučaiová, Z., Bačkor, M., 2014a. Impact of Silicon on Maize Seedlings Exposed to Short-Term Uv-B Irradiation. Biologia 69, 1349-1355.

Malčovská, M.S., Dučaiová, Z., Maslaňáková, I., Bačkor, M., 2014b. Effect of Silicon on Growth, Photosynthesis, Oxidative Status and Phenolic Compounds of Maize (Zea Mays L.) Grown in Cadmium Excess. Water, Air, & Soil Pollution 225, 11.

Martínez-Atienza, J., Jiang, X., Garciadeblas, B., Mendoza, I., Zhu, J.-K., Pardo, J.M., Quintero, F.J., 2007. Conservation of the Salt Overly Sensitive Pathway in Rice. Plant Physiology 143, 1001-1012.

Moran, R., 1982. Formulae for Determination of Chlorophyllous Pigments Extracted with N,N-Dimethylformamide. Plant Physiology 69, 1376-1381.

Mustard, J., Renault, S., 2004. Effects of Nacl on Water Relations and Cell Wall Elasticity and Composition of Red-Osier Dogwood (Cornus Stolonifera) Seedlings. Physiol Plant 121, 265-271.

Netto, A., Campostrini, E., Oliveira, J., Bressan-Smith, R., 2005. Photosynthetic Pigments, Nitrogen, Chlorophyll a Fluorescence and Spad-502 Readings in Coffee Leaves.

Nieboer, E., Richardson, D.H.S., 1980. The Replacement of the Nondescript Term 'Heavy Metals' by a Biologically and Chemically Significant Classification of Metal Ions. Environmental Pollution Series B, Chemical and Physical 1, 3-26.

Obel, N., Erben, V., Schwarz, T., Kühnel, S., Fodor, A., Pauly, M., 2009. Microanalysis of Plant Cell Wall Polysaccharides. Molecular Plant 2, 922-932.

Oliver, M.J., Velten, J., Mishler, B.D., 2005. Desiccation Tolerance in Bryophytes: A Reflection of the Primitive Strategy for Plant Survival in Dehydrating Habitats?1. Integrative and Comparative Biology 45, 788-799.

Pascual, M.B., Echevarria, V., Gonzalo, M.J., Hernandez-Apaolaza, L., 2016. Silicon Addition to Soybean (Glycine Max L.) Plants Alleviate Zinc Deficiency. Plant Physiology and Biochemistry 108, 132-138.

Pavlović, D., Nikolić, B., Đurović, S., Waisi, H., Anđelković, A., Marisavljević, D., 2014. Chlorophyll as a Measure of Plant Health: Agroecological Aspects. Pesticides and Phytomedicine (Belgrade) 29, 13.

Possnig, U., 2011. Das Wachstumsverhalten Von Moos-Protonemata Unter Osmotischen Stressbedingungen, Fakultät für Lebenswissenschaften. Universität Wien, Vienna, p. 102.

Prasad, M.N.V., 2004. Heavy Metal Stress in Plant: From Molecules to Ecosystems., 2nd Ed. ed. Springer, Berlin.

Pressel, S., Ligrone, R., Duckett, J.G., 2008. Cellular Differentiation in Moss Protonemata: A Morphological and Experimental Study. Annals of Botany 102, 227-245.

Qiu, Y.L., Li, L.B., Wang, B., Chen, Z.D., Knoop, V., Groth-Malonek, M., Dombrovska, O., Lee, J., Kent, L., Rest, J., Estabrook, G.F., Hendry, T.A., Taylor, D.W., Testa, C.M., Ambros, M., Crandall-Stotler, B., Duff, R.J., Stech, M., Frey, W., Quandt, D., Davis, C.C., 2006. The Deepest Divergences in Land Plants Inferred from Phylogenomic Evidence. Proceedings of the National Academy of Sciences of the United States of America 103, 15511-15516.

Rasband, W., 2015, Fiji Imagej V1.50e.

Rios, J.J., Martínez-Ballesta, M.C., Ruiz, J.M., Blasco, B., Carvajal, M., 2017. Silicon-Mediated Improvement in Plant Salinity Tolerance: The Role of Aquaporins. Frontiers in Plant Science 8, 948.

Ronen, R., Galun, M., 1984. Pigment Extraction from Lichens with Dimethyl Sulfoxide (Dmso) and Estimation of Chlorophyll Degradation. Environmental and Experimental Botany 24, 239-245.

Ross, I.S., Old, K.M., 1973. Thiol Compounds and Resistance of Pyrenophora Avenae to Mercury. Transactions of the British Mycological Society 60, 301-310.

Ruplitsch, B., 2011. Das Moos Physcomitrella Unter Uv-Stress, Fakultät für Lebenswissenschaften. University of Vienna, Vienna, p. 91.

Saglam, A., Terzi, R., Demiralay, M., 2014. Effect of Polyethylene Glycol Induced Drought Stress on Photosynthesis in Two Chickpea Genotypes with Different Drought Tolerance. Acta Biol Hung 65, 178-188.

Sassmann, S., Adlassnig, W., Puschenreiter, M., Cadenas, E.J.P., Leyvas, M., Lichtscheidl, I.K., Lang, I., 2015a. Free Metal Ion Availability Is a Major Factor for Tolerance and Growth in Physcomitrella Patens. Environmental and Experimental Botany 110, 1-10.

Sassmann, S., Weidinger, M., Adlassnig, W., Hofhansl, F., Bock, B., Lang, I., 2015b. Zinc and Copper Uptake in Physcomitrella Patens: Limitations and Effects on Growth and Morphology. Environmental and Experimental Botany 118, 12-20.

Scheller, H.V., Jensen, J.K., Sørensen, S.O., Harholt, J., Geshi, N., 2007. Biosynthesis of Pectin, Physiologia Plantarum, pp. 283-295.

Schiller, W., 1974. Versuche Zur Kupferresistenz Bei Schwermetallökotypen Von Silene Cucubalus Wib. Flora 163, 327-341.

Schlee, D., 1986. Ökologische Biochemie. VEB Gustav Fischer Verlag Jena.

Shakoor, S.A., 2014. Silicon Biomineralisation in Plants: A Tool to Adapt Global Climate Change Journal of Research in Biological Sciences 1, 3 pp.

Shen, X., Li, Z., Duan, L., Eneji, A.E., Li, J., 2014. Silicon Mitigates Ultraviolet-B Radiation Stress on Soybean by Enhancing Chlorophyll and Photosynthesis and Reducing Transpiration. Journal of Plant Nutrition 37, 837-849.

Sokal, R.R., Rohlf, F.J., 1994. Biometry: The Principles and Practices of Statistics in Biological Research, 3rd Edition ed. Palgrave Macmillan.

StatPoint Technologies Inc., 2010, Statgraphics Centurion Xvi v16.1.11 (64-bit).

Stoláriková, M., Vaculík, M., Lux, A., Di Baccio, D., Minnocci, A., Andreucci, A., Sebastiani, L., 2012. Anatomical Differences of Poplar (Populus × Euramericana Clone I-214) Roots Exposed to Zinc Excess. Biologia 67, 483-489.

Trembath-Reichert, E., Wilson, J.P., McGlynn, S.E., Fischer, W.W., 2015. Four Hundred Million Years of Silica Biomineralization in Land Plants. Proceedings of the National Academy of Sciences of the United States of America 112, 5449-5454.

Tripathi, D.K., Singh, S., Yadav, V., Arif, N., Singh, S., Dubey, N.K., Chauhan, D.K., 2017. Silicon: A Potential Element to Combat Adverse Impact of Uv-B in Plants, in: Singh, V.P., Singh, S., Prasad, S.M., Parihar, P. (Eds.), Uv-B Radiation: From Environmental Stressor to Regulator of Plant Growth. Wiley Blackwell.

Url, W.G., 1956. "Über Schwermetall- Zumal Kupferresistenz Einiger Moose.". Protoplasma 46, 786-793.

Vaculík, M., 2009. Silicon Mitigates Cadmium Inhibitory Effects in Young Maize Plants. Environmental and Experimental Botany 67, 52-58.

Vaculík, M., Landberg, T., Greger, M., Luxová, M., Stoláriková, M., Lux, A., 2012. Silicon Modifies Root Anatomy, and Uptake and Subcellular Distribution of Cadmium in Young Maize Plants. Annals of Botany 110, 433-443.

Vaculíková, M., Vaculík, M., Tandy, S., Luxová, M., Schulin, R., 2016. Alleviation of Antimonate (Sbv) Toxicity in Maize by Silicon (Si). Environmental and Experimental Botany 128, 11-17.

Vidali, L., Rounds, C.M., Hepler, P.K., Bezanilla, M., 2009. Lifeact-Megfp Reveals a Dynamic Apical F-Actin Network in Tip Growing Plant Cells. PLoS ONE 4, e5744.

Wellburn, A.R., 1994. The Spectral Determination of Chlorophylls a and B, as Well as Total Carotenoids, Using Various Solvents with Spectrophotometers of Different Resolution. Journal of Plant Physiology 144, 307-313.

Werner, D., Roth, R., 1983. Silica Metabolism. Springer-Verlag, New York.

Wernitznig, S., 2009. Die Schwermetalltoleranten Moose Mielichhoferia Elongata Und Pohlia Drummondii Und Ihre Reaktion Gegenüber Schwermetallstress. Universität Wien, Wien, p. 110.

Whitmarsh, J., Govindjee, 1999. The Photosynthetic Process, in: Singhal, G.S., Renger, G., Sopory, S.K., Irrgang, K.-D., Govindjee (Eds.), Concepts in Photobiology: Photosynthesis and Photomorphogenesis. Narosa Publishers; Kluwer Academic, New Delhi; Dordrecht, pp. 11-51.

Wojtala, A., Bonora, M., Malinska, D., Pinton, P., Duszynski, J., Wieckowski, M.R., 2014. Methods to Monitor Ros Production by Fluorescence Microscopy and Fluorometry. Methods Enzymol 542, 243-262.

Wolf, L., Rizzini, L., Stracke, R., Ulm, R., Rensing, S.A., 2010. The Molecular and Physiological Responses of *Physcomitrella Patens* to Ultraviolet-B Radiation. Plant Physiology 153, 1123-1134.

Yamasaki, H., Pilon, M., Shikanai, T., 2008. How Do Plants Respond to Copper Deficiency? Plant Signaling & Behavior 3, 231-232.

Zhu, J.-K., 2001. Plant Salt Stress, Els. John Wiley & Sons, Ltd.

Zörb, C., Mühling, K.H., Kutschera, U., Geilfus, C.-M., 2015. Salinity Stiffens the Epidermal Cell Walls of Salt-Stressed Maize Leaves: Is the Epidermis Growth-Restricting? PLoS ONE 10, e0118406.